A CLASS OF THREE DIMENSIONAL OPTIMUM WINGS IN HYPERSONIC FLOW

Thesis by

Tse-Fou Zien

In Partial Fulfillment of the Requirements

For the Degree of

Doctor of Philosophy

California Institute of Technology

Pasadena, California

1967

(Submitted May 1, 1967)

Acknowledgment

I am greatly indebted to Professor Julian D. Cole who, in addition to providing guidance to my research in general, suggested this problem in particular and gave constant advice and encouragement throughout the investigation. Various difficulties in the present study were overcome through numerous stimulating discussions with him. My association with him in these four years at the California Institute of Technology has indeed made this last part of my student's life the most enjoyable and memorable.

Thanks are also due to Kiku Matsumoto for her assistance in the numerical programming; to Viv Pickelsimer for her excellent typing of the thesis.

It is a great pleasure to express my gratitude to my dear parents who have given me encouragement and support in all respects during the entire course of my graduate study.

Lastly, but not leastly, I wish to record my deep appreciation to my wife, Suzy Shen, whose understanding and unfailing encouragement contributed the most to the success of my graduate study.

The research was supported in part by Grant 6655 from the National Science Foundation.

Abstract

The idea of using streamlines of a certain known flow field to construct generally three-dimensional lifting surfaces together with the method of evaluating the aerodynamic forces on the surfaces, developed by Nonweiler, Jones and Woods, has been extended and applied to axisymmetric hypersonic flow fields associated with a class of slender power-law shock waves of the form $r \sim \tau x^n$ in the limit of infinite free stream Mach number. For this purpose, the basic flow fields associated with concave shocks ($n > 1$) have first been calculated numerically at a fixed value of the ratio of specific heats $\gamma = 1.40$, and the results are presented in tabulated form, covering a wide range of values of n. The method of constructing a lifting surface either by prescribing its leading edge shape on the basic shock or by specifying its trailing edge shape in the plane $x = 1$ is then discussed. Expressions for lift and drag on the surface are derived. A class of optimum shapes giving minimum pressure drag at a fixed value of lift has been determined for every basic flow field with n ranging from 1/2 to 10 at $\gamma = 1.40$.

Table of Contents

List of Figures

List of Symbols

$A = \mathscr{D}/\mathscr{L}$ (Eq. 4.5)

B = equation of lifting surface

C = elevation of the leading edge

D = drag integral (Eq. 3.41)

$G = r/x^n$

$\overline{G} = r$

H = hypersonic similarity parameter $1/M_\infty^2\delta^2$, also functional of variational problems

L = lift integral (Eq. 3.42), also leading edge function (Eq. 3.9)

P = pressure similarity function (Eq. 2.40b)

$Q = d\Phi(r)/dr$ (Eq. 4.4a)

R = density similarity function (Eq. 2.40c)

S = shock function, leading term of $g(x^*,\tau)$

T = side thrust integral, temperature field, also D/L

V = velocity similarity function (Eq. 2.40a)

a = speed of sound

b = body shape factor

f = body shape function

g = shock shape function

$(\vec{i},\vec{j},\vec{k})$ = unit vectors of the Cartesian coordinate system

j = equal to zero for two dimensional use, equal to 1 for axisymmetric case

(k_1,k_2) = elevation of trailing edge

n = exponent, $S(x) = x^n$

$\vec{q}$ = velocity vector

r = distance from the axis of symmetry

s = area

u = non-dimensional axial velocity component

v = non-dimensional transverse velocity component

(x,y,z) = cartesian coordinates system

α = invariant coordinate (Eq. 2.41)

β = invariant coordinate (Eq. 2.41)

γ = specific heats ratio

δ = characteristic shock angle, also variation

η = similarity variable, $2\Psi/x^{2n}$

$\bar{\eta}$ = basic similarity variable r/x^n

$(\lambda_1^*,\lambda_2^*)$ = Lagrange multipliers

ξ = auxiliary coordinate (Eq. 2.42)

ζ = auxiliary coordinate (Eq. 2.42)

ρ = density

Σ^* = control surface

σ = non-dimensional density

τ = thickness parameter

ϕ = azimuthal angle

Ψ = stream function

Ω = lifting surface

$\mathscr{L}$ = lift function

$\mathscr{D}$ = drag function

Subscripts

∞ = conditions upstream of the shock wave

s = conditions downstream of the shock wave

b = conditions on the body surface

Superscripts

* = physical quantities

I. Introduction

Recent advances in technology have made flight at hypersonic speeds realizable. As a consequence, the practical problem of the optimum design of the aerodynamic shapes in this speed range is beginning to attract considerable attention from many aerodynamicists, and significant progress has been achieved. Perhaps the most up-to-date survey of the current status of this subject is given by Miele.[1] However, most of the available analyses seem to be restricted to two dimensional or axisymmetric shapes; also the Newtonian approximation of pressure distribution is widely adopted in the analyses. The treatment of general three dimensional shapes without the simplifying assumption of Newtonian pressure distribution appears to be formidable because of the inherent difficulties of solving the strongly non-linear set of equations of gasdynamics in any generality. This is true even for slender shapes where the simplified equations of the hypersonic small disturbance theory (henceforth referred to as HSDT) can be successfully applied.

Nevertheless, a relatively new method of constructing lifting surfaces within the framework of inviscid gasdynamic theory has recently been developed. This method furnishes a fairly wide class of three dimensional surfaces whose aerodynamic characteristics can be determined exactly. This method, first developed by Nonweiler,[2] consists of using the streamlines in some basic known flow field as the elements of the surface. If an arbitrary curve prescribed on the shock surface of the basic flow field is taken as the leading edge of the lifting surface, then the lifting surface is formed by those

streamlines that penetrate the basic shock surface through the points on the leading edge curve. Obviously this lifting surface will have a shock wave of known shape attached all along its leading edge. That part of the original flow field between the lifting surface and the shock wave attached along its leading edge will remain unaltered regardless of the replacement of the original body by the lifting surface. Therefore, the forces acting on the surface are accessible to exact calculations. Nonweiler illustrated the idea by taking the flow field behind a plane oblique shock wave generated by a two dimensional wedge flying at supersonic speeds as the basic flow field. Later Jones[3] and Woods[4,5] carried the idea over to the case where an axisymmetric supersonic cone field is taken as the basic field. They indicated a procedure of constructing the surface geometrically as well as a method of numerically evaluating the aerodynamic forces on it.

It now seems feasible to generate a fairly wide class of three dimensional lifting surfaces from some known two dimensional or axisymmetric flow fields. The same idea can equally well be applied to hypersonic flow fields and hence to the design of a class of three dimensional hypersonic lifting surfaces. In both the supersonic and the hypersonic cases, the solution to the basic flow field is essential.

Among the limited number of existing exact solutions to the equations of hypersonic small disturbance theory, the self-similar flow behind an axisymmetric power-law shock wave of the form $r^* \sim \tau x^{*n}$, seems to be the most interesting one for this purpose. A detailed account of this flow field can be found in a survey article by Mirels,[6] in

which the discussion is limited to the non-concave shapes of the body and shock only, i.e., $n \leq 1$. Extensive numerical results for the corresponding flow field have also been tabulated in Chernyi[7] and Gersten and Nicolai.[8] For concave shapes, the flow field also exhibits similarity, but the only investigation considers a two dimensional case (Sullivan[9]). The numerical calculations for the corresponding axisymmetric case do not seem to exist in the literature.

In the present thesis, the previously mentioned method of constructing the lifting surface is extended and applied to the limiting hypersonic small disturbance flow field (i.e., $H \equiv 0$) associated with an axisymmetric slender power law shocks of the form $r^* \sim \tau x^{*n}$ for all n greater than 1/2. The surfaces under consideration have the following general properties: (1) the trailing edge when projected onto the plan is straight and perpendicular to the axis of symmetry of the basic field. (2) the leading edge is on the original shock surface and is symmetric with respect to a meridian plane of the basic axisymmetric field. To do this, the numerical solutions of the concave shock case are first obtained in Chapter 2 by reformulating the problem in terms of similarity variables and then solving it numerically on the IBM 7094 digital computer for $\gamma = 1.40$ and a wide range of n. Certain singular behavior of the solution is noted and discussed. Then in Chapter 3, the geometrical construction of the surface is discussed in detail for both the case of prescribed leading edge shape and for the case of prescribed trailing edge shape. The method of calculating the lift and drag forces on the surface is also presented and the expressions for

the forces are given in terms of single integrals. The integrals are in the trailing edge plane and involve a function which characterizes the shape of the trailing edge. A variational problem is then formulated and solved in Chapter 4 to find an optimum family of shapes which, for a given set of values of n and γ, gives minimum drag for a fixed lift. Certain geometrical constraints derived from some practical considerations arise naturally. Typical results on the optimum shapes and the associated formulae for the minimum drag are also presented, covering a wide range of n for $\gamma = 1.4$.

It is to be noted here that the treatment of the problem in general supersonic case is possible for the exceptional value of n equal to unity, i.e., the axisymmetric cone field, simply because of the fact that exact solution of the flow field is available for that exceptional case without using the approximations of HSDT. However, calculations would then have to be made for every set of values of M_∞ and θ_s (or θ_b), the half shock cone angle (or half body cone angle). By studying the limiting case of hypersonic flow corresponding to $M_\infty = \infty$, the great simplification is achieved that only one optimum shape exists.

II. Solution of the Hypersonic Small Disturbance Equations for the Axisymmetric Flow Associated With A Power-Law Shock

2.1. Formulation of the Problem.

In this section, the limiting HSDT equations and boundary conditions are derived from the exact, inviscid gasdynamic equations and shock wave relations as well as the conditions of tangential flow on the body surface. Next, specialization to the class of the flow associated with power-law shape of shock wave is made and the similarity formulation of the problem is given.

(2.1.1) Derivation of the Limiting HSDT Equations.

The derivation of the HSDT equations is well-known (see, for example, Van Dyke[10]); however, it is included here for completeness.

Consider the steady, uniform flow of a stream of calorically perfect gas at Mach number M_∞ over a slender body of revolution of the form

$$r^* = \tau f(x^*) \qquad f(o) = o \tag{2.1}$$

where x^* and r^* are the streamwise and transverse coordinates respectively, and τ is a small parameter characterizing the body surface inclination to the free stream.

As a working hypothesis, the associated shock wave shape is postulated to have the following form of expansion in terms of τ:

$$r^* = g(x^*,\tau) = \tau S(x^*) + O(\tau^2) \tag{2.2}$$

Let the quantity δ be defined as a characteristic angle which the shock wave makes with the free stream, i.e.,

$$\tan \delta = \frac{d}{dx^*} g(x^*,\tau) = \tau \frac{d}{dx^*} S(x^*) + O(\tau^2). \tag{2.3}$$

Since $\tau \to 0$, (2.3) implies that the angle also tends to zero uniformly if $S'(x^*)$ is uniformly of $O(1)$ throughout the flow field.

We now consider the following limit:

$$M_\infty \to \infty, \qquad \delta \to 0 \qquad \text{such that } H \equiv \frac{1}{M_\infty^2 \delta^2} \to 0. \tag{2.4}$$

The equations of motion derived from the exact, inviscid gasdynamic equations under the limit (2.4) are the limiting HSDT equations. It is to be noted here that in the class of problem considered later, the assumptions (2.4) underlying the approximation may break down locally and thus results in certain singular behavior of the solutions. More explicitly, for the class of flow where

$$S(x^*) = x^{*n}$$

the assumption of small flow deflection $\delta \to 0$ breaks down at $x^* = o$ for $n < 1$ because $S'(x^*) = \infty$ there. On the other hand, the assumption of strong shock $1/M_\infty^2 \delta^2 = 0$ is violated at $x^* = o$ for $n > 1$ because $S'(x^*) = 0$ at the tip. These singularities will be discussed later.

We will assume here that $S'(x^*)$ is generally of $O(1)$ except for some local points, so that δ and τ will be of the same order of magnitude.

The physical interpretations of the limit (2.4) are as follows. The limit $M_\infty \to \infty$ corresponds to the case that the free stream sound speed $a_\infty \to o$ while the free stream density ρ_∞ and speed U_∞ are kept fixed, or equivalently, the ambient pressure p_∞ and temperature T_∞ tend to zero. The limit $\delta \to 0$ (or $\tau \to 0$) corresponds to the case of small flow deflection. The strong shock limit $1/M_\infty^2\delta^2 = 0$ (or $1/M_\infty^2\tau^2 = 0$) indicates the fact that the free stream Mach angle vanishes faster than the local shock wave angle does, because the product $M_\infty\delta$ can be interpreted as the ratio of the characteristic shock angle to the free stream Mach angle.

In carrying out this limiting process, the strained coordinates $r = r^*/\tau$, $x = x^*$ are used and kept fixed in order to keep the relative position of a field point and the body surface invariant.

The exact conditions across the shock wave in uniform stream can be expressed as[11]

$$\frac{p_s^* - P_\infty}{\rho_\infty U_\infty^2} = \frac{2}{\gamma + 1}\left(\sin^2\delta - \frac{1}{M_\infty^2}\right) \tag{2.5a}$$

$$\frac{\rho_s^*}{\rho_\infty} = \frac{\gamma + 1}{\gamma - 1}\left[1 + \frac{2}{\gamma - 1}\left(\frac{1}{M_\infty \sin\delta}\right)^2\right]^{-1} \tag{2.5b}$$

$$\frac{v_s^*}{U_\infty} = \frac{2}{\gamma + 1}\sin\delta\cos\delta\left[1 - \left(\frac{1}{M_\infty \sin\delta}\right)^2\right] \tag{2.5c}$$

$$\frac{u_s^* - U_\infty}{U_\infty} = \frac{2}{\gamma + 1} \sin^2 \delta \left[1 - \left(\frac{1}{M_\infty \sin \delta}\right)^2\right] \tag{2.5d}$$

where the subscripts ∞ and s represent conditions on the upstream and downstream sides of the shock surface respectively.

A study of Eqs. (2.5) under the limit (2.4) suggests the following representations of the exact flow fields:

$$\begin{aligned} u^*(x^*,r^*,\tau) &= 1 + \tau^2 u(x,r) + 0(\tau^4) \\ v^*(x^*,r^*,\tau) &= \tau v(x,r) + 0(\tau^3) \\ p^*(x^*,r^*,\tau)/\rho_\infty U_\infty^2 &= \tau^2 p(x,r) + 0(\tau^4) \\ \rho^*(x^*,r^*,\tau)/\rho_\infty &= \sigma(x,r) + 0(\tau^2) \end{aligned} \tag{2.6}$$

where the fact that $\lim \delta/\tau = 0(1)$ is used and the velocity field $\vec{q}^*$ is represented by $\vec{q}^*(x^*,r^*,\tau) = U_\infty \left[\vec{\ell}_x u^*(x^*,r^*,\tau) + \vec{\ell}_r v^*(x^*,r^*,\tau)\right]$.

The exact equations of steady motion of an inviscid, nonconducting gas in an axisymmetric field are:

$$\text{continuity:} \quad \frac{\partial}{\partial x^*}(\rho^* u^* r^*) + \frac{\partial}{\partial r^*}(\rho^* v^* r^*) = 0 \tag{2.7a}$$

$$\text{axial momentum:} \quad u^* \frac{\partial u^*}{\partial x^*} + v^* \frac{\partial u^*}{\partial r^*} + \frac{1}{\rho^* U_\infty^2} \frac{\partial p^*}{\partial x^*} = 0 \tag{2.7b}$$

$$\text{transverse momentum:} \quad u^* \frac{\partial v^*}{\partial x^*} + v^* \frac{\partial v^*}{\partial r^*} + \frac{1}{\rho^* U_\infty^2} \frac{\partial p^*}{\partial x^*} = 0 \tag{2.7c}$$

$$\text{entropy:} \quad \left(u^* \frac{\partial}{\partial x^*} + v^* \frac{\partial}{\partial r^*}\right)\left[\frac{p^*}{(\rho^*)^\gamma}\right] = 0. \qquad (2.7d)$$

The exact boundary condition of tangential flow at body surface is expressed as

$$\vec{q}^* \cdot \nabla^*[r^* - \tau f(x^*)] = 0 \quad \text{on} \quad r^* = \tau f(x^*). \qquad (2.8)$$

Application of the expressions (2.6) and the limit (2.4) to the equations (2.5), (2.7) and (2.8) results in the following system of equations for the leading terms of the expansion:

$$\text{continuity:} \quad \frac{\partial}{\partial x}(r\sigma) + \frac{\partial}{\partial r}(r\sigma v) = 0$$

$$\text{transverse momentum:} \quad \left(\frac{\partial}{\partial x} + v\frac{\partial}{\partial r}\right) v + \frac{1}{\sigma}\frac{\partial p}{\partial r} = 0 \qquad (2.9)$$

$$\text{entropy:} \quad \left(\frac{\partial}{\partial x} + v\frac{\partial}{\partial r}\right)\frac{p}{\sigma^\gamma} = 0$$

$$\text{shock conditions} \qquad v[x,S(x)] = \frac{2}{\gamma+1} S'(x)$$

$$p[x,S(x)] = \frac{2}{\gamma+1} S'^2(x) \qquad (2.10)$$

$$\sigma[x,S(x)] = \frac{\gamma+1}{\gamma-1}$$

and body surface condition

$$v[x,f(x)] = f'(x). \qquad (2.11)$$

The system of Eqs. (2.9), (2.10) and (2.11) constitutes a complete problem for the quantities $v(x,r)$, $\sigma(x,r)$ and $p(x,r)$ and are referred to as the limiting HSDT equations. The direct problem is the one with $f(x)$ given and $S(x)$ found together with the solutions, whereas the inverse problem deals with a prescribed shock shape and an unknown body shape.

As is well known, these equations of motion are exactly analogous to those describing the exact unsteady motion in a transverse plane. One significant feature of the HSDT equations is that the axial perturbation velocity $u(x,r)$ is uncoupled from other quantities, and thus the number of the differential equations in the system is reduced by one. The solution of $u(x,r)$ can be most conveniently obtained from the following energy integral in the limiting HSDT form:

$$u + \frac{1}{2} v^2 + \frac{\gamma}{\gamma - 1} \frac{p}{\sigma} = 0 \qquad (2.12)$$

after the solutions of $v(x,r)$, $p(x,r)$ and $\sigma(x,r)$ are obtained.

(2.1.2) Special Class of Similarity Solutions--Power-law Shocks.

The limiting HSDT equations obtained in the previous section exhibits significant simplification compared to the original set of equations, however, the nonlinearity is still associated with the system and the task of finding general solutions is still intractable. A class of similarity solutions associated with power-law shocks (and bodies) is well known to be admissible to the HSDT system. The set of partial differential equations is therefore reducible to an

equivalent set of ordinary differential equations for this special class of flow fields. The details of the formal deduction of similarity solutions is omitted here and the reader is referred to Mirels[6] or Sedov.[12] We only note here that for a class of bodies of the form $r \sim x^n$, associated shocks must also have the shapes $r \sim x^n$ so that both the shock surface and the body surface can be represented in terms of constant values of similarity variable r/x^n. Now, the body surface boundary condition (Eq. 2.11) shows that on the body surface,

$$v \sim x^{n-1}.$$

The shock wave conditions (Eqs. 2.10) further demand that

$$p \sim v^2$$

$$\sigma \sim 1$$

on the shock surface. Therefore, we see immediately that the representations of $p(x,r)$, $v(x,r)$ and $\sigma(x,r)$ for this class of similarity solutions must be

$$p(x,r) \sim x^{2(n-1)}\, \bar{P}(\bar{\eta}) \tag{2.13a}$$

$$v(x,r) \sim x^{n-1}\, \bar{V}(\bar{\eta}) \tag{2.13b}$$

$$\sigma(x,r) \sim \bar{R}(\bar{\eta}) \tag{2.13c}$$

where $\bar{\eta}$ is the basic similarity variable defined by

$$\bar{\eta} \equiv \frac{r}{x^n}\,. \tag{2.14}$$

In the following, one convenient form of the similarity formulation for the problem will be given with a prescribed shock wave

$$r = S(x) = x^n \ . \tag{2.15}$$

The body shape is represented by

$$r = f(x) = bx^n \tag{2.16}$$

where b, the body shape factor, is to be found.

With the shock wave shape given in Eqs. (2.15), the following boundary value problem is formulated using Eqs. (2.9), (2.10) and (2.11).

$$\begin{aligned} &\frac{\partial}{\partial x}(r\sigma) + \frac{\partial}{\partial r}(r\sigma v) = 0 \\ &\left(\frac{\partial}{\partial x} + v\frac{\partial}{\partial r}\right) v + \frac{1}{\sigma}\frac{\partial p}{\partial r} = 0 \\ &\left(\frac{\partial}{\partial x} + v\frac{\partial}{\partial r}\right)\frac{p}{\sigma^\gamma} = 0 \end{aligned} \tag{2.17}$$

$$\begin{aligned} v(x,x^n) &= \frac{2}{\gamma+1} n x^{n-1} \\ p(x,x^n) &= \frac{2}{\gamma+1} n^2 x^{2(n-1)} \\ \sigma(x,x^n) &= \frac{\gamma+1}{\gamma-1} \end{aligned} \tag{2.18}$$

and the body shape factor b is determined from

$$bnx^{n-1} = v(x,bx^n) \ . \tag{2.19}$$

It is convenient to express the equations of motion in terms of a stream function defined by

$$\begin{aligned} \Psi_r &= r\sigma \\ \Psi_x &= - r\sigma v \end{aligned} \tag{2.20}$$

so that the continuity equation is satisfied identically.

The transformation from the coordinate system (x,r) to the coordinate system (x,Ψ) is carried out by observing that

$$\frac{\partial}{\partial x} \to \frac{\partial}{\partial x} - r\sigma v \frac{\partial}{\partial \Psi}, \quad \frac{\partial}{\partial r} \to r\sigma \frac{\partial}{\partial \Psi} \tag{2.21}$$

so that the derivative along a streamline is

$$D \equiv \frac{\partial}{\partial x} + v \frac{\partial}{\partial r} \to \frac{\partial}{\partial x} .$$

Also, in the following, Physicist's notation will be used, i.e.,

$$f(x,r) = f(x,\Psi) .$$

In terms of the new independent variables, Eqs. (2.17) are rewritten as

$$\begin{aligned} \frac{1}{\sigma^2} \frac{\partial \sigma}{\partial x} + r \frac{\partial v}{\partial \Psi} + \frac{v}{r\sigma} &= 0 \\ \frac{\partial}{\partial x} v + r \frac{\partial p}{\partial \Psi} &= 0 \\ \frac{p}{\sigma^\gamma} &= \Phi(\Psi) . \end{aligned} \tag{2.22}$$

$\Phi(\Psi)$ is the entropy function which should be evaluated at the shock wave. The mapping of the shock wave from the (x,r) plane to the (x,Ψ) plane can be effected by using the following relation in the (x,r) plane:

$$\left.\frac{d\Psi}{dx}\right|_{s.w.} = \left.\frac{\partial\Psi}{\partial x}\right|_{s.w.} + \left.\frac{\partial\Psi}{\partial r}\right|_{s.w.} (nx^{n-1}) = (-r\sigma v)_{s.w.} + (r\sigma)_{s.w.}\, nx^{n-1} .$$

Therefore, we get

$$\left.\frac{d\Psi}{dx}\right|_{s.w.} = nx^{2n-1} \tag{2.23}$$

on using the shock conditions (2.18).

Equation (2.23) is readily integrated to give

$$\Psi(x,x^n) = \frac{1}{2}\, x^{2n} \tag{2.24}$$

because $\Psi(o,o) = 0$. This result could be derived directly from physical reasoning. The value of Ψ measures the mass flow between a stream surface and the axis.

The mapping of body surface is done similarly by noting that

$$\frac{d}{dx}\,\Psi\big|_{body} = (-r\sigma v)_{body} + (r\sigma)_{body}\,(bnx^{n-1})$$

from which it follows that

$$\frac{d\Psi}{dx} = 0 \tag{2.25}$$

on using the boundary condition (2.19). This merely verifies that the body surface is a stream surface.

Equation (2.25) is also readily integrated to give $\Psi(x,bx^n) = 0$ as expected. Therefore, in (x,Ψ) plane, the shock and the body are represented by

$$\Psi = \frac{1}{2} x^{2n} \qquad \text{shock}$$

and

$$\Psi = 0 \qquad \text{body}$$

respectively.

The function $\Phi(\Psi)$ can then be determined as follows:

$$\Phi(\Psi) = \tag{2.26}$$

$$\left.\frac{p}{\sigma^\gamma}\right|_{s.w.} = \left(\frac{\gamma - 1}{\gamma + 1}\right)^\gamma \frac{2}{\gamma + 1} n^2 x^{2(n-1)} = \frac{2}{\gamma + 1} \left(\frac{\gamma - 1}{\gamma + 1}\right)^\gamma n^2 (2\Psi)^{\frac{n-1}{n}}$$

in which the relation $\Psi_s = \frac{1}{2} x^{2n}$ has been used.

Let $r = \bar{G}(x,\Psi)$. Then we have

$$\left.\frac{\partial r}{\partial r}\right|_x = 1 = \sigma r \bar{G}_\Psi = \sigma \bar{G}\, \bar{G}_\Psi$$

and

$$\left.\frac{\partial r}{\partial x}\right|_r = 0 = \bar{G}_x - r\sigma v \bar{G}_\Psi = \bar{G}_x - \sigma v \bar{G}\, \bar{G}_\Psi \, .$$

Thus

$$\frac{1}{\sigma} = \bar{G}\,\bar{G}_{\Psi} \tag{2.27}$$

$$v = \bar{G}_{x} \tag{2.28}$$

Equation (2.28) states that the transverse component of the velocity is equal to the slope of the streamline which is also obvious physically. Substituting Eqs. (2.26), (2.27) and (2.28) into Eq. (2.22), we obtain the following system of equations for the unknowns $p(x,\Psi)$ and $\bar{G}(x,\Psi)$:

$$\begin{aligned} p^{-1/\gamma}\left[\frac{2}{\gamma+1}\,n^{2}(2\Psi)^{\frac{n-1}{n}}\right]^{1/\gamma}\frac{\gamma-1}{\gamma+1} &= \bar{G}\,\frac{\partial \bar{G}}{\partial \Psi} \\ \frac{\partial^{2}\bar{G}}{\partial x^{2}} + \bar{G}\,\frac{\partial p}{\partial \Psi} &= 0\ . \end{aligned} \tag{2.29}$$

The corresponding set of boundary conditions (2.18) is transformed accordingly as follows:

$$\bar{G}_{x}\left(x,\ \frac{1}{2}\,x^{2n}\right) = v_{s} = \frac{2}{\gamma+1}\,x^{n-1} \tag{2.30a}$$

Also

$$\bar{G}\left(x,\ \frac{1}{2}\,x^{2n}\right) = x^{n} \tag{2.30b}$$

and

$$\bar{G}(x,o) = bx^n \ . \tag{2.30c}$$

The shock condition on p remains the same, i.e.,

$$p\left(x, \frac{1}{2} x^{2n}\right) = \frac{2}{\gamma + 1} n^2 x^{2(n-1)} . \tag{2.30d}$$

Now, the results of the similarity discussion will be applied. First note that the basic similarity variable $\bar{\eta}$ is constant along the lines $r \sim x^n$. In (x,Ψ) plane, a corresponding similarity variable η can thus be defined as

$$\eta \equiv 2 \frac{\Psi}{x^{2n}} \tag{2.31}$$

because a typical similarity line in the (x,r) plane, e.g., the shock wave, $r = x^n$ is mapped to a line $\Psi = \frac{1}{2} x^{2n}$ in the (x,Ψ) plane.

Therefore, we write

$$p(x,\Psi) = \frac{2}{\gamma + 1} n^2 x^{2(n-1)} \ P(\eta) \tag{2.32}$$

$$\bar{G}(x,\Psi) = x^n G(\eta) \tag{2.33}$$

where $P(\eta)$ is equal to $p(x,\Psi)/p_s$.

The derivatives $\partial\bar{G}/\partial x$, $\partial\bar{G}/\partial\Psi$, $\partial p/\partial\Psi$ etc. are evaluated according to

$$\frac{\partial G}{\partial x} = nx^{n-1}\, G(\eta) + x^n \left(\frac{dG}{d\eta}\right) \eta_x$$

$$\frac{\partial G}{\partial \psi} = x^n \frac{dG}{d\eta}\, \eta_\psi$$

$$\frac{\partial p}{\partial \psi} = \frac{2}{\gamma+1}\, n^2 x^{2(n-1)} \frac{dP}{d\eta}\, \eta_\psi$$

where

$$\eta_x = -\, 2n \frac{\eta}{x}$$

$$\eta_\psi = \frac{2}{x^{2n}} \cdot$$

Equations (2.29) are thus transformed into

$$\left.\begin{aligned} G\, G' &= \frac{1}{2} \frac{\gamma - 1}{\gamma + 1} P^{-1/\gamma}\, \eta^{\frac{n-1}{n} \frac{1}{\gamma}} && (2.34a) \\ 4n\eta^2 G'' + 2\eta G' + (n-1)\, G + \frac{4}{\gamma+1}\, \eta G P' &= 0 && (2.34b) \end{aligned}\right\} 0 \le \eta \le 1$$

with the boundary conditions specified along the line $\eta = 1$ as

$$\left.\begin{aligned} G(1) &= 1 \\ P(1) &= 1 \end{aligned}\right\} \qquad (2.35)$$

and the body shape factor determined by

$$G(o) = b\ . \qquad (2.36)$$

Further elimination in the system (2.34) is possible by writing Eq. (2.34a) as

$$P(\eta) = \left(\frac{1}{2}\frac{\gamma - 1}{\gamma + 1}\right)^{\gamma} \eta^{\frac{n-1}{n}} (GG')^{-\gamma} \tag{2.37}$$

and substituting into (2.34b). The result is a second order nonlinear ordinary differential equation for $G(\eta)$:

$$G''(\eta) =$$

$$\frac{2\frac{\eta}{n}G' + \left(1 - \frac{1}{n}\right)G + \frac{4}{\gamma + 1}\left(\frac{1}{2}\frac{\gamma - 1}{\gamma + 1}\right)^{\gamma} \eta^{\frac{n-1}{n}} G^{(1-\gamma)}(G')^{-\gamma}\left(\frac{n - 1}{n}\frac{1}{\eta} - \gamma\frac{G'}{G}\right)}{\frac{4\gamma}{\gamma + 1}\left(\frac{1}{2}\frac{\gamma - 1}{\gamma + 1}\right)^{\gamma} \eta^{(n-1)/n} G^{(1-\gamma)} (G')^{-(\gamma+1)} - 4\eta^2}$$

$$0 \le \eta \le 1 \tag{2.38}$$

with the initial conditions

$$G(1) = 1 \ ,$$

$$G'(1) = \frac{1}{2}\frac{\gamma - 1}{\gamma + 1} \ . \tag{2.39}$$

Equations (2.38) and (2.39) constitute a complete problem for $G(\eta)$ and the flow quantities v, p, σ are all determined in terms of $G(\eta)$ as

$$v(x,\eta) = \bar{G}_x(x,\eta) = nx^{n-1}\left[G(\eta) - 2\eta G'(\eta)\right] \ ,$$

$$p(x,\eta) = \frac{2}{\gamma + 1} n^2 x^{2(n-1)} P(\eta) = \frac{2}{\gamma + 1} n^2 x^{2(n-1)} \left[\left(\frac{1}{2}\frac{\gamma - 1}{\gamma + 1}\right)^{\gamma} \eta^{\frac{n-1}{n}} (GG')^{-\gamma}\right] \ ,$$

$$\sigma(x,\eta) = \frac{1}{\bar{G}(x,\eta)\ \bar{G}_{\psi}(x,\eta)} = \frac{1}{2}\frac{1}{G(\eta)}\frac{1}{G'(\eta)} \ .$$

If $v(x,\eta)$, $p(x,\eta)$, $\sigma(x,\eta)$ are expressed as

$$v(x,\eta) = \frac{2}{\gamma + 1} n x^{n-1} V(\eta) ,$$

$$p(x,\eta) = \frac{2}{\gamma + 1} n^2 x^{2(n-1)} P(\eta) ,$$

$$\sigma(x,\eta) = \frac{\gamma + 1}{\gamma - 1} R(\eta) .$$

so that

$$V(\eta) = \frac{v(x,\eta)}{v_s} ,$$

$$P(\eta) = \frac{p(x,\eta)}{p_s} ,$$

$$R(\eta) = \frac{\sigma(x,\eta)}{\sigma_s} ,$$

then $V(\eta)$, $p(\eta)$ and $R(\eta)$ are determined by $G(\eta)$ as

$$V(\eta) = \frac{\gamma + 1}{2} [G(\eta) - 2\eta G'(\eta)] \qquad (2.40a)$$

$$P(\eta) = \left(\frac{1}{2} \frac{\gamma - 1}{\gamma + 1}\right)^{\gamma} \eta^{\frac{n-1}{n}} [G(\eta)G'(\eta)]^{-\gamma} \qquad (2.40b)$$

$$R(\eta) = \frac{1}{2} \frac{\gamma - 1}{\gamma + 1} \frac{1}{G(\eta)G'(\eta)} , \qquad (2.40c)$$

and the body shape factor b determined by Eq. (2.36).

One advantage of this formulation is that the location of the body surface ($\eta = 0$) which will be shown to be a singularity of the flow field for $n \neq 1$ involves explicitly the independent variable η only.

This fact facilitates somewhat the procedure of the numerical integration.

It is noted here that the above formulation is essentially the same as that adopted by Gersten and Nicolai.[8]

2.2. Behavior of the Solutions Near the Body Surface.

For the case $n \leq 1$, an extensive literature on the solutions of the problem exists (Refs. 6,7,8). Only the main results will be recapitulated here for the sake of comparison with the results for $n > 1$ to be obtained in this section. From forebody drag considerations it is concluded that physically realistic flow exists for $n \geq 2/(3 + j)$ where $j = o$ for two dimensional case and $j = 1$ for axisymmetric flow. The limiting case $n = 2/(3 + j)$ corresponds to constant forebody drag, i.e., the drag on the body is independent of the length of the body. Therefore it corresponds to a sudden release of a certain constant amount of energy at the body nose. Also $b = o$ everywhere except at the nose where it is undetermined. Physically, this flow pattern corresponds to that due to flow over a blunt nose followed by a circular cylindrical afterbody (in two dimensional flow, to the flow over a blunt-nosed flat plate). The density R is zero on the body surface for all realistic values of γ and $2/(3 + j) \leq n < 1$, while pressure P and velocity V are finite everywhere in the flow field.

In the following, a detailed analysis of the solutions near the surface ($\eta = 0$) is presented for axisymmetric flow, with special emphasis on $n > 1$.

The starting point is the equations (2.34). It is noticed that the system of equations is invariant under the following affine transformation: $\eta \to a\eta$, $G \to a^{(1/2)(1-1/n\gamma)} G$, $P \to aP$. Therefore the following set of invariant coordinates α,β is introduced.

$$\alpha = \frac{G}{\eta^{\frac{1}{2}\left(1 - \frac{1}{n\gamma}\right)}}, \qquad \beta = \frac{P}{\eta} \tag{2.41}$$

together with the auxiliary coordinates ξ,ζ defined by

$$\xi = \eta^{(1/2)(1+1/n\gamma)} \frac{dG}{d\eta}, \qquad \zeta = \frac{dP}{d\eta}. \tag{2.42}$$

Due to the invariant properties of the differential equations, the system is reducible to a single first order differential equation in (α,β) plane. The reduction is accomplished as follows: First, two mapping equations from Eqs. (2.41)

$$\frac{d\eta}{\eta} = \frac{d\alpha}{\xi - \frac{1}{2}\left(1 - \frac{1}{n\gamma}\right)\alpha} \tag{2.43}$$

$$\frac{d\eta}{\eta} = \frac{d\beta}{\zeta - \beta} \tag{2.44}$$

are obtained by directly differentiating the equations (2.41) with respect to η and using Eqs. (2.42).

With the aid of the above mapping formulas, the original differential equations (2.34) are written in terms of these new variables as follows:

$$4n\left\{\left[\xi - \frac{1}{2}\left(1 - \frac{1}{n\gamma}\right)\alpha\right]\frac{d\xi}{d\alpha} - \frac{1}{2}\left(1 + \frac{1}{n\gamma}\right)\xi\right\} + 2\xi + (n-1)\alpha + \frac{4}{\gamma+1}\, n\alpha\zeta = 0 \tag{2.45a}$$

$$\alpha\xi = \frac{1}{2}\,\frac{\gamma-1}{\gamma+1}\,\beta^{-1/\gamma}\,. \tag{2.45b}$$

The next step is to eliminate ξ and ζ in favor of α and β. Equation (2.45b) gives

$$\frac{d\xi}{d\alpha} = -\frac{1}{2}\,\frac{\gamma-1}{\gamma+1}\,\frac{\beta^{-1/\gamma}}{\alpha}\left(\alpha + \frac{1}{\gamma}\,\frac{1}{\beta}\,\frac{d\beta}{d\alpha}\right)\,. \tag{2.46}$$

Also combination of Eqs. (2.43) and (2.44) gives

$$\zeta = \beta + \frac{d\beta}{d\alpha}\left[\xi - \frac{1}{2}\left(1 - \frac{1}{n\gamma}\right)\alpha\right]$$

which on using (2.45b) yields

$$\zeta = \beta + \frac{d\beta}{d\alpha}\left[\frac{1}{2}\,\frac{\gamma-1}{\gamma+1}\,\beta^{-1/\gamma}\,\alpha^{-1} - \frac{1}{2}\left(1 - \frac{1}{n\gamma}\right)\alpha\right]\,. \tag{2.47}$$

Finally, the single differential equation in (α,β) plane is obtained as

$$\frac{d\beta}{d\alpha} =$$

$$\frac{\frac{\beta}{\alpha}\,\frac{\gamma-1}{\gamma+1} + \frac{2}{n\gamma}\,\alpha^2\beta^{1/\gamma} - \frac{1}{n}\,\alpha^2\beta^{1/\gamma} - \left(1 - \frac{1}{n}\right)\frac{\gamma+1}{\gamma-1}\,\alpha^4\beta^{2/\gamma} - \frac{4}{\gamma-1}\,\alpha^4\beta^{(2/\gamma)+1}}{-\frac{\gamma-1}{\gamma+1}\,\frac{1}{\gamma} + \frac{1}{\gamma}\left(1 - \frac{1}{n\gamma}\right)\alpha^2\beta^{1/\gamma} + \frac{2}{\gamma+1}\,\beta^{1+(1/\gamma)}\,\alpha^2 - \frac{2}{\gamma-1}\,\alpha^4\beta^{(2/\gamma)+1}} \tag{2.48}$$

after substituting Eqs. (2.46) and (2.47) into Eq. (2.45a) and rearranging terms. The boundary condition associated with Eq. (2.48) is easily obtained from the defining Eq. (2.41) and the boundary condition on P and G at shock $\eta = 1$. It is simply

$$\alpha = 1, \qquad \beta = 1 \ . \tag{2.49}$$

Actually, Eqs. (2.48) and (2.49) represent the complete solutions of the problem and qualitative discussions on the behavior of the solutions are possible through the study of integral curves in (α,β) plane, known as the phase plane. Since numerical results are essential to the work in this thesis, it seems preferable to integrate the original equations directly. However, the behavior of the solutions near the body surface can be deduced from these phase plane equations.

Let us first investigate the behavior of the equation (2.48) as $\alpha \to \infty$. It can be shown from Eq. (2.48) that the only self-consistent assumption on β is that

$$\beta \sim \alpha^{k_1} \tag{2.50a}$$

where

$$k_1 = \frac{2n\gamma}{n\gamma - 1} \ . \tag{2.50b}$$

Therefore, $\beta \to \infty$ for $n > 1$ because $\gamma > 1$.

Then the behavior of η as $\alpha \to \infty$ is similarly deduced from the following equation

$$\frac{d\alpha}{d\eta} = \frac{1}{2}\frac{1}{\eta}\left[\frac{\gamma - 1}{\gamma + 1}\,\alpha^{-\left(1+\frac{2n}{n\gamma-1}\right)} - \left(1 - \frac{1}{n\gamma}\right)\alpha\right] \tag{2.51}$$

which is obtained by eliminating ξ from Eq. (2.43) in favor of α, using Eq. (2.45b). It can also be shown from Eq. (2.51) that as $\alpha \to \infty$, the only self-consistent assumption on η is

$$\eta \sim \alpha^{k_2} \tag{2.52a}$$

where

$$k_2 = -\frac{2n\gamma}{n\gamma - 1} = -k_1 \,. \tag{2.52b}$$

It is then true that $\eta \to 0$ as $\alpha \to \infty$ for $n > 1$, and consequently that $\alpha = \infty$ corresponds to the body surface. Also obvious from Eq. (2.52) is the fact that

$$\lim_{\eta\to 0} G(\eta) = \lim_{\eta\to 0}\left[\alpha\,\eta^{(1/2)(1-1/n\gamma)}\right] = \text{finite} \,. \tag{2.53}$$

Thus, the body shape factor b is always finite for concave power-law shock flows.

The behavior of ξ as $\eta \to 0$ can also be deduced from Eq. (2.45b) as

$$\xi \sim \alpha^{-1}\beta^{-1/\gamma} \sim \alpha^{-\left(1+\frac{2n}{n\gamma-1}\right)} \sim \eta^{\frac{n\gamma+2n-1}{2n\gamma}} \tag{2.54}$$

from which the behavior of $G'(\eta)$ as $\eta \to 0$ is found from Eqs. (2.42) to be

$$G'(\eta) \sim \xi\eta^{-(1/2)(1+1/n\gamma)} = C_1\ \eta^{(n-1)/n\gamma} \to 0 \text{ for } n > 1 \qquad (2.55)$$

where C_1 is a constant.

Finally, the behavior of $P(\eta)$, $V(\eta)$ and $R(\eta)$ as $\eta \to 0$ is obtained, using Eqs. (2.53) and (2.55) together with Eqs. (2.40). The results show that both P and V are finite as $\eta \to 0$ whereas

$$R(\eta) = C_2\ \eta^{-(n-1)/n\gamma} \qquad (2.56)$$

where C_2 = constant and thus $R(\eta)$ tends to infinite at the surface for $n > 1$, in contrast to the result for $n < 1$. Note also that

$$\lim_{\eta\to 0}\left[G'R\right] = \frac{1}{2}\frac{\gamma+1}{\gamma-1}\frac{1}{G(o)} = \text{finite}\ . \qquad (2.57)$$

It is important to remark here that the pressure field is regular in the whole flow field so that the lift and drag forces on any stream surfaces should be finite, regardless of the singular density field.

2.3 Numerical Integration of the Differential Equations.

Equation (2.38) with the initial conditions Eqs. (2.39) was programmed and integrated numerically on IBM 7094 digital computer, using a fourth order Runge-Kutta method. The solutions of $P(\eta)$, $V(\eta)$ and $R(\eta)$ are obtained in terms of $G(\eta)$ through the use of Eqs. (2.40). The integration is started at $\eta = 1$ and continued toward $\eta = 0$. The

value of γ is fixed at 1.40 while the values of n ranges from 1 to 10. As the results presented in Fig. 2 shows, the flow field at n = 10 already approaches that of the exponential flow field (see Ref. 7) which is a limiting case of the power-law flow field; it does not seem necessary to go beyond n = 10.

Except for the case n = 1, the point $\eta = 0$ is a singularity of the differential equation and therefore integration can only be continued to a point close to $\eta = 0$. The step size $\Delta\eta$ used in the integration is usually 10^{-3} at the beginning and reduced to 2×10^{-4} for $\eta \leq 5\times10^{-2}$. Values of $G(\eta)$, $G'(\eta)$, $P(\eta)$, $V(\eta)$ and $R(\eta)$ are obtained for each value of η. Since we know from the local behavior analysis made in previous section that

$$G'(\eta) = C_1 \, \eta^{\frac{n-1}{n\gamma}} \tag{2.55}$$

as $\eta \to 0$, the numerical integration is stopped at some small positive η_e where $G'(\eta)$ is satisfactorily described by Eq. (2.55). More explicitly, the computation stops at $\eta = \eta_e$ when the neighboring points of η_e, called η_{e_1}, η_{e_2}, η_{e_3}, etc. have the property that the ratios $G'(\eta_{e_1})/\eta_{e_1}^{(n-1)/n\gamma}$, $G'(\eta_{e_2})/\eta_{e_2}^{(n-1)/n\gamma}$ and $G'(\eta_{e_3})/\eta_{e_3}^{(n-1)/n\gamma}$ are approximately equal to four significant digits. Values of η_e found in the present investigation are usually of the order of 10^{-4}.

Since G(o) is finite, we can integrate Eq. (2.55) to give

$$G(\eta) = b + \frac{C_1}{\frac{n-1}{n\gamma} + 1} \, \eta^{\left(\frac{n-1}{n\gamma} + 1\right)}. \tag{2.58}$$

Therefore, the body shape factor b is found to be

$$b = G(\eta_e) - \frac{C_1}{\frac{n-1}{n\gamma} + 1} \eta_e^{\left(\frac{n-1}{n\gamma} + 1\right)}. \qquad (2.58b)$$

Also the surface value of $P(\eta)$ can be obtained from Eq. (2.40b) as

$$p(o) = \left(\frac{1}{2}\frac{\gamma - 1}{\gamma + 1}\right)^{\gamma} (C_1 b)^{-\gamma} \qquad (2.59)$$

where C_1 is the constant obtained from the ratios $G'(\eta_{e_1})/\eta_{e_1}^{(n-1)/n\gamma}$ etc., and Eqs. (2.55) and (2.58) have been used. The surface value of $V(\eta)$ is simply

$$V(o) = \frac{\gamma + 1}{2} b \,. \qquad (2.60)$$

Finally, Eq. (2.56) should be used to describe the density field near the surface with C_2 determined in a way similar to C_1, and of course,

$$R(o) = \infty \qquad (\text{for } n > 1) \qquad (2.61)$$

It is noted here that for a fixed set of values (n,γ), the values of P, V and G are practically constant to no less than four decimal places when η falls below 10^{-3}. Therefore, for our purpose, the accuracy of the equations for surface values derived above is more than sufficient.

The numerical results are plotted in Figs. 2, 3, 4 and also tabulated in a familiar form with P, V and R as functions of G. Certain linear interpolation of the computer results is involved in the

conversion, but the accuracy of the results is believed to be unaffected due to the small step size $\Delta\eta$ used in the calculation. In the following chapters, the Physicist's notation will be used, i.e., we shall write

$$P(\eta) = P(G) \qquad \text{etc.}$$

unless otherwise stated.

III. Geometrical and Aerodynamic Properties of the Lifting Surface.

3.1 General Considerations.

A lifting surface is defined here as a stream surface, one side of which is used as the compression side of an actual wing. The lifting surface considered in this thesis is the stream surface generated by a sheet of streamlines which originate from a curve drawn on the slender axisymmetric shock surface of the form $r^* = \tau x^{*n}$ considered in Chapter 2. This curve is called the leading edge of the lifting surface. The segment of the basic shock wave downstream of the leading edge will therefore be attached to the lifting surface all along its leading edge. In the region bounded by this segment of the basic shock wave and the lifting surface, the original flow field will remain unchanged when the original axisymmetric power-law body $r^* = \tau_b x^{*n}$ is replaced by such a lifting surface, generally three dimensional. Therefore, the flow field is known in this region and the forces acting on that side of the lifting surface which faces the attached shock wave can be calculated using the solutions of the basic flow field. It is this shock-facing side of the surface that will be used as the lower surface of an actual wing. The calculation is exact with regard to the HSDT equations, although it is still asymptotic as far as the complete gasdynamic equations are concerned.

In the following, the geometry and aerodynamics of the lifting surface will be discussed in terms of a set of cylindrical coordinate system (x,r,ϕ) in which x and r denote the streamwise and transverse coordinates respectively as defined in Chapter 2, and ϕ denotes the

azimuthal angle. A related rectangular cartesian coordinate system (x,y,z) with its origin fixed at the nose of the basic shock wave will also be used for auxiliary purpose. The relation of the two system is given as follows (see Fig. 1):

$$\begin{aligned} x &= x \\ r^2 &= y^2 + z^2 \\ \phi &= \tan^{-1} \frac{z}{y} , \end{aligned} \tag{3.1}$$

and

$$\begin{aligned} \vec{\ell}_x &= \vec{i} \\ \vec{\ell}_r &= \vec{k} \sin \phi + \vec{j} \cos \phi \\ \vec{\ell}_\phi &= \vec{k} \cos \phi - \vec{j} \sin \phi \end{aligned} \tag{3.2}$$

where $(\vec{\ell}_x, \vec{\ell}_r, \vec{\ell}_\phi)$ and $(\vec{i}, \vec{j}, \vec{k})$ denote two sets of unit vectors associated with the cylindrical system and the cartesian system respectively. It should be recalled here that both systems refer to the so-called hypersonic coordinates in the sense that the lateral coordinates y,z in the cartesian system and r in the cylindrical system have been stretched by τ in accordance with the HSDT analysis.

The lifting surfaces investigated in the present thesis have these geometrical properties in common: (1) A plane of symmetry exists and is taken to be $\phi = o$, hence the leading edge and trailing edge are also symmetric with respect to $\phi = o$; (2) the trailing edge lies in the plane

$x = 1$ (henceforth referred to as the trailing edge plane) and joins the leading edge which lies on the basic shock wave at two points on the shock surface. Thus the closed curve formed by these edges is the boundary line of the surface; (3) the azimuthal dimension of the surface is such that $|\phi| \leq \frac{\pi}{2}$; and (4) no expansion region exists on the shock facing side of the lifting surface. Property (2) above is sufficient to assure a supersonic trailing edge so that the flow field upstream of the trailing edge will not be influenced by any downstream conditions; it also simplifies the calculations significantly. Property (4) is introduced to make sure that the calculation of the aerodynamic forces is indeed made on the high pressure side of the surface.

3.2 The Expression of the Stream Function.

In this section, an analytic expression of the stream function Ψ is derived for the axisymmetric flow field considered in Chapter 2. This forms the basis of the geometrical aspect of the problem and is consequently essential to the calculation of the aerodynamic forces on the lifting surface.

Recall from Eq. (2.33) that a stream function $\Psi(x,r)$ was defined as satisfying the continuity equation identically, i.e.,

$$\frac{\partial \Psi}{\partial x}(x,r) = -r\sigma v, \qquad \frac{\partial \Psi}{\partial r}(x,r) = r\sigma \tag{2.33}$$

Next we introduce the similarity properties of the flow.

If we follow the Physicist's convention and write $\Psi(x,r) = \Psi(x,G)$ etc., then on transforming the independent variables from (x,r) into (x,G), we have

$$\frac{\partial}{\partial x}\,\Psi(x,r) = \left(\frac{\partial}{\partial x} - n\,\frac{G}{x}\,\frac{\partial}{\partial G}\right)\Psi(x,G)$$

$$\frac{\partial}{\partial r}\,\Psi(x,r) = \frac{1}{x^n}\,\frac{\partial}{\partial G}\,\Psi(x,G)\ .$$

Also, using the similarity properties of the functions σ,v, we have

$$\sigma(x,r) = R(G) \tag{3.3a}$$

$$v(x,r) = \frac{2}{\gamma+1}\,nx^{n-1}\,V(G)\ . \tag{3.3b}$$

Therefore, Eqs. (2.33) become

$$\frac{1}{x^n}\,\frac{\partial}{\partial G}\,\Psi(x,G) = x^n GR(G) \tag{3.4a}$$

$$\left(\frac{\partial}{\partial x} - n\,\frac{G}{x}\,\frac{\partial}{\partial G}\right)\Psi(x,G) = -\,\frac{2}{\gamma+1}\,nx^{2n-1}\,GV(G)R(G)\ . \tag{3.4b}$$

To solve the system (3.4) for $\Psi(x,G)$, Eq. (3.4a) is first substituted into (3.4b) to yield

$$\frac{\partial}{\partial x}\,\Psi(x,G) = nx^{2n-1}\,GR\left(G - \frac{2}{\gamma+1}\,V\right)$$

which is immediately integrated along a similarity line G = constant to give

$$\Psi(x,G) = \frac{x^{2n}}{2}\,GR\left(G - \frac{2}{\gamma+1}\,V\right) + F(G) \tag{3.5}$$

where F(G) is an arbitrary function.

Differentiating Eq. (3.5) with respect to G and using Eq. (3.4a), we have an equation for F(G) as

$$F'(G) = -\frac{1}{2} x^{2n} \left[G^2 R' - \frac{2}{\gamma + 1} (RV + GR'V + GRV') \right] .$$

The original continuity equation (2.17a) in (x,G) coordinates takes the form

$$G^2 R' - \frac{2}{\gamma + 1} (RV + GR'V + GRV') = 0 \qquad (3.6)$$

after using the similarity representation (3.3) for σ and v.

Thus $F'(G) = 0$ and $F(G) = \text{const} = 0$ so that $\Psi(o,G) = 0$. Finally, the analytic representation of Ψ is obtained as

$$\Psi(x,r) = \frac{x^{2n}}{2} \frac{r}{x^n} R\left(\frac{r}{x^n}\right) \left[\frac{r}{x^n} - \frac{2}{\gamma + 1} V\left(\frac{r}{x^n}\right) \right] \qquad (3.7)$$

and a streamline in this flow field is represented by

$$\begin{cases} \Psi(x,r) = \frac{1}{2} r x^n R\left(\frac{r}{x^n}\right) \left[\frac{r}{x^n} - \frac{2}{\gamma + 1} V\left(\frac{r}{x^n}\right) \right] = \text{const.} \\ \phi = \text{const.} \end{cases} \qquad (3.8)$$

3.3. Geometry of the Lifting Surface.

It seems convenient for the purpose of discussion to divide the lifting surfaces into two types; (A) the surface contains a portion of the basic body surface $r = bx^n$; (B) the surface does not have any portion in common with the basic body surface.

The lifting surface can be determined either by prescribing its leading edge shape on the basic shock wave or by prescribing its trailing edge shape in the plane x = 1. These two methods will be discussed in the following.

3.3.1. Lifting Surface With Prescribed Leading Edge.

Suppose that the leading edge is prescribed on the shock surface as

$$\begin{cases} r = x^n \\ |\phi| = L(x) \le \frac{\pi}{2}, \qquad x_o \le x \le 1 \ , \end{cases} \tag{3.9}$$

so that it is symmetric with respect to $\phi = 0$. The condition $L(x_o) = 0$ for $x_o > 0$ is imposed on the function L(x) to assure the continuity of the leading edge curve at $x = x_o$. However $L(o) = 0$ is not necessary because $x = o$ represents only a point on the shock surface, i.e., the nose, hence continuity is implied if the leading edge goes through the nose. The significance of the non-negative constant x_o is that it serves to distinguish type A surface ($x_o = o$) from type B surface ($x_o > 0$). This will be discussed later in this section.

The streamline that penetrates the shock wave at the point $(x,r,\phi) = [x_*, x_*^n, \pm L(x_*)]$ on the leading edge has the following parametric representation in terms of the parameter x_*, according to Eq. (3.8):

$$\begin{cases} r x^n R\left(\frac{r}{x^n}\right)\left[\frac{r}{x^n} - \frac{2}{\gamma+1} V\left(\frac{r}{x^n}\right)\right] = x_*^{2n} R_s \left(1 - \frac{2}{\gamma+1} V_s\right) & (3.10a) \\ |\phi| = L(x_*) \qquad x_o \le x_* \le 1 \ . & (3.10b) \end{cases}$$

Equation (3.10a) can be solved explicitly for x_*, using $R_s = V_s = 1$, to give

$$x_* = \left[\frac{\gamma + 1}{\gamma - 1}\, r x^n\, R\left(\frac{r}{x^n} - \frac{2}{\gamma + 1}\, V\right)\right]^{1/2n} \tag{3.11}$$

Combining Eq. (3.11) with Eq. (3.10b), we get an analytic expression for the lifting surface:

$$\left\{\begin{array}{c} |\phi| = L(x_*) \\ \text{with } x_o \le x_*(x,r) = \left\{\dfrac{\gamma + 1}{\gamma - 1}\, r x^n\, R\left(\dfrac{r}{x^n}\right)\left[\dfrac{r}{x^n} - \dfrac{2}{\gamma + 1}\, V\left(\dfrac{r}{x^n}\right)\right]\right\}^{1/2n} \le 1. \end{array}\right. \tag{3.12}$$

The trailing edge of this surface is the intersection of this surface and the plane $x = 1$ and is hence easily found to have the following representation:

$$\left\{\begin{array}{c} x = 1 \\ |\phi| = L(r_*) \\ \text{with } x_o \le r_*(r) = \left\{\dfrac{\gamma + 1}{\gamma - 1}\, r R(r)\, \left[r - \dfrac{2}{\gamma + 1}\, V(r)\right]\right\}^{1/2n} \le 1; \end{array}\right. \tag{3.13}$$

the relation between the function x_* in Eq. (3.12) and the function r_* in Eq. (3.13) being that

$$x_*(1,r) \equiv r_*(r)\ . \tag{3.13a}$$

The boundary line of the lifting surface has thus been determined and some of its normal projections will be deduced below:

Projection onto the Trailing Edge Plane:

Elimination of x from Eq. (3.10) gives the leading edge projection:

$$|\phi| = L\left(r^{1/n}\right) . \tag{3.14}$$

Obviously, the trailing edge has its true shape in this plane.

Projection onto the Plane y = o: (Planform)

Elimination of y from Eq. (3.10) and conversion into the cartesian coordinates (using Eq. (3.1)) give the leading edge projection in terms of cartesian coordinates,

$$|z| = \left(x^{2n} - z^2\right)^{1/2} \tan\left[L(x)\right]$$

or equivalently

$$|z| = x^n \sin\left[L(x)\right] . \tag{3.15}$$

The trailing edge is projected as a segment of x = 1 in the x-z plane.

Projection onto the Plane z = o: (Elevation)

Elimination of z from Eq. (3.10) and conversion into the cartesian coordinates give the leading edge projection:

$$y \tan\left[L(x)\right] = \left(x^{2n} - y^2\right)^{1/2}$$

or equivalently

$$y = x^n \cos [L(x)] \ . \tag{3.16}$$

Again, the trailing edge projection is simply a segment of the straight line x = 1.

The equation of the center line of the lifting surface can also be obtained. Due to the assumed symmetry of the surface, this line is simply the streamline lying in the plane ϕ = o and originating from the point $(x,r,\phi) = (x_*, x_*^n, L(x_*))$ on the leading edge with $L(x_*)$ = o. Its equation in the plane ϕ = o (z = o) is implicitly given as [see Eq. (3.12)]

$$L\left\{\left[\frac{\gamma+1}{\gamma-1}\, y\, x^n\, R\left(\frac{y}{x^n}\right)\left(\frac{y}{x^n} - \frac{2}{\gamma+1}\, V\left(\frac{y}{x^n}\right)\right)\right]^{1/2n}\right\} = 0 \ , \tag{3.17}$$

because y = r in the plane ϕ = 0. A more convenient expression will be derived later in an example where an explicit form of L(x) is given.

It is noted here that the shapes of trailing edge and the center line serve to give some feeling of the transverse and longitudinal curvature respectively of the lifting surface.

Finally, it will be shown that the case $x_o = 0$ corresponds to type A surface whereas the case $x_o > 0$ corresponds to type B surface. This is done with a study of the equation of the trailing edge (3.13). First, it is observed that the parameter $r_*(r)$ defined in Eq. (3.13) has the property that $r_*(1) = 1$ and $r_*(b) = 0$ and is monotone in $0 \le r \le 1$ for all values of n considered in the thesis. The fact that $r_*(1) = 1$

can easily be shown by using the shock wave conditions on V and R. That $r_*(b) = 0$ is obvious for the case $n \leq 1$ where it has been shown that $R(b) = 0$ or finite and also $\left[r - \frac{2}{\gamma + 1} V(r)\right] = 0$ at $r = b$ due to the body surface condition of the original basic flow. For $n > 1$, it has been established (see section 2.2) that $R \to C_2 \eta^{-(n-1)/n\gamma}$ [Eq. (2.56)], $\frac{2}{\gamma + 1} V \to r - 2\eta C_1 \eta^{(n-1)/n\gamma}$ [Eqs. (2.40) and (2.55)] as $\eta \to 0$, hence $r_* \sim \eta^{1/2n} \to 0$ as $\eta \to 0$. Now consider

Case (i): $x_o > 0$: In this case $r_*(r)$ will not go to zero. Therefore in the plane $x = 1$, the trailing edge defined by Eq. (3.13) will be such that $r > b$ throughout. Consequently no point on the body surface ($r = b$) exists in the trailing edge. Since neither the leading edge nor the trailing edge contains any point on the surface of the basic body, the lifting surface must have no portion in common with the basic body surface. This conclusion is actually obvious from physical considerations. Note that Eq. (3.13) represents the complete trailing edge in this case, the two branches join continuously at a point $(r,\phi) = (r_o,0)$ where r_o is defined as $r_*(r_o) = x_o$.

Case (ii): $x_o = 0$: In this case $r_*(r)$ will range from zero to one, hence the trailing edge does intersect with the circle $r = b$ (the basic body surface). At the point of intersection $|\phi|$ takes on the value $L(o)$ which is not necessarily zero. Let $L(o) = \Phi_b$. Thus the two branches of the curve given by Eq. (3.13) end on the circle $r = b$ at the points (b,Φ_b) and $(b,-\Phi_b)$ respectively, and they mark the trace in the plane $x = 1$ of the streamlines originating from the points on

the two branches of the leading edge. The complete trailing edge must consist of a circular arc: $r = b$, $-\Phi_b \le \phi \le \Phi_b$ in addition to the curves given by Eq. (3.13). This segment of the circle represents a segment of the basic power-law body surface $r = bx^n$, "wet" by the streamlines originating from the nose ($x = o$). It can further be shown that the area of this segment of the basic body surface (measured by Φ_b) increases with increasing value of L(o) which is the angle extended by the two branches of leading edge at $x = o$. If $L(o) = o$, we have $\Phi_b = o$ and this part of the surface degenerates to a line, i.e., $\phi = o$, $r = bx^n$.

An example: Let the leading edge be prescribed as

$$r = x^n$$

$$\phi = \cos^{-1}\frac{C}{x^n} \equiv L(x) \le \frac{\pi}{2},\ 0 < C^{1/n} = x_o \le x \le 1\ .$$

The leading edge has constant elevation $y = C > 0$.

The equation of the lifting surface is then [see Eq. (3.12)]

$$|\phi| = \cos^{-1}\frac{C}{x_*^n}$$

$$C^{1/n} \le x_* = \left\{\frac{\gamma+1}{\gamma-1}\, rx^n\, R\left(\frac{r}{x^n}\right)\left[\frac{r}{x^n} - \frac{2}{\gamma+1}\, V\left(\frac{r}{x^n}\right)\right]\right\}^{1/2n} \le 1\ , \tag{3.18}$$

or simply

$$\cos\phi = C\left\{\frac{\gamma+1}{\gamma-1}\, rx^n\, R\left(\frac{r}{x^n}\right)\left[\frac{r}{x^n} - \frac{2}{\gamma+1}\, V\left(\frac{r}{x^n}\right)\right]\right\}^{-1/2} \tag{3.18a}$$

The trailing edge is described by [see Eq. (3.13)]

$$x = 1$$

$$|\phi| = \cos^{-1} \frac{C}{r_*^n} \tag{3.19}$$

$$\text{with } C^{1/n} \le r_* = \left\{ \frac{\gamma + 1}{\gamma - 1} rR(r) \left[r - \frac{2}{\gamma + 1} V(r) \right] \right\}^{1/2n} \le 1 ,$$

or simply

$$\begin{cases} x = 1 \\ \cos \phi = C \left\{ \dfrac{\gamma + 1}{\gamma - 1} rR(r) \left[r - \dfrac{2}{\gamma + 1} V(r) \right] \right\}^{-1/2}, \quad r_o \le r \le 1 \\ \text{where } r_o \text{ is defined by } \left\{ \dfrac{\gamma + 1}{\gamma - 1} r_o R(r_o) \left[r_o - \dfrac{2}{\gamma + 1} V(r_o) \right] \right\}^{1/2} = C . \end{cases} \tag{3.19a}$$

The planform is [Eq. (3.15)]

$$|z| = x^n \sin \cos^{-1} \frac{C}{x^n} = \left(x^{2n} - C^2 \right)^{1/2} , \tag{3.20}$$

bounded by $x = 1$.

The projection in the plane $z = 0$ takes the form [Eq. (3.16)]

$$y = C, \qquad 0 < x \le 1$$

as expected.

The boundary line of the surface when projected onto the trailing edge plane becomes the closed curve bounded by the trailing edge curve [Eq. (3.19a)] and $r \cos \phi = C$.

The center line of the lifting surface is [Eq. (3.17)]

$$\cos^{-1} \frac{C}{\left\{ \frac{\gamma+1}{\gamma-1} y x^n R\left(\frac{y}{x^n}\right)\left[\frac{y}{x^n} - \frac{2}{\gamma+1} V\left(\frac{y}{x^n}\right)\right]\right\}^{1/2}} = 0$$

or

$$C^2 = \frac{\gamma+1}{\gamma-1} \frac{y}{x^n} x^{2n} R\left(\frac{y}{x^n}\right)\left[\frac{y}{x^n} - \frac{2}{\gamma+1} V\left(\frac{y}{x^n}\right)\right] .$$

In view of the fact that functions R,V are tabulated as functions of $G\left(\equiv \frac{r}{x^n}\right)$, the practical computation of the above equation can be facilitated by using the following parametric representation

$$\begin{aligned} x &= \left\{ C^2 \frac{\gamma-1}{\gamma+1} \frac{1}{GR(G)\left[G - \frac{2}{\gamma+1} V(G)\right]} \right\}^{\frac{1}{2n}} \qquad r_o \le G \le 1 \\ y &= Gx^n = G\left\{ C^2 \frac{\gamma-1}{\gamma+1} \frac{1}{GR(G)\left[G - \frac{2}{\gamma+1} V(G)\right]} \right\}^{1/2} . \end{aligned} \tag{3.21}$$

Finally, it is obvious that in this example, $x_o = C^{1/n} > 0$ and hence the lifting surface belongs to type B.

3.3.2. Lifting Surface With Prescribed Trailing Edge.

Let the trailing edge of the lifting surface be prescribed in the plane x = 1 as

$$\begin{cases} |\phi| = \Phi(r) \\ x = 1 \end{cases} \tag{3.22}$$

where the function $\Phi(r)$ is defined as follows:

Type A: $\Phi(r)$ defined for $r\epsilon[1,b]$ with $\Phi(b) \equiv \Phi_b > 0$ (3.22a)

Type B: $\Phi(r)$ defined for $r\epsilon[1,r_o]$ with $r_o > b$ and $\Phi(r_o) = 0$. (3.22b)

Of course, for type A surface, the trailing edge is completed by a circular arc $r = b$ between $\phi = -\Phi_b$ and $\phi = \Phi_b$.

In this section, the geometry of the lifting surface will be discussed in terms of the trailing edge function $\Phi(r)$ in general. However, it is understood that the surface referred to in the following is the whole lifting surface excluding that portion which is in common with the basic power-law body $r = bx^n$, in the case of Type A surface, i.e., in the case $\Phi(b) > 0$.

Consider a streamline that leaves the trailing edge plane at a point on the trailing edge, $(x,r,\phi) \equiv [1,\tilde{r},\pm\Phi(\tilde{r})]$. Its equation is, according to Eq. (3.8)

$$\begin{cases} rx^n R\left(\dfrac{r}{x^n}\right)\left[\dfrac{r}{x^n} - \dfrac{2}{\gamma+1} V\left(\dfrac{r}{x^n}\right)\right] = \tilde{r}R(\tilde{r})\left[\tilde{r} - \dfrac{2}{\gamma+1} V(\tilde{r})\right] \\ |\phi| = \Phi(\tilde{r}) \ . \end{cases} \tag{3.23}$$

Considering $\tilde{r}$ as a parameter and letting it vary from one to r_o (or b), we have Eq. (3.23) as a parametric representation of the lifting surface.

The leading edge is the trace of the lifting surface on the basic shock surface $r = x^n$. Its equation is thus obtained as

$$\begin{cases} rx^n\, R\left(\dfrac{r}{x^n}\right)\left[\dfrac{r}{x^n} - \dfrac{2}{\gamma+1}\, V\left(\dfrac{r}{x^n}\right)\right] = \tilde{r}\, R(\tilde{r})\left[\tilde{r} - \dfrac{2}{\gamma+1}\, V(\tilde{r})\right] \\ |\phi| = \Phi(\tilde{r}) \\ r = x^n \end{cases}$$

Realizing that $\dfrac{r}{x^n}$, $R\left(\dfrac{r}{x^n}\right)$ and $V\left(\dfrac{r}{x^n}\right)$ on $r = x^n$ all take on the value of unity, we rewrite the above equation in a form which represents a parametrized curve on the shock surface $r = x^n$:

$$\begin{cases} x = \left\{\dfrac{\gamma+1}{\gamma-1}\, \tilde{r}\, R(\tilde{r})\left[\tilde{r} - \dfrac{2}{\gamma+1}\, V(\tilde{r})\right]\right\}^{1/2n} \\ |\phi| = \Phi(\tilde{r}) \\ r = x^n \ . \end{cases}$$

Now that the geometry of the surface and its boundary line is completed, a few projections will be given below:

Projection in the trailing edge plane (x = 1):

Elimination of x from Eq. (3.24) gives the leading edge projection as

$$\begin{cases} r = \left\{\dfrac{\gamma+1}{\gamma-1}\, \tilde{r}\, R(\tilde{r})\left[\tilde{r} - \dfrac{2}{\gamma+1}\, V(\tilde{r})\right]\right\}^{1/2} \\ |\phi| = \Phi(\tilde{r}) \ . \end{cases} \qquad (3.25)$$

The trailing edge has its true shape in this plane.

Projection in the plane y = o (planform)

Elimination of y from Eq. (3.24) and conversion into cartesian coordinates give the leading edge projection:

$$\begin{cases} x = \left\{ \dfrac{\gamma + 1}{\gamma - 1} \tilde{r} \, R(\tilde{r}) \left[\tilde{r} - \dfrac{2}{\gamma + 1} V(\tilde{r}) \right] \right\}^{1/2n} \\ |z| = x^n \sin \Phi(\tilde{r}) \ . \end{cases} \tag{3.26}$$

The trailing edge projects as x = 1 in this plane.

Projection in the plane z = o (Elevation)

Elimination of z from Eq. (3.24) gives the leading edge projection as

$$\begin{cases} x = \left\{ \dfrac{\gamma + 1}{\gamma - 1} \tilde{r} \, R(\tilde{r}) \left[\tilde{r} - \dfrac{2}{\gamma + 1} V(\tilde{r}) \right] \right\}^{1/2n} \\ y = x^n \cos \Phi(\tilde{r}) \ . \end{cases} \tag{3.27}$$

Again the trailing edge projection is x = 1 in this plane.

The equation of the center line of the lifting surface is obviously given by

$$\begin{cases} r = bx^n \\ \phi = 0 \end{cases}$$

for the type A surface, and according to Eq. (3.23),

$$x^{2n} \frac{y}{x^n} R\left(\frac{y}{x^n}\right) \left[\frac{y}{x^n} - \frac{2}{\gamma + 1} V\left(\frac{y}{x^n}\right) \right] = r_o R(r_o) \left[r_o - \frac{2}{\gamma + 1} V(r_o) \right]$$

with r_o defined by $\Phi(r_o) = 0$

for the type B surface. The equation above can further be parametrized as follows:

$$x = \left\{ \frac{r_o R(r_o)\left[r_o - \frac{2}{\gamma+1} V(r_o)\right]}{GR(G)\left[G - \frac{2}{\gamma+1} V(G)\right]} \right\}^{1/2n}$$

$$y = Gx^n = G\left\{ \frac{r_o R(r_o)\left[r_o - \frac{2}{\gamma+1} V(r_o)\right]}{GR(G)\left[G - \frac{2}{\gamma+1} V(G)\right]} \right\}^{1/2} \qquad r_o \le G \le 1 \qquad (3.28)$$

An Example: Let the trailing edge be prescribed as

$$\text{(i)} \quad \begin{cases} x = 1 \\ r\cos\phi = k_1 \end{cases} \qquad k_1 > b\ , \quad \text{Type A}$$

or

$$\text{(ii)} \quad \begin{cases} x = 1 \\ r\cos\phi = k_2 < b & \text{for } b \le r \le 1 \\ r = b & \text{for } |\phi| \in \left[-\cos^{-1}\frac{k_2}{b},\ \cos^{-1}\frac{k_2}{b}\right] \end{cases} \qquad \text{Type B}$$

where k_1, k_2 are constants so that the trailing edge is at constant elevation $y = k_1$ (or k_2). Evidently case (i) corresponds to type B surface and case (ii) to type A surface. For the purpose of illustration, only case (i) will be considered below.

We have

$$\Phi(r) \equiv \cos^{-1}\frac{k_1}{r}$$

The equation of the lifting surface takes the following parametric form [see Eq. (3.23)]

$$\begin{cases} rx^n R\left(\frac{r}{x^n}\right)\left[\frac{r}{x^n} - \frac{2}{\gamma+1} V\left(\frac{r}{x^n}\right)\right] = \tilde{r} R(\tilde{r}) \left[\tilde{r} - \frac{2}{\gamma+1} V(\tilde{r})\right] \\ \phi = \cos^{-1} \frac{k_1}{\tilde{r}} \, . \end{cases} \tag{3.29}$$

The leading edge representation is also parametrized as [see Eq. (3.24)]

$$\begin{aligned} x &= \left\{\frac{\gamma+1}{\gamma-1} \tilde{r} R(\tilde{r}) \left[\tilde{r} - \frac{2}{\gamma+1} V(\tilde{r})\right]\right\}^{1/2n} \\ \phi &= \cos^{-1} \frac{k_1}{\tilde{r}} \\ r &= x^n \, . \end{aligned}$$

The projection of the boundary line onto the trailing edge plane is a closed curve represented by

$$\begin{aligned} r &= \left\{\frac{\gamma+1}{\gamma-1} \tilde{r} R(\tilde{r}) \left[\tilde{r} - \frac{2}{\gamma+1} V(\tilde{r})\right]\right\}^{1/2} \\ \phi &= \cos^{-1} \frac{k_1}{\tilde{r}} \end{aligned} \tag{3.30}$$

and the real trailing edge.

The planform is [see Eq. (3.26)]

$$\begin{cases} x = \left\{\frac{\gamma+1}{\gamma-1} \tilde{r} R(\tilde{r}) \left[\tilde{r} - \frac{2}{\gamma+1} V(\tilde{r})\right]\right\}^{1/2n} \\ |z| = \frac{x^n}{\tilde{r}} \left(\tilde{r}^2 - k_1^2\right)^{1/2} \end{cases} \qquad k_1 \le \tilde{r} \le 1 \tag{3.31}$$

closed by the trailing edge projection $x = 1$.

The projection of the boundary line in the plane z = o is

$$\begin{cases} x = \left\{ \dfrac{\gamma+1}{\gamma-1}\,\tilde{f}\,R(\tilde{f})\left[\tilde{f} - \dfrac{2}{\gamma+1}\,V(\tilde{f})\right]\right\}^{1/2n} \\ y = \dfrac{x^n}{\tilde{f}}\,k_1 \end{cases} \qquad k_1 \le \tilde{f} \le 1 \qquad (3.32)$$

also joined by the segment of the straight line x = 1.

The equation of the center line of the surface is [see Eq. (3.28)]

$$x = \left\{ \frac{k_1 R(k_1)\left[k_1 - \dfrac{2}{\gamma+1}\,V(k_1)\right]}{GR(G)\left[G - \dfrac{2}{\gamma+1}\,V(G)\right]} \right\}^{1/2n}$$

$$y = G\left\{ \frac{k_1 R(k_1)\left[k_1 - \dfrac{2}{\gamma+1}\,V(k_1)\right]}{GR(G)\left[G - \dfrac{2}{\gamma+1}\,V(G)\right]} \right\}^{1/2} \qquad k_1 \le G \le 1 \qquad (3.33)$$

The analytical discussion of the geometry of the lifting surface presented above should be sufficient to illustrate the geometrical aspect of the surface. Further information can be obtained by properly using the equations derived above. It is seen that in a given basic flow field, i.e., for a given set of values of n and γ, a lifting surface is determined by specifying either the leading edge shape on the basic shock surface $r = x^n$ or the trailing edge in the plane x = 1. Graphical construction of the actual three dimensional surface can be done with the aid of the tabulated results of the flow field, using Eqs. (3.12) or (3.23). This will not be included in the present thesis.

3.4. Aerodynamic Forces on the Lifting Surface.

In this section, methods of evaluating the lift and drag forces on the shock-facing side of the lifting surface will be given. First a direct method is discussed. An indirect method is presented next by constructing a control volume. The results of this indirect method will be shown to be accessible to actual calculation. Original physical coordinates and flow variables are used in deriving the formulae and HSDT expansions introduced in Chapter 2 are used afterwards to get the leading terms. The order of magnitude of the error terms will thus become evident in the process.

3.4.1. Direct Method.

Let the lifting surface be denoted by Ω^*. Then the pressure force acting on the shock-facing side of it is the following integral over the lifting surface.

$$-\int_{\Omega^*}\int \vec{n}\, p^*\, ds^*$$

where $\vec{n}$ is the unit normal of the lifting surface directed away from the side on which the pressure acts. If we denote by L^*, D^* and T^* the lift force (acting in $(-\vec{j})$ direction), the drag force (acting in $\vec{i}$ direction) and the side thrust (acting in $\vec{k}$ direction), then we have

$$L^* = \int_{\Omega_y^*}\int p^*\, ds_y^*$$

$$D^* = -\int_{\Omega_{x^*}} \int p^* \, ds^*_{x^*}$$

$$T^* = -\int_{\Omega_{z^*}} \int p^* \, ds^*_{z^*}$$

in which $ds^*_{y^*}$ is the normal projection of ds^* onto the plan, i.e.,

$$ds^*_{y^*} = \vec{j} \cdot \vec{n} \, ds^*$$

and Ω_{y^*} is consequently the planform of the lifting surface. $ds^*_{x^*}$, Ω_{x^*} and $ds^*_{z^*}$, Ω_{z^*} are similarly defined.

Now, in the HSDT limit,

$$p^* = \tau^2 p + 0(\tau^4)$$

$$ds^*_{y^*} = \tau dxdz \text{ etc.}$$

Therefore, the lift force, for example, can be expressed as

$$L^* = \tau^3 \int_{\Omega_y} \int p \, dxdz + 0(\tau^5) \, .$$

Here p is a known function, i.e.,

$$p = \frac{2}{\gamma + 1} n^2 \, x^{2(n-1)} \, P\left(\frac{r}{x^n}\right)$$

but in order to calculate the leading term of L, the function $P\left(\frac{r}{x^n}\right)$ must be expressed as a function of (x,z), using the equation of the lifting surface

$$B(x,r,\phi) = 0$$

to eliminate $r = (y^2 + z^2)^{1/2}$ in favor of (x,z) and then carry out the integration over the planform.

As shown in the previous section, the function $B(x,r,\phi)$ is very implicit, hence the process of eliminating r from $P\left(\frac{r}{x^n}\right)$ would be extremely laborious. Therefore, the direct method is inconvenient for practical purpose, although it is applicable in principle.

3.4.2. Indirect Method.

Consider a fixed control volume bounded by a closed surface Σ^* in a flow field discussed in Chapter 2. Application of the laws of conservation of mass and momentum to the fluid inside this volume gives the following equations:

$$\iint_{\Sigma^*} \rho^* \vec{q}^* \cdot \vec{n}\, ds^* = 0 \tag{3.34}$$

$$\iint_{\Sigma^*} \vec{q}^* (\rho^* \vec{q}^* \cdot \vec{n}) + p^* \vec{n}\, ds^* = 0 \tag{3.35}$$

if the effect of body force is neglected.

Generalizing Woods'[5] idea, we choose a control volume with its bounding surface formed by these elements: (see Fig. 5)

(1) Ω^*: the lifting surface

(2) s_1^*: in plane x = 1, bounded by a segment of the trace of the basic shock wave and the complete trailing edge of the lifting surface.

(3) $s_2^* + s_3^*$: s_2^* is the normal projection of the lifting surface onto the plane $x^* = x_o$, which is perpendicular to the undisturbed streamlines and passing through the apex of the lifting surface; s_3^* is the normal projection of s_1^* onto the plane $x^* = x_o$ and is thus its true shape.

(4) s_4^*: A surface formed by the sheet of undisturbed streamlines which connect the boundary line of $s_2^* + s_3^*$ with the leading edge and the upper boundary of s_1^*, which is a segment of the trace of the basic shock wave in the trailing edge plane.

With elements of Σ^* so chosen, we have the following results:

On Ω^*: $\vec{q}^* \cdot \vec{n} = 0$, $\vec{n}$ = unit normal vector directed toward the pressure-acting side.

On $(s_2^* + s_3^*)$: $p^* = p_\infty$, $\rho = \rho_\infty$, $\vec{q}^* = U_\infty \vec{i}$, $\vec{n} = -\vec{i}$

On s_4^*: $p^* = p_\infty$, $\rho = \rho_\infty$, $\vec{q}^* = U_\infty \vec{i}$, $\vec{n} = \vec{\ell}_r$, $\vec{n} \cdot \vec{q}^* = 0$

On s_1^*: $\vec{n} = \vec{i}$.

Therefore Eqs. (3.34) and (3.35) become, respectively:

$$-\iint_{s_2^*+s_3^*} \rho_\infty U_\infty ds^* + \iint_{s_1^*} \rho^* \left(\vec{q}^* \cdot \vec{i}\right) ds^* = 0 \tag{3.36}$$

$$\iint_{s_1^*} \left[\rho^* \vec{q}^* \left(\vec{q}^* \cdot \vec{i}\right) + p^* \vec{i}\right] ds^* + \iint_{s_2^*+s_3^*} \left[- p_\infty \vec{i} - \rho_\infty U_\infty^2 \vec{i}\right] ds^*$$

$$+ \iint_{s_4^*} (p_\infty \vec{\ell}_r) ds^* + \iint_{\Omega^*} (p^* \vec{n}) ds^* = 0 \tag{3.37}$$

The last term in Eq. (3.37) is the pressure force exerted on the lifting surface by the fluid. We write

$$\iint_{\Omega^*} (p^* \vec{n}) ds^* = D^* \vec{i} - L^* \vec{j} + T^* \vec{k}$$

as in section 3.4.1 and remark again that the lift force L^* is taken in the negative $\vec{j}$ direction. Also, we consider $p_\infty = 0$. Then Eq. (3.37) becomes

$$D^* \vec{i} - L^* \vec{j} + T^* \vec{k} = \iint_{s_1^*} \left[U_\infty \rho^* \left(\vec{q}^* \cdot \vec{i} \right) \vec{i} - \rho^* \vec{q}^* \left(\vec{q}^* \cdot \vec{i} \right) - p^* \vec{i} \right] ds^*$$

after Eq. (3.36) has been used.

Notice from above that the aerodynamic forces are expressible in terms of integrals in the trailing edge plane.

Introducing the limiting HSDT expansions of Chapter 2 [Eq. (2.6)]

$$\frac{1}{U_\infty} \vec{q}^* = \left[1 + \tau^2 u + 0(\tau^4) \right] \vec{i} + \left[\tau v + 0(\tau^3) \right] \vec{\ell}_r$$

$$\frac{1}{\rho_\infty U_\infty^2} p^* = \tau^2 p + 0(\tau^4)$$

$$\frac{1}{\rho_\infty} \rho^* = \sigma + 0(\tau^2)$$

$$ds^* = r^* dr^* d\phi = \tau^2 r dr d\phi$$

we get

$$\frac{1}{\rho_\infty U_\infty^2}\left[D^*\vec{i} - L^*\vec{j} + T^*\vec{k}\right]$$

$$= \tau^2 \iint_{S_1} \left\{\sigma(1+\tau^2 u)\vec{i} - \sigma\left[(1+\tau^2 u)\vec{i} + \tau v\vec{\ell}_r\right](1+\tau^2 u) - \tau^2 p\vec{i}\right\} r\,dr\,d\phi$$

$$= \tau^2 \iint_{S_1} \left\{\left[\tau^2(-u\sigma - p) + O(\tau^4)\right]\vec{i} - \left[\sigma v\tau + O(\tau^3)\right]\vec{\ell}_r\right\} r\,dr\,d\phi \ .$$

Using the relation $\vec{\ell}_r = \vec{k}\sin\phi + \vec{j}\cos\phi$, we obtain the following formula

$$\frac{1}{\rho_\infty U_\infty^2} D^* = \tau^4 \iint_{S_1} (-u\sigma - p) r\,dr\,d\phi + O(\tau^6) \tag{3.38}$$

$$\frac{1}{\rho_\infty U_\infty^2} L^* = \tau^3 \iint_{S_1} \sigma v \cos\phi\ r\,dr\,d\phi + O(\tau^5) \tag{3.39}$$

$$\frac{1}{\rho_\infty U_\infty^2} T^* = \tau^3 \iint_{S_1} \sigma v \sin\phi\ r\,dr\,d\phi + O(\tau^5) \ . \tag{3.40}$$

The quantity u in Eq. (3.38) can be eliminated by using Eq. (2.12) to give

$$\frac{1}{\rho_\infty U_\infty^2} D^* = \tau^4 \iint_{S_1} \left(\frac{\sigma}{2} v^2 + \frac{1}{\gamma - 1} p\right) r\,dr\,d\phi \tag{3.38a}$$

Recall that we have

$$v(x,r) = \frac{2}{\gamma + 1} n x^{n-1} V\left(\frac{r}{x^n}\right)$$

$$p(x,r) = \frac{2}{\gamma + 1} n^2 x^{2(n-1)} P\left(\frac{r}{x^n}\right)$$

$$\sigma(x,r) = \frac{\gamma + 1}{\gamma - 1} R\left(\frac{r}{x^n}\right)$$

Thus, in s_1 where $x = 1$ the quantities v,p,σ are all functions of r alone and if we write

$$\frac{1}{\rho_\infty U_\infty^2} D^* = \tau^4(2D) + \tau^6(2D_1) + \ldots$$

$$\frac{1}{\rho_\infty U_\infty^2} L^* = \tau^3(2L) + \tau^5(2L_1) + \ldots$$

$$\frac{1}{\rho_\infty U_\infty^2} T^* = \tau^3(2T) + \tau^5(2T_1) + \ldots$$

then we get

$$2D = \frac{2}{\gamma + 1} n^2 \iint_{s_1} \left[\frac{R(r)}{\gamma - 1} V^2(r) + \frac{1}{\gamma - 1} P(r)\right] r dr d\phi$$

$$2L = \frac{2}{\gamma - 1} n \iint_{s_1} R(r)\, V(r) \cos\phi \; r dr d\phi$$

$$2T = \frac{2}{\gamma - 1} n \iint_{s_1} R(r)\, V(r) \sin\phi \; r dr d\phi \; .$$

Note that (2D), (2L) and (2T) are the leading terms of the dimensionless drag, lift and side thrust respectively and that they are all expressed as integrals in the trailing edge plane. The area s_1 is

bounded by the trailing edge curve and a segment of the basic shock wave and is hence symmetric with respect to $\phi = o$. If we first integrate along r = const. from $\phi = -\Phi(r)$ to $\phi = +\Phi(r)$ then the following results are obtained:

$$D = \frac{2n^2}{\gamma^2 - 1} \int_{r_a}^{1} (RV^2 + P)\, \Phi(r) r dr \tag{3.41}$$

$$L = \frac{2}{\gamma - 1} n \int_{r_a}^{1} RV \sin \Phi(r)\, r dr \tag{3.42}$$

$$T = 0 \tag{3.43}$$

where $|\phi| = \Phi(r)$ is the trailing edge equation which, in the case of type A surface, does not include the circular arc r = b. Also, $r_a = r_o > b$ with $\Phi(r_o) = o$ for a type B surface and $r_a = b$ for a type A surface.

In order to facilitate writing, the following notations are introduced

$$\mathcal{L}(r;n,\gamma) = \text{drag function} = \frac{2}{\gamma^2 - 1} n^2 (RV^2 + P) r \tag{3.44}$$

$$\mathcal{D}(r;n,\gamma) = \text{lift function} = \frac{2}{\gamma - 1} nRVr \tag{3.45}$$

so that

$$D = \int_{r_a}^{1} \mathcal{D}(r) \Phi(r) dr \tag{3.41a}$$

$$L = \int_{r_a}^{1} \mathcal{L}(r) \sin \Phi(r) dr. \tag{3.42a}$$

It is seen that the calculation of D and L involves only single integrations. Functions $\mathcal{D}(r;n,\gamma)$ and $\mathcal{L}(r;n,\gamma)$ are fixed functions of r for every given flow field and thus can be calculated once for all with given n and γ, using table 1. Once $\Phi(r)$ is specified, the evaluation of D and L is so simple that even hand calculation is practical. The advantage of this method over the previous one is thus evident.

It might appear that a difficulty exists for a type A surface with $n > 1$ because we have then $r_a = b$ and $\mathcal{L}, \mathcal{D}(b) = \infty$. However it will be shown below that this singularity is an integrable one. Consider the contribution to the lift from the elements between $r = r_\ell$ and $r = b$ where r_ℓ is slightly greater than b, and denote this local contribution by L_ℓ. Then,

$$L_\ell = \int_{b}^{r_\ell} \mathcal{L}(r) \sin \Phi(r) dr = \frac{2n}{\gamma - 1} \int_{o}^{\eta_\ell} G(\eta)\, R(\eta)\, V(\eta)\, \frac{dG}{d\eta} \sin \Phi \, d\eta$$

where η_ℓ is defined as $G(\eta_\ell) = r_\ell$ and again the Physicist's convention $R(G) = R(\eta)$ etc. has been used.

According to the analysis of the local behavior of the functions R, V, G, G' in section 2.2, we have

$$\lim_{\eta \to 0} \left[R(\eta)\, \frac{dG}{d\eta} \right] = \text{finite constant} \tag{3.43}$$

and also $V(\eta)$, $G(\eta)$ and $\sin \Phi$ are constants as $\eta \to 0$.

In the actual calculation, use must be made of the original computer results, that is, the table in which P, V, R and G′ are given as functions of η, and η_ℓ is so chosen that the product $\sin \Phi\ R(\eta_\ell)\ V(\eta_\ell)\ G(\eta_\ell)\ \frac{dG}{d\eta}(\eta_\ell) = \mathcal{L}_\ell$ = constant to four significant digits. Then

$$L_\ell = \left(\frac{2n}{\gamma - 1}\ \eta_\ell\right)\mathcal{L}_\ell = \text{finite constant.}$$

A similar procedure is used for D_ℓ where we have

$$D_\ell = \frac{2}{\gamma^2 - 1}\ n^2 \int_0^{\eta_\ell} (P + R(\eta)\ V^2)\frac{dG}{d\eta}\ \Phi\ d\eta = \frac{2}{\gamma^2 - 1}\ n^2\ \eta_\ell\ \mathcal{D}_\ell = \text{finite constant.}$$

In all cases considered in this thesis, L_ℓ and D_ℓ turn out to be only about 5 percent of the total L and D.

Therefore, we conclude that the lift and drag formulae (3.41), (3.42) give finite values for L and D even in the use of type A surface with $n > 1$. This fact is consistent with the physical reasoning that finite surface pressure should result in finite total forces.

In closing this chapter, the following remark will be made. The trailing edge function $\Phi(r)$ has been shown to play a decisive role in the whole analysis. It determines the geometry of the lifting surface on the one hand and absorbs the dependence of the aerodynamics upon the geometry of the lifting surface on the other. The distinction between the type A surface and the type B surface is also evident in the definition of the function $\Phi(r)$. If $\Phi(r)$ is defined for $b \le r \le 1$, the

surface belongs to type A; if it is defined for $b < r_o \leq r \leq 1$ with $\Phi(r_o) = o$, the surface belongs to type B.

In the next chapter, further investigation of the lifting surface will be based on the trailing edge function $\Phi(r)$.

IV. Optimum Shapes.

4.1. General Discussions.

It has been shown in the previous chapter that a rather wide class of three dimensional lifting surfaces can be constructed in a flow field associated with a slender axisymmetric power-law shock wave in limiting HSDT flows by specifying the trailing edge shape which in turn completely determines the aerodynamic properties of the surface. A practical question naturally arises as to the feasibility of obtaining, in a specific flow field, a particular surface which has optimum aerodynamic properties. Among all optimum shapes, the one giving minimum drag with fixed lift seems to be the most interesting and useful from a practical point of view. As revealed in the last section of the previous chapter, the expressions of lift and drag are given as

$$L^* = \tau^3 \int_{r_a}^{1} \mathcal{L}(r) \sin \bar{\Phi}(r) dr \tag{4.1}$$

$$D^* = \tau^4 \int_{r_a}^{1} \mathcal{D}(r) \bar{\Phi}(r) dr \tag{4.2}$$

They all involve the trailing edge shape function $\bar{\Phi}(r)$ and the thickness ratio τ, thus the questions can obviously be answered by seeking a solution to a certain variational problem to determine the function $\bar{\Phi}(r)$ and the associated value of τ which serve the purpose.

In this chapter, a variational problem will first be formulated under certain constraints. Then the solutions of Euler equations are discussed in details, the behavior of the solutions for different basic flow fields being noted and explored.

4.2. Constraints.

4.2.1. Isoperimetric Constraint.

Since a set of solutions $\Phi(r)$ and τ is sought which gives minimum D^* with a fixed L^*, the following isoperimetric constraint

$$\tau^3 \int_{r_a}^{1} \mathscr{L}(r) \sin \Phi(r) dr = \text{constant} \tag{4.3}$$

is imposed.

4.2.2. Differential Constraint.

It has been mentioned in Section (3.1) that the lifting surfaces considered in this thesis is of such a geometry that the side on which aerodynamic forces are calculated is completely the compression side, i.e., at positive angle of attack. It can be shown that this restriction of the surface geometry amounts to following constraint on the trailing edge shape (see Appendix I).

$$\frac{d\Phi(r)}{dr} \geq 0 \qquad r_a \leq r \leq 1 \tag{4.4}$$

This inequality constraint can be replaced by the following equality constraint if we introduce an auxiliary real function Q(r) such that

$$\frac{d\Phi(r)}{dr} - Q^2(r) = 0 \tag{4.4a}$$

4.3. The Role of the Function $A(r) \equiv \mathcal{D}(r)/\mathcal{L}(r)$.

The variational problem to be considered in this chapter is essentially that of determining the function $\Phi(r)$ which minimizes D^* and gives a specified value of L^* where D^* and L^* are given by Eqs. (4.1) and (4.2). The constraint that $\Phi'(r) \geq 0$, $r_a \leq r \leq 1$ brings out the significance of the function A(r) defined as

$$A(r) \equiv \frac{\mathcal{D}(r)}{\mathcal{L}(r)} = \frac{n}{\gamma + 1}\left(V + \frac{P}{RV}\right) \tag{4.5}$$

To see this, let us first consider very crudely the variational problem just stated. Following the usual method of the calculus of variations, we form the functional

$$\tilde{H}[\Phi(r)] = \int_{r_a}^{1} \left[\tau^4 \mathcal{D}(r)\ \Phi(r) - \lambda_1^* \tau^3 \mathcal{L}(r)\ \sin\ \Phi(r)\right] dr$$

If a solution exists at all, it must satisfy the Euler equation, namely,

$$\frac{\partial}{\partial \Phi}\left[\tau^4 \mathcal{D}(r)\ \Phi(r) - \lambda_1^* \tau^3 \mathcal{L}(r)\ \sin\ \Phi(r)\right] = 0$$

from which we obtain an equation for $\Phi(r)$ as

$$\cos \Phi(r) = \frac{\tau}{\lambda_1^*} \frac{\mathcal{D}(r)}{\mathcal{L}(r)} = \frac{\tau}{\lambda_1^*} A(r) \tag{4.6}$$

Note here that λ_1^* must be chosen to be positive in order to satisfy the condition $0 < \Phi(r) \leq \frac{\pi}{2}$, since $\mathcal{D}(r)$, $\mathcal{L}(r)$ and τ are all positive definite quantities.

From Eq. (4.6), we see that

$$\Phi'(r) = - \frac{\tau}{\lambda_1^*} \frac{A'(r)}{\sin \Phi(r)} \tag{4.7}$$

Equation (4.7) reveals the significance of the function $A(r)$. If $A'(r) \leq 0$ for $r_a \leq r \leq 1$, the solution $\Phi(r)$ given by Eq. (4.6) (to be referred to as the regular arc later) is compatible with the constraint $\Phi'(r) \geq 0$, although other conditions such as transversality conditions etc. still remain to be verified. However, if $A'(r) \leq 0$ is not true for $r_a \leq r \leq 1$, the regular arc solution violates the differential constraint and hence the introduction of this constraint into the basic formulation of the variational problem becomes inevitable.

It is obvious that $A(r)$ is a characteristic property of the basic flow field, therefore, we should expect that the optimum shapes will have basically different geometry for basically different flow fields. A detailed analytical study of the function $A(r)$ is impossible simply due to the impossibility of obtaining analytical solutions for a general flow field. However, the function $A'(r)$ (and of course, $A(r)$) can be studied analytically at the boundary points $r = 1$ and $r = b$ as

a function of the parameters n and γ, using the shock boundary values and the established behavior of the solutions near the basic body surface. The details of the calculation are presented in Appendix II and the results are seen plotted in Fig. 6 in a (n,γ) plane. It is noted that $A'(b)$ tends to $+\infty$ or $-\infty$ according as n is greater or less than unity, and is finite for $n = 1$, the result being true for all realistic values of γ. Nevertheless, the behavior of $A'(1)$ shows a substantial dependence on γ in addition to n. A boundary line exists in the region $n \geq 1$, across which $A'(1)$ changes signs. Therefore there is a finite domain in the (n,γ) plane in which $A'(1)A'(b) < 0$, i.e., the function $A(r)$ is not monotone. For the rest of the domain in the (n,γ) plane, the function $A(r)$ may be monotone. To fix the idea, we shall consider $\gamma = 1.40$. For this specific value of γ, the following observations can be made (see Fig. 6): (1). $A(r)$ may be a monotone increasing function of r for $n > 1.065$, because both $A'(b)$ and $A'(1)$ are positive; (2) $A(r)$ must at least have one maximum for $1.000 < n < 1.065$, because $A'(b) > 0$ while $A'(1) < 0$; (3) $A(r)$ may be monotone decreasing, because both $A'(1)$ and $A'(b)$ are negative. Notice that the above observations are inconclusive, owing to the fact that they are based merely on the behavior at the boundary points. Actual numerical calculations for $A(r)$ have been carried out for $n = 0.50, 0.65, 0.75, 1.00, 1.05, 1.50, 2.00, 3.00, 4.00$ at this fixed value of $\gamma = 1.40$. The results are also plotted in Fig. 7. They confirm the above conjectures. Based on the analytical dependence of the flow fields on the parameters n and γ, it seems justified to draw the following conclusions for $\gamma = 1.40$:

(i) $n > 1.065$: $A'(r) > 0$ and $A(r)$ bounded for $b \leq r \leq 1$;

(ii) $1.065 > n > 1$: $A'(r) \leq 0$ for $r_m \leq r \leq 1$;

$A'(r) > 0$ for $b \leq r < r_m$; and

$A(r)$ bounded for $b \leq r \leq 1$.

(iii) $n = 1$: $A'(r) < 0$ for $A(r)$ bounded for $b \leq r \leq 1$.

(iv) $\frac{1}{2} \leq n < 1$: $A'(r) < 0$ for $b \leq r \leq 1$, $A(b) = \infty$.

4.4. Optimum Shapes for $\frac{1}{2} \leq n < 1$, $\gamma = 1.40$.

It has been revealed in the previous section that $A'(r) < 0$ for $b \leq r \leq 1$ in this case, therefore the regular arc to be obtained can be used throughout and as a consequence, the introduction of the differential constraint $\Phi'(r) \geqslant 0$ becomes unnecessary.

We shall first state the variational problem as follows: The function $\Phi(r)$ and the parameter τ are to be determined which minimize the drag

$$D^* = \tau^4 \int_{r_o}^{1} \mathcal{D}(r) \quad \Phi(r)dr$$

under the isoperimetric constraint that the lift

$$L^* = \tau^3 \int_{r_o}^{1} \mathcal{L}(r) \sin \Phi(r)dr$$

is fixed.

The end conditions on $\Phi(r)$ are

$$\Phi(1) = \text{free}$$

$$\Phi(r_o) = 0$$

where r_o is free and $b \leq r_o < 1$.

Note that the derivative of the unknown function $\Phi(r)$ does not appear in the above variational problem and hence the Euler equation will be an algebraic equation instead of a differential equation. Therefore, the fact that end conditions are free is a necessary condition for the solution to exist.

Following the usual procedure of the indirect method of calculus of variations, we introduce a constant Lagrange multiplier λ_1^* and reduce the problem to that of minimizing the functional

$$H[\Phi,\tau] = \int_{r_o}^{1} \left[\tau^4 \mathcal{D}(r)\ \Phi(r) - \lambda_1^* \tau^3 \mathcal{L}(r)\ \sin\ \Phi(r)\right] dr \qquad (4.8)$$

under the constraint

$$\tau^3 \int_{r_o}^{1} \mathcal{L}(r)\ \sin\ \Phi(r) dr = L^* = \text{fixed} \qquad (4.9)$$

Since τ is a constant parameter, the usual method of differential calculus can be employed to yield the first equation:

$$\frac{\partial H}{\partial \tau} = 0: \quad \int_{r_o}^{1} \mathcal{D}(r)\Phi(r) dr = \frac{3}{4} \frac{\lambda_1^*}{\tau} \int_{r_o}^{1} \mathcal{L}(r)\ \sin\ \Phi(r) dr \qquad (4.10)$$

Then, we consider the first variation of the functional H, taking into account the variation of the end point r_o. We have from Eq. (4.8)

$$\delta H = \int_{r_o}^{1} \left[\tau^4 \mathcal{D}(r) - \lambda_1^* \tau^3 \mathcal{L}(r) \cos \Phi(r)\right] \delta\Phi dr$$

$$- \left[\tau^4 \mathcal{D}(r_o)\Phi(r_o) - \lambda_1^* \tau^3 \mathcal{L}(r_o) \sin \Phi(r_o)\right] \delta r_o = 0 \qquad (4.11)$$

Consider now a sub-class of the comparison arcs for which the variations of the end points vanish. If $\bar{\Phi}(r)$ is the solution of the original more general problem, it certainly has to be the solution of this restrictive problem. Therefore the above equation asserts the validity of the Euler equation, i.e.,

$$\mathcal{D}(r) = \frac{\lambda_1^*}{\tau} \mathcal{L}(r) \cos \Phi(r)$$

or

$$\cos \Phi(r) = \frac{1}{\lambda_1} A(r) \qquad (4.12)$$

where $\lambda_1 = \lambda_1^*/\tau$.

Then the tranversality condition follows from Eq. (4.11),

$$\tau^4 \mathcal{D}(r_o)\Phi(r_o) - \lambda_1^* \tau^3 \mathcal{L}(r_o) \sin \Phi(r_o) = 0 \qquad (4.11a)$$

Note that the Euler equation and the transversality condition actually can be obtained by applying the results of usual variational calculus directly (for example, see Ref. 13). The transversality condition in general serves to determine the value of r_o. However it is

important to note here that it is automatically satisfied in this case since $\Phi(r_o)$ vanishes (by the end condition) and $(\mathcal{D}(r_o), \mathcal{L}(r_o))$ are all finite for this range of n. This result is by no means trivial, because it allows the end coordinate to be determined by the solution after it is found. Were it not so, a solution might not exist at all.

Now the Eqs. (4.9), (4.10) and (4.12) form a complete system which determines the unknowns $\Phi(r)$, τ and λ_1^*.

To proceed, first rewrite Eq. (4.10) as

$$D = \frac{3}{4} \lambda_1 L \tag{4.13}$$

Then Eqs. (4.12) and (4.13) determine λ_1 in the following way. For a given basic flow field, A(r) is a known function. Thus, varying λ_1 gives a family of functions $\Phi(r)$ through Eq. (4.12) with r_o determined by $\Phi(r_o) = 0$. Note here that since $A(1) \leq A(r) < \infty$ for $b < r \leq 1$ in this range of n, there always exists such an r_o, $b < r_o < 1$ that $A(r_o) = \lambda_1$ (i.e., $\Phi(r_o) = 0$) for any value of λ_1 greater than A(1), however large. Each member $\Phi(r)$ gives a set of corresponding values of D and L and hence the ratio D/L. Therefore for a given flow field (i.e., given n) D/L can be found as a function of λ_1, and we write

$$\frac{D}{L} = T(\lambda_1)$$

This function $T(\lambda_1)$ must be found numerically using the solutions of the basic flow field to evaluate $\mathcal{L}(r)$ and $\mathcal{D}(r)$. The functions $T(\lambda_1)$ for n = 0.50, 0.65 and 0.75 have actually been established and plotted in Fig. 8. Then Eqs. (4.13) serves to single out the particular value

of λ_1, called λ_{1p}, and hence the corresponding values of L and D denoted by L_p and D_p by stating that $(\lambda_{1p}, T(\lambda_{1p})$ is the location of the intersection of the curve $D/L = T(\lambda_1)$ with the straight line $D/L = 3/4\ \lambda_1$, if the two do intersect, i.e.,

$$T(\lambda_{1p}) = \frac{3}{4}\lambda_{1p} \tag{4.14}$$

Equation (4.14) has been solved graphically (see Fig. 8) for n = 0.50, 0.65, 0.75 and it is found that intersections do occur. The results are approximately as follows:

$$\begin{aligned}
&n = 0.50: \quad \lambda_{1p} = 0.72, \quad L_p = 0.100, \quad D_p = 0.0536, \quad r_o = 0.878 \\
&n = 0.65: \quad \lambda_{1p} = 0.93, \quad L_p = 0.173, \quad D_p = 0.121, \quad r_o = 0.872 \\
&n = 0.75: \quad \lambda_{1p} = 1.04, \quad L_p = 0.223, \quad D_p = 0.173, \quad r_o = 0.881
\end{aligned} \tag{4.15}$$

Finally, Eq. (4.9) determines the value of τ associated with every specified value of L^* as

$$\tau_p = \left(\frac{L^*}{L_p}\right)^{1/3} \tag{4.16}$$

Now that the solution has been completed, it has to be checked if the necessary condition, known as Legendre condition, for the extremal to be a minimal is satisfied. This is done by studying the second variation of the functional H given by Eq. (4.8).

Following the line of reasoning used in deducing the Euler equation from the first variation of H, we again consider a subclass of the comparison arcs for which the variation of the end point vanishes. Therefore

$$\delta H = \int_{r_o}^{1} \left[\tau^4 \mathcal{D}(r) - \lambda_1^* \tau^3 \mathcal{L}(r) \cos \Phi(r)\right] \delta\Phi dr$$

Therefore,

$$\delta^2 H = \int_{r_o}^{1} \tau^4 \lambda_1 \mathcal{L}(r) \sin \Phi(r) (\delta\Phi)^2 dr$$

Along the extremal, $\tau = \tau_p$, $\lambda_1 = \lambda_{1p}$ and $\Phi(r) = \Phi_p(r) = \cos^{-1} 1/\lambda_{1p} A(r)$, therefore, along the extremal

$$\delta^2 H = \tau_p^4 \lambda_{1p} \int_{r_o}^{1} \mathcal{L}(r) \sin \Phi_p(r) (\delta\Phi)^2 dr \qquad (4.17)$$

Since the right hand side of Eq. (4.17) is positive definite, we conclude that $\delta^2 H > 0$ along the extremal. This shows that the extremal

$$\Phi_p(r) = \cos^{-1} \frac{A(r)}{\lambda_{1p}} \qquad (4.18)$$

satisfies the necessary condition for being a minimal.

Summarizing, we shall state that the optimum shapes for $\gamma = 1.40$ and $1/2 \leq n < 1$ have been determined. The trailing edge function $\Phi(r)$ is given by Eq. (4.18) and the optimum thickness ratio τ is given by Eq. (4.17). The associated minimum drag is

$$D^*_{min} = \tau_p^4 D_p \qquad (4.19)$$

Values of λ_{1p}, D_p and L_p for n = 0.50, 0.65 and 0.75 have been tabulated in Eq. (4.15).

Note that the optimum surfaces can be constructed based on $\bar{\Phi}_p(r)$ using the results established in Chapter 3. They all belong to type B surfaces for this range of n.

4.5. Optimum Shape for n = 1, γ = 1.40.

This is the cone field in limiting hypersonic small disturbance flow. As was noted before, $A'(r) < 0$ throughout and hence the differential constraint is again unnecessary. Therefore, the formulation together with the method of solution for this case is exactly the same as that for the case $1/2 \leq n < 1$. However, one distinction has to be borne in mind while carrying out the calculation. In contrast to the previous case, the function A(r) here is bounded on both ends, more explicitly, $A(1) = 0.8334 \leq A(r) \leq A(b) = 0.8422$. This fact causes the following complication in the analysis, namely, if the particular value of λ_{1p} found in the same way as in previous section is greater than A(b), then the regular arc will continue until it hits the body surface r = b but with $\bar{\Phi}(b) > 0$. As a consequence, $\bar{\Phi}(r_o) = 0$ is not satisfied by this regular arc and the transversality condition, Eq. (4.11a) is violated.

Following the same procedure outlined in the last section, a curve $D/L = T(\lambda_1)$ is first established for this case (see also Fig. 8) and the particular value λ_{1p} defined by Eq. (4.14) is then determined graphically. The results are approximately

$$\lambda_{1p} = 1.26, \qquad L_p = 0.325, \qquad D_p = 0.308, \qquad r_o = b \tag{4.20}$$

Notice that the regular arc given by

$$\phi = \Phi_p(r) = \cos^{-1} \frac{A(r)}{1.26} \tag{4.21}$$

ends on $r = b = 0.915$ beyond which the function $A(r)$ is no longer defined, but we have $\Phi_p(b) = \cos^{-1} 0.8422/1.26 = 0.815 > 0$. Therefore the difficulty noted above does arise.

This difficulty suggests the imposition of another inequality constraint

$$r - b \geq 0$$

into the formulation of the variational problem. If this is done formally, the Euler equations will lead to the result that the optimum trailing edge arc consists of two subcases, one being the regular arc and the other being the circular arc $r = b$ (to be referred to as the limiting arc later). A corner point thus exists and has to be taken care of by formal mathematics.

However, the following rather intuitive approach seems to be more direct in getting the same answer. The end point of the regular arc $(r,\phi) = (b, \Phi_p(b))$ can obviously be brought to the point $(r,\phi) = (b,o)$ by the limiting arc so that the complete trailing edge function satisfies the condition $\Phi(r_o) = 0$ and hence the transversality condition. Since the addition of this limiting arc to the trailing edge arc does not affect either the value of D^* or the value of L^*, the optimum

property originally associated with the regular arc still remains with this combined arc.

Therefore, the optimum shape of the trailing edge for this case is a regular arc given by Eq. (4.21) joined by a limiting arc $r = b$, $0 \le \phi \le 0.815$. Again, the optimum thickness ratio τ is (see Eqs. (4.16) and (4.20))

$$\tau_p = (L^*/0.325)^{1/3} \tag{4.22}$$

and the associated minimum drag is

$$D^*_{min} = 0.308\ \tau_p^4 \tag{4.23}$$

It is noted that the optimum surface belongs to type A.

4.6. Optimum Shapes for $n > 1$, $\gamma = 1.4$.

It is known that the function $A(r)$ is not monotone decreasing for this range of n, consequently, the introduction of the differential constraint $\Phi'(r) \ge 0$ is necessary. To facilitate the presentation, type A surfaces and type B surfaces will be discussed separately, that is, optimum type A surface and optimum type B surface will be discussed separately for this range of n.

4.6.1. Case $1 < n < 1.065$.

The function $A(r)$ for this case is such that $A'(r) < 0$ for $r_m < r \le 1$ and $A'(r) > 0$ for $b \le r < r_m$ with $A'(r_m) = 0$. Therefore, the regular arc is not allowed to be used for $r < r_m$ and another arc has to be joined to the regular one at $r = r_c$ with $r_c \ge r_m$. A corner point is thus expected.

(i) Type A surface:

The problem here is to find an arc $\phi = \Phi(r)$ running from the shock circle $r = 1$ to the body circle $r = b$, and the thickness parameter τ such that

$$D^* = \tau^4 \int_b^1 \mathcal{D}(r)\Phi(r)dr = \text{minimum}$$

with

$$L^* = \tau^3 \int_b^1 \mathcal{L}(r) \sin \Phi(r)dr = \text{given constant.}$$

The end conditions are

$$\Phi(1) = \text{free}$$
$$\Phi(b) = \text{free} \qquad (4.24)$$

Notice that the limits of integration here, unlike those of sections (4.4) and (4.5), are fixed.

To proceed formally, we follow the multiplier rule of the indirect method of calculus of variation by introducing a constant Lagrange multiplier λ_1^* and a variable Lagrange multiplier $\lambda_2^*(r)$ and form the following functional H

$$H[\Phi,Q;\tau] = \left(\int_b^{r_c} + \int_{r_c}^1\right)\Big\{\tau^4\mathcal{D}(r)\Phi(r) - \lambda_1^*\tau^3\mathcal{L}(r)\sin\Phi(r)$$
$$+ \lambda_2^*(r)\left[\Phi'(r) - Q^2(r)\right]\Big\}dr \qquad (4.25)$$

the integral being divided at $r = r_c$ to allow for the discontinuity of $\Phi'(r)$ at $r = r_c$.

The variational problem is then formulated as follows: "In the class of functions $\Phi(r)$ and $Q(r)$ and constants τ which satisfy the differential equation

$$\frac{d}{dr}\,\Phi(r) = Q^2(r) \tag{4.26}$$

and the condition

$$\tau^3 \int_b^1 \mathcal{L}(r)\,\sin\,\Phi(r)\,dr = L^* = \text{constant} \tag{4.27}$$

find that special set which minimizes the functional H given by Eq. (4.25), the end conditions being given by Eq. (4.24)."

The procedure for solution goes as follows. First, since τ is a constant parameter, the usual technique in differential calculus for finding an extremum may be applied, i.e., $\partial H/\partial\tau = 0$ which gives

$$\int_b^1 \mathcal{D}(r)\,\Phi(r)\,dr = \frac{3}{4}\,\frac{\lambda_1^*}{\tau}\int_b^1 \mathcal{L}(r)\,\sin\,\Phi(r)\,dr$$

or

$$D = \frac{3}{4}\,\lambda_1\,L \tag{4.28}$$

where λ_1 is, as before, defined as λ_1^*/τ and also the integral above need not be divided because only $\Phi(r)$ which is continuous appears.

The variation of H due to $\Phi(r)$ and $Q(r)$ is then calculated and set equal to zero.

$$\delta H = \left(\int_b^{r_c} + \int_{r_c}^{1}\right)\Big\{\tau^4 \mathcal{D}(r)\delta\Phi - \lambda_1^* \tau^3 \mathcal{L}(r) \cos \Phi(r)\delta\Phi$$

$$+ \lambda_2^*(r)\delta\Phi' - 2\lambda_2^*(r)Q(r)\delta Q\Big\}dr$$

Integrating the term associated with $\lambda_2^*(r)\delta\Phi'$ by parts and rearranging, we obtain

$$\delta H = \left(\int_b^{r_c} + \int_{r_c}^{1}\right)\Big[\tau^4 \mathcal{D}(r) - \lambda_1^* \tau^3 \mathcal{L}(r) \cos \Phi(r) - \lambda_2^{*\prime}(r)\Big]\delta\Phi dr$$

$$- 2\left(\int_b^{r_c} + \int_{r_c}^{1}\right) \lambda_2^*(r)Q(r)\delta Q dr + \Big[\lambda_2^*(r)\delta\Phi(r)\Big]_{r=b}^{r=1}$$

$$- \Big[\lambda_2^*(r)\delta\Phi(r)\Big]_{r=r_c^-}^{r=r_c^+} = 0 \qquad (4.29)$$

where as usual, $[f(x)]_{x=b}^{x=a}$ stands for $f(a) - f(b)$.

Now, consider a sub-class of the comparison arcs for which the variations of the coordinates of the end points and those of the corner point vanish and the variation of $Q(r)$, i.e., the variation of $\Phi'(r)$, vanish for $b \le r \le 1$. Since if $\Phi(r)$ is to be the solutions to the original more general variational problem it certainly must be the solution to this rather restrictive problem, we deduce the first Euler equation from Eq. (4.29), i.e.,

$$\tau^4 \mathcal{D}(r) - \lambda_1^* \tau^3 \mathcal{L}(r) \cos \Phi(r) - \lambda_2^{*\prime}(r) = 0 \qquad (4.30)$$

Using the same line of reasoning, we can deduce the second Euler equation as

$$\lambda_2^*(r) Q(r) = 0 \qquad (4.31)$$

Equations (4.26), (4.27), (4.28), (4.30) and (4.31) constitute a complete system from which the five unknowns $\Phi(r)$, $Q(r)$, τ, λ_1^* and $\lambda_2^*(r)$ can be determined.

Also deducible from the Eq. (4.29) are the usual transversality conditions

$$\lambda_2^*(1) = \lambda_2^*(b) = 0 \qquad (4.32)$$

and the corner conditions

$$\lambda_2^*(r_c^+) = \lambda_2^*(r_c^-) = 0 \qquad (4.33)$$

using the arbitrariness of $\Phi(r)$ at the ends and at the corner.

Equations (4.30) and (4.31) state that the solution arc may be composed of two subarcs, namely,

Regular arc: $\lambda_2^*(r) \equiv 0$, $\mathcal{D}(r) = \lambda_1 \mathcal{L}(r) \cos \Phi(r)$, $r_c \le r \le 1$ (4.34a)

and

Singular arc: $Q(r) = 0$, $\Phi = \Phi_c = \text{constant}$, $b \le r \le r_c$ (4.34b)

The task is first to determine the location of the corner point which marks the junction of the two arcs. This is done by integrating Eq. (4.30) along the singular arc $\Phi = \Phi_c$ = constant, using the fact that $\lambda_2^*(r_c) = \lambda_2^*(b) = 0$, and the result is

$$\lambda_2^*(r_c) = \int_b^{r_c} \tau^4 \left[\mathcal{D}(r) - \lambda_1 \mathcal{L}(r) \cos \Phi_c \right] dr = 0 \qquad (4.35)$$

Since the continuity of $\Phi(r)$ must be satisfied at the corner, Φ_c is determined from the regular arc, i.e.,

$$\cos \Phi_c = \frac{1}{\lambda_1} \quad \frac{\mathcal{D}(r_c)}{\mathcal{L}(r_c)} = \frac{1}{\lambda_1} A(r_c) \qquad (4.36)$$

Combining Eqs. (4.35) and (4.36), we obtain an equation which determines r_c,

$$\int_b^{r_c} \left[\mathcal{D}(r) - \frac{\mathcal{D}(r_c)}{\mathcal{L}(r_c)} \mathcal{L}(r) \right] dr = 0 \qquad (4.37)$$

Note that the corner point location depends on the basic flow field only and is independent of λ_1 and therefore independent of the specified value of lift.

The next step is to determine the shape of the regular arc, i.e., to single out the special value of λ_1 in Eq. (4.34a). This is done in much the same way as in Section 4.4. Rewrite Eqs. (4.28) and (4.34a) as

$$\Phi_c \int_b^{r_c} \mathcal{D}(r)\,dr + \int_{r_c}^{1} \mathcal{D}(r)\,\Phi(r)\,dr = \frac{3}{4}\,\lambda_1 \left\{ \sin \Phi_c \int_b^{r_c} \mathcal{L}(r)\,dr + \int_{r_c}^{1} \mathcal{L}(r)\,\sin \Phi(r)\,dr \right\} \tag{4.38}$$

$$\cos \Phi(r) = \frac{1}{\lambda_1}\,\frac{\mathcal{D}(r)}{\mathcal{L}(r)} \tag{4.39}$$

Specifying a value of λ_1 determines $\Phi(r)$ and hence $\Phi_c \equiv \Phi(r_c)$ through Eq. (4.39). This expression of $\Phi(r)$ is then substituted into Eq. (4.38) which in turn gives a value of λ_1. Therefore Eqs. (4.38) and (4.39) can, in principle, be solved simultaneously by iteration to yield the special value of λ_1, called λ_{1p}, and hence the regular arc and $\Phi(r_c)$ can be determined.

The complete solution arc is thus:

$$\phi = \Phi(r) = \cos^{-1} \frac{A(r)}{\lambda_{1p}} \qquad r_c \le r \le 1 \tag{4.40a}$$

and

$$\phi = \Phi_c \equiv \Phi(r_c) \qquad b \le r \le r_c \tag{4.40b}$$

with r_c determined by Eq. (4.37).

Using the solution arc above, L_p can be evaluated as

$$L_p = \sin \Phi_c \int_b^{r_c} \mathcal{L}(r)\,dr + \int_{r_c}^{1} \mathcal{L}(r) \sin \Phi(r)\,dr \qquad (4.41)$$

The optimum value of τ is then obtained from Eqs. (4.27) as

$$\tau_p = \left(L^*/L_p\right)^{1/3}$$

It should be mentioned here that the above is a general outline of the procedure for determining a possible solution. The value of r_c determined by Eq. (4.37) must be greater than or equal to r_m where $A'(r_m) = 0$. Also the combined solution arc Eq. (4.40) must be such that the Legendre condition is satisfied along each subarc. The last statement can be made more explicit by writing down the expression for the second variation of H. Using the arguments given in Section 4.4, we have

$$\delta^2 H = \int_b^1 \left[\lambda_1 \tau^4 \mathcal{L}(r) \sin \Phi(r)\right](\delta\Phi)^2 dr - 2\int_b^1 \lambda_2^*(r)(\delta Q)^2 dr$$

Since the integrand of the first integral is always positive along the combined arc, it will suffice to require that

$$\lambda_2^*(r) \leq 0 \qquad (4.42)$$

along the solution arc in order to fulfill the necessary requirement for the solution arc to be a minimal, namely, $\delta^2 H \geq 0$. Along regular arc, $\lambda_2^*(r) \equiv 0$, therefore the Legendre condition will be satisfied if

$$\int_b^r \left[\mathcal{D}(r') - \lambda_1 \mathcal{L}(r') \cos \Phi_c\right] dr' \leq 0$$

or equivalently

$$\int_{r_c}^r \left[\mathcal{D}(r') - \lambda_1 \mathcal{L}(r') \cos \Phi_c\right] dr' \leq 0$$

in view of Eq. (4.35).

Note that $\cos \Phi_c = 1/\lambda_1 \, A'(r_c)$, so that a simpler expression for the Legendre condition may be used, i.e.,

$$\int_{r_c}^r \mathcal{D}(r')dr' \leq A(r_c) \int_{r_c}^r \mathcal{L}(r')dr' \tag{4.43}$$

No numerical solutions for this case are included in this thesis.

(ii) Type B Surface.

The only difference in the formulation of this variational problem compared to that of the type A surface exists in the end point condition. The Euler equations are hence still the same. Therefore, we state that if the solution is to exist, it may still only be composed of two types of subarcs, namely, the regular arc starting from the shock circle and the singular arc which follows. However, the singular arc is radial and hence must run into the body circle because the possibility of joining it with another regular arc is ruled out due to the fact that for $r < r_c$, regular arcs are all incompatible with the constraint $\Phi'(r) \geq 0$. Therefore, the surface will not be of type B. We then arrive at the conclusion that optimum type B shape does not exist for this range of n.

4.6.2. Case $n > 1.065$.

This case is characterized by the fact that the regular arc is not allowed to be used at all because $A'(r) > 0$ for $b \leq r \leq 1$. The singular arc is therefore expected to prevail in $b \leq r \leq 1$. The formal analysis will be given below.

(i) Type A Surface.

The problem here is again to find an arc $\phi = \Phi(r)$ joining two circles $r = 1$ and $r = b$ and the thickness parameter τ such that

$$D^* = \tau^4 \int_b^1 \mathcal{D}(r)\,\Phi(r)\,dr = \text{minimum}$$

with

$$L^* = \tau^3 \int_b^1 \mathcal{L}(r) \sin \Phi(r)\,dr = \text{given constant.}$$

The end conditions are also of the free type

$$\Phi(1) = \text{free}$$

$$\Phi(b) = \text{free}$$

Following the procedure used in Section 4.6.1, a constant Lagrange multiplier λ_1^* and a variable Lagrange multiplier $\lambda_2^*(r)$ are introduced and the problem is reduced to that of finding a set of functions $\Phi(r)$, $Q(r)$ and the parameter τ which minimizes the functional H, where

$$H[\Phi,Q,\tau] = \int_b^1 \Big\{ \tau^4 \mathcal{D}(r)\Phi(r) - \lambda_1^* \tau^3 \mathcal{L}(r) \sin \Phi(r)$$

$$+ \lambda_2^*(r) \left[\Phi'(r) - Q^2(r) \right] \Big\} dr \qquad (4.44)$$

subject to the constraints

$$\tau^3 \int_b^1 \mathcal{L}(r) \sin \Phi(r) dr = L^* \qquad (4.45)$$

and

$$\frac{d}{dr} \Phi(r) = Q^2(r) \qquad (4.46)$$

The end conditions are $\Phi(1)$ = free, $\Phi(b)$ = free.

This problem is the same as that discussed in Section 4.6.1 except that the complication due to the corner point is removed. Therefore, the results obtained previously are directly applicable to this case with the corner conditions deleted. That is, we have the Euler equations

$$\tau^4 \mathcal{D}(r) - \lambda_1^* \tau^3 \mathcal{L}(r) \cos \Phi(r) - \lambda_2^{*\prime}(r) = 0 \qquad (4.47)$$

$$\lambda_2^*(r) Q(r) = 0 \qquad (4.48)$$

and the equation of $\partial H/\partial \tau = 0$, i.e.,

$$D = \frac{3}{4}\frac{\lambda_1^*}{\tau} L = \frac{3}{4}\lambda_1 L \tag{4.49}$$

The transversality conditions remain the same

$$\lambda_2^*(1) = \lambda_2^*(b) = 0 \tag{4.50}$$

Again, the system of Eqs. (4.45) through (4.49) together with the transversality conditions completely determines the solutions for $\Phi(r)$, $Q(r)$, λ_1^*, $\lambda_2^*(r)$ and τ.

Euler equations still assert that the solution arc may consist of two types of subarcs, namely, regular arc and singular arc. However, as was stated before, $A'(r) > 0$ for $b \le r \le 1$, thus the regular arc does not exist in this case. The Euler equations will be satisfied in this case by choosing

$$Q(r) \equiv 0 \qquad b \le r \le 1 \tag{4.51}$$

and

$$\lambda_2^{*\prime}(r) = \tau^4\left[\mathcal{D}(r) - \lambda_1 \mathcal{L}(r) \cos \Phi(r)\right] \tag{4.52}$$

Equation (4.51) when combined with Eq. (4.46) yields

$$\Phi(r) \equiv \Phi_c = \text{constant}. \tag{4.53}$$

Therefore, we have

$$\lambda_2^{*\prime}(r) = \tau^4\left[\mathcal{D}(r) - \lambda_1 \mathcal{L}(r) \cos \Phi_c\right] \tag{4.54}$$

Integrating (4.54) noting that $\lambda_2^*(b) = 0$, we obtain

$$\lambda_2^*(r) = \tau^4 \int_b^r \left[\mathcal{D}(r') - \lambda_1 \mathcal{L}(r') \cos \Phi_c \right] dr' \qquad (4.55)$$

Equations (4.55) furnishes one equation for determining λ_1 and Φ_c if we use the fact that $\lambda_2^*(1) = 0$, i.e.,

$$\int_b^1 \mathcal{D}(r)dr = \lambda_1 \cos \Phi_c \int_b^1 \mathcal{L}(r)dr$$

Writing

$$\int_b^1 \mathcal{D}(r)dr \equiv D_A \qquad (4.56)$$

$$\int_b^1 \mathcal{L}(r)dr \equiv L_A \qquad (4.57)$$

which are the properties of the basic flow field, we have

$$D_A = \left(\lambda_1 \cos \Phi_c\right) L_A \qquad (4.58)$$

Rewriting Eq. (4.49) as

$$\Phi_c \int_b^1 \mathcal{D}(r)dr = \frac{3}{4} \lambda_1 \sin \Phi_c \int_b^1 \mathcal{L}(r)dr$$

using the fact that $\Phi(r) \equiv \Phi_c$ = constant, we get another equation for determining Φ_c and λ_1, i.e.,

$$\Phi_c D_A = \frac{3}{4} \lambda_1 \sin \Phi_c L_A \tag{4.59}$$

Equations (4.58) and (4.59) give the results that

$$\Phi_c = \frac{3}{4} \tan \Phi_c \tag{4.60}$$

$$\lambda_1 \equiv \frac{\lambda_1^*}{\tau} = \frac{D_A}{L_A} \frac{1}{\cos \Phi_c} \tag{4.61}$$

It must be remarked that the result of Φ_c as shown in Eq. (4.60) is surprisingly simple. Since D_A and L_A drop out in this equation, Φ_c is independent of the property of the basic flow field and hence has the same value for all n in this range, i.e.,

$$\Phi_c = 0.846 = 48.5 \text{ deg} \tag{4.62}$$

Corresponding to this value of Φ_c, L can be calculated to be

$$L_p = \int_b^1 (\sin \Phi_c) \mathcal{L}(r) dr = 0.749 \, L_A$$

Equation (4.45) can then be used to determine the optimum value of τ.

$$\tau_p = \left(\frac{L^*}{0.749 \, L_A} \right)^{1/3} = 1.101 \left(\frac{L^*}{L_A} \right)^{1/3} \tag{4.63}$$

Values of L_A together with those of D_A for n = 1.5, 3.0, 6.0, 10.0 have been calculated numerically and the results are plotted in Fig. 9.

Now that a solution arc $\phi = \Phi_c$ has been found, the remaining task is to verify that along this arc, Legendre condition is satisfied. The second variation $\delta^2 H$ is given by Eq. (4.41).

$$\delta^2 H = \tau^4 \lambda_1 \int_b^1 \mathcal{L}(r) \sin \Phi(r) (\delta\Phi)^2 dr - 2 \int_b^1 \lambda_2^*(r) (\delta Q)^2 dr$$

Along the arc $\phi = \Phi_c$, $\tau = \tau_p$, $\lambda_1 = \lambda_{1p}$

$$\delta^2 H = \tau_p^4 \lambda_{1p} \sin \Phi_c \int_b^1 \mathcal{L}(r) (\delta\Phi)^2 dr - 2 \int_b^1 \lambda_2^*(r) (\delta Q)^2 dr$$

where $\lambda_2^*(r)$ is given by Eqs. (4.55) and (4.58).

Since the first term on the right hand side of the above equation is positive definite, $\delta^2 H > 0$ is satisfied if

$$\lambda_2^*(r) \leq 0 \qquad b \leq r \leq 1 \tag{4.64}$$

Now since

$$\lambda_2^*(r) = \tau_p^4 \int_b^r \left[\mathcal{D}(r') - \frac{D_A}{L_A} \mathcal{L}(r') \right] dr', \quad \lambda_2^*(1) = 0 \tag{4.65}$$

the quantity

$$\lambda_2(r) \equiv \int_b^r \left[\mathcal{D}(r') - \frac{D_A}{L_A} \mathcal{L}(r') \right] dr' \tag{4.66}$$

is required to be negative for $b \leq r \leq 1$.

Using the results of the flow field, $\lambda_2(r)$ as defined by Eq. (4.66) can be calculated numerically for each flow field, i.e., for each value of n. This has actually been done for n = 1.5, 3.0, 6.0, 10.0 and the results are plotted in Fig. 10. It is revealed in this figure that

$$\lambda_2(r) \leq 0 \qquad \text{for} \qquad b \leq r \leq 1$$

is actually satisfied. Since analytical dependence of $\lambda_2(r)$ on the parameter n is expected, it seems reasonable to draw the conclusion from the results for these typical values of n listed above that

$$\lambda_2(r) \leq 0, \qquad b \leq r \leq 1$$

holds for all n in this range. Therefore, the Legendre condition is satisfied by this arc $\phi = \Phi_c = 0.846$.

In concluding this section, we shall summarize the results obtained as follows: the optimum trailing edge is

$$\phi = \Phi_c = 0.846$$

for all values of n. However, the optimum value of τ is given by Eq. (4.63) which evidently varies with different basic flow fields. The associated minimum drag is

$$D^*_{min} = \tau_p^4 \, \Phi_c D_A \tag{4.67}$$

(ii). Type B Surface.

The formulation of this problem differs from that of the previous problem only in the end point conditions. Therefore the Euler equations

remain the same, consequently the optimum arc can only be the singular arc alone. However the singular arc is radial and must run into the body surface r = b. Therefore again the conclusion is reached that the optimum type B surface does not exist in this range of n.

4.7. Concluding Remark.

To conclude the discussion on optimum shapes, the geometrical aspects of the optimum surfaces are worked out for the range of n between 1/2 and 1, using the results obtained in this chapter and the methods given in the last chapter. These results are shown in Figs. 11 through 15.

Appendix I

Let the trailing edge of the lifting surface be represented by

$$\phi = \Phi(r)$$

$$x = 1$$

It is proposed to show in this appendix that the condition

$$\Phi'(r) \geq 0 \tag{a}$$

is both necessary and sufficient to insure that

$$\frac{d\phi}{dr} \geq 0$$

on the lifting surface at an arbitrary station $x = x^*$ where $0 \leq x_o \leq x_* \leq 1$.

That the condition is necessary is obvious because otherwise $d\phi/dr$ is negative at least at the trailing edge plane $x = 1$.

To show that it is also sufficient, we need to investigate the geometry of the lifting surface determined from the given trailing edge function $\Phi(r)$.

Let the curve

$$\phi = \Phi_p(r)$$

$$x = 1$$

represent the normal projection of the leading edge corresponding to the given trailing edge onto the plane $x = 1$.

Then from section 3.3.2 we have a parametric representation for the curve $\phi = \Phi_p(r)$ as

$$r = \left\{ \frac{\gamma + 1}{\gamma - 1} \tilde{r} \, R(\tilde{r}) \left[\tilde{r} - \frac{2}{\gamma + 1} V(\tilde{r}) \right] \right\}^{1/2} \tag{b}$$

$$\phi = \Phi(\tilde{r}) = \Phi_p(r) \tag{c}$$

Now, it is obvious that the occurrence of

$$\frac{d\phi}{dr} < 0$$

at a certain station $x = x_*$ means that $\Phi_p(r) < \Phi(r)$ for some r between b and 1. Therefore, to rule out this possibility we must have

$$\Phi_p(r) \geq \Phi(r) \tag{d}$$

where equality holds only at r = 1.

Numerical evidence shows that in Eq. (b)

$$\tilde{r} \geq r \tag{e}$$

for all $n \geq 1/2$, equality holding only at $\tilde{r} = b$ and $\tilde{r} = 1$.

Since Eq. (d) requires that

$$\Phi(\tilde{r}) \geq \Phi(r)$$

we conclude that the function $\Phi(r)$ must be such that

$$\Phi'(r) \geq 0$$

in view of Eq. (e). That is, Φ must be a monotone increasing function of r.

Appendix II

Recall that the function A(r) was defined as

$$A(r) \equiv \frac{\mathcal{D}(r)}{\mathcal{L}(r)} = \tilde{A}(G)\Big|_{x=1} \tag{a}$$

where

$$\tilde{A}(G) = \frac{n}{\gamma + 1}\left[V(G) + \frac{P}{RV}(G)\right] \tag{b}$$

and

$$G \equiv \frac{r}{x^n} \tag{c}$$

Therefore, it follows that

$$\frac{dA}{dr} = \frac{d\tilde{A}}{dG}\bigg|_{x=1}$$

and

$$\frac{dA}{dr}\bigg|_{r=1} = \frac{d\tilde{A}}{dG}\bigg|_{G=1}, \qquad \frac{dA}{dr}\bigg|_{r=b} = \frac{d\tilde{A}}{dG}\bigg|_{G=b} \tag{d}$$

To study the behavior of $\frac{dA}{dr}\Big|_{r=1}$ and $\frac{dA}{dr}\Big|_{r=b}$, it therefore suffices to study $\frac{d\tilde{A}}{dG}\Big|_{G=1}$ and $\frac{d\tilde{A}}{dG}\Big|_{G=b}$ respectively.

It is convenient to go back to the original independent variable η used in the solution of the basic flow fields for this purpose. We will write

$$\tilde{A}(G) = \tilde{A}(G(\eta)) = \frac{n}{\gamma + 1}\left[V(\eta) + \frac{P}{RV}(\eta)\right]$$

where physicist's notation is being used again. Then

$$\frac{d\tilde{A}}{dG} = \left(\frac{d\tilde{A}}{d\eta}\right)\Big/\left(\frac{dG}{d\eta}\right) \tag{f}$$

Let us calculate $d\tilde{A}/d\eta$. From Eq. (e), we have

$$\frac{d\tilde{A}}{d\eta} = \frac{n}{\gamma + 1}\left\{V' + \frac{P}{RV}\left(\frac{P'}{P} - \frac{R'}{R} - \frac{V'}{V}\right)\right\}$$

Using Eqs. (2.53), we obtain $P'(\eta)$, $V'(\eta)$ and $R'(\eta)$ as follows

$$\frac{P'}{P} = \frac{d}{d\eta}\log P = \frac{n - 1}{n}\frac{1}{\eta} - \gamma\frac{G'}{G} - \gamma\frac{G''}{G'}$$

$$\frac{V'}{V} = \frac{d}{d\eta}\log V = -\frac{G' + 2\eta G''}{G - 2\eta G'}$$

$$\frac{R'}{R} = \frac{d}{d\eta}\log R = -\left[\frac{G'}{G} + \frac{G''}{G'}\right]$$

(i) Consider $\left.\frac{d\tilde{A}}{d\eta}\right|_{\eta=1}$:

$$\frac{d\tilde{A}}{d\eta}(1) = \frac{n}{\gamma + 1}\left\{V'(1) + \frac{P(1)}{R(1)V(1)}\left[\frac{P'}{P}(1) - \frac{R'}{R}(1) - \frac{V'}{V}(1)\right]\right\}$$

The boundary conditions $G(1) = 1$ and $G'(1) = \frac{1}{2}\frac{\gamma - 1}{\gamma + 1}$ enable us to calculate $G''(1)$ through Eq. (2.51). The result is

$$G''(1) = \frac{1}{4}\frac{\gamma - 1}{(\gamma + 1)^2}\left(-\frac{6}{n} + \frac{-\gamma^2 + 8\gamma + 5}{\gamma + 1}\right)$$

Therefore, we have

$$\frac{P'}{P}(1) = \frac{1}{\gamma+1}\left(\frac{2\gamma-1}{n} + \frac{1-3\gamma^2}{\gamma+1}\right)$$

$$\frac{V'}{V}(1) = -\frac{\gamma-1}{2(\gamma+1)}\left(-\frac{3}{n} + \frac{5\gamma+3}{\gamma+1}\right)$$

$$\frac{R'}{R}(1) = -\frac{1}{\gamma+1}\left(-\frac{3}{n} + 2\,\frac{2\gamma+1}{\gamma+1}\right)$$

Finally, on using P(1) = V(1) = R(1) = 1. We have

$$\frac{d\tilde{A}}{d\eta}(1) = \frac{1}{(\gamma+1)^3}\left[2(\gamma-2)(\gamma+1) + n(-3\gamma^2+4\gamma+3)\right]$$

and hence

$$\left.\frac{d\tilde{A}}{dG}\right|_{G=1} = \frac{2}{(\gamma-1)(\gamma+1)^2}\left[2(\gamma-2)(\gamma+1) + n(-3\gamma^2+4\gamma+3)\right]$$

in view of Eq. (f).

Therefore, we conclude that

$$\left.\frac{dA}{dr}\right|_{r=1} \gtrless 0 \quad \text{if} \quad 2(\gamma-2)(\gamma+1) + n(-3\gamma^2+4\gamma+3) \gtrless 0$$

and the boundary line, i.e., $\left.\frac{dA}{dr}\right|_{r=1} = 0$, is thus

$$2(\gamma-2)(\gamma+1) + n(-3\gamma^2+4\gamma+3) = 0$$

which is drawn in Fig. 6 in a (n,γ) plane.

(ii) Consider $\frac{d\tilde{A}}{d\eta}$ as $\eta \to 0$:

We know that

$$G \to b, \qquad G' \to C_1 \eta^{\frac{n-1}{n\gamma}} \quad (C_1 > 0), \quad \text{as} \quad \eta \to 0$$

Thus

$$G''(\eta) \sim \frac{\frac{4}{\gamma+1}\left(\frac{1}{2}\frac{\gamma-1}{\gamma+1}\right)^{\gamma} b^{1-\gamma} \frac{1}{\eta} \frac{n-1}{n} C_1^{-\gamma}}{\frac{4\gamma}{\gamma+1}\left(\frac{1}{2}\frac{\gamma-1}{\gamma+1}\right)^{\gamma} b^{1-\gamma} C_1^{-(\gamma+1)} \eta^{-\frac{n-1}{n\gamma}}} = \frac{n-1}{n\gamma} C_1 \eta^{-1+\frac{n-1}{n\gamma}}$$

Therefore,

$$\frac{P'}{P} \sim \frac{n-1}{n}\frac{1}{\eta} - \gamma C_1 \frac{\eta^{\frac{n-1}{n\gamma}}}{b} - \gamma \frac{n-1}{n\gamma}\frac{1}{\eta} \sim \gamma \frac{C_1}{b} \eta^{\frac{n-1}{n\gamma}}$$

$$\frac{V'}{V} \sim -\left(\frac{C_1}{b} \eta^{\frac{n-1}{n\gamma}} + 2\eta \frac{C_1^{\frac{n-1}{n\gamma}}}{b} \eta^{\frac{n-1}{n\gamma}} - 1\right) = -\eta^{\frac{n-1}{n\gamma}} \frac{C_1}{b}\left(1 + 2\frac{n-1}{n\gamma}\right)$$

$$\frac{R'}{R} \sim -\frac{n-1}{n\gamma}\frac{1}{\eta}$$

and hence $\left|\frac{R'}{R}\right| \gg \left|\frac{V'}{V}\right|, \left|\frac{P'}{P}\right|$ as $\eta \to 0$.

Also,

$$V \to \frac{\gamma+1}{2} b$$

$$R \to \frac{1}{2}\frac{\gamma-1}{\gamma+1}\frac{1}{b}\frac{1}{C_1} \eta^{-\frac{n-1}{n\gamma}}$$

$$P \to \left(\frac{1}{2}\frac{\gamma - 1}{\gamma + 1}\right)^{\gamma} (C_1 b)^{-\gamma}$$

Thus,

$$\lim_{\eta \to 0} \left[\left(\frac{P}{RV}\right)\frac{R'}{R}\right] = O\left(\eta^{\frac{n-1}{n\gamma} - 1}\right) \gg \lim_{\eta \to 0} V'(\eta) = O\left(\eta^{\frac{n-1}{n\gamma}}\right)$$

Therefore,

$$\lim_{\eta \to 0} \frac{d\tilde{A}}{d\eta} \sim \frac{n - 1}{\gamma(\gamma + 1)} \eta^{\frac{n-1}{n\gamma}}$$

and

$$\lim_{G \to 0} \frac{d\tilde{A}}{dG} = \lim_{\eta \to 0} \left[\left(\frac{d\tilde{A}}{d\eta}\right) \Big/ \left(\frac{dG}{d\eta}\right)\right] \sim \frac{n - 1}{\gamma(\gamma + 1)} \frac{1}{\eta}$$

Therefore, we conclude that

$$\frac{dA}{dr}(b) = \begin{array}{ll} + \infty & \text{if } n > 1 \\ - \infty & \text{if } n < 1 \end{array}$$

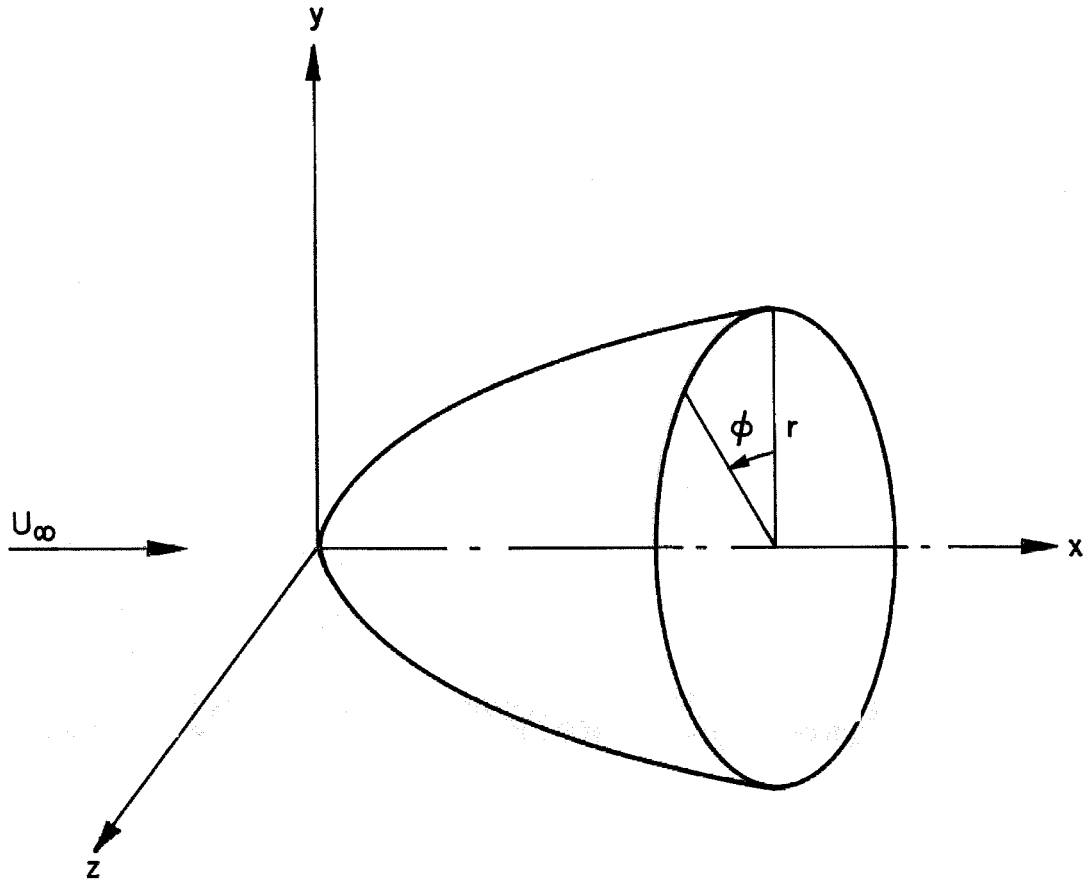

$$x = x$$

$$r = \sqrt{y^2 + z^2}$$

$$\phi = \tan^{-1} z/y$$

Fig. 1 COORDINATE SYSTEM

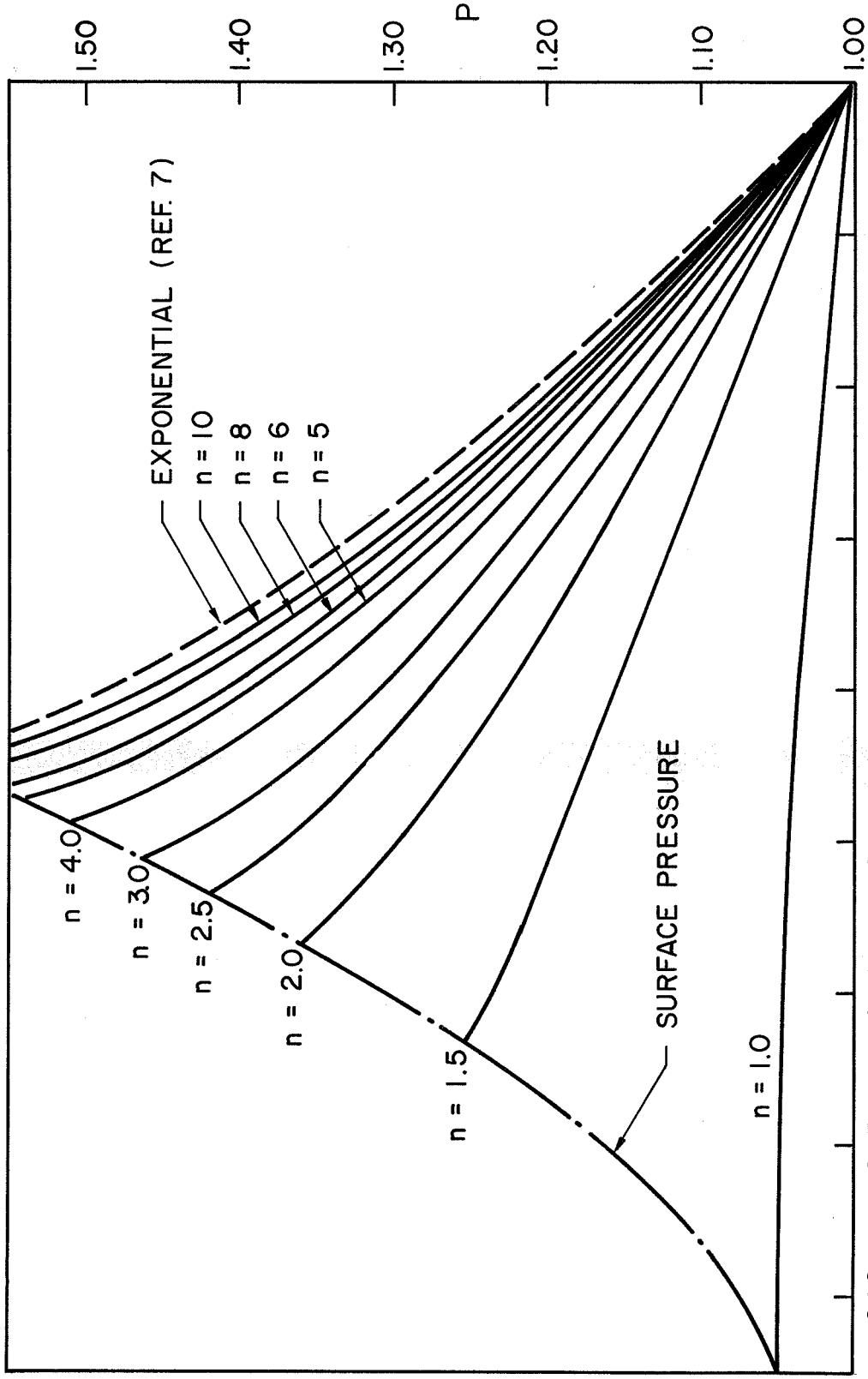

Fig. 2 PRESSURE FIELD ($\gamma = 1.40$)

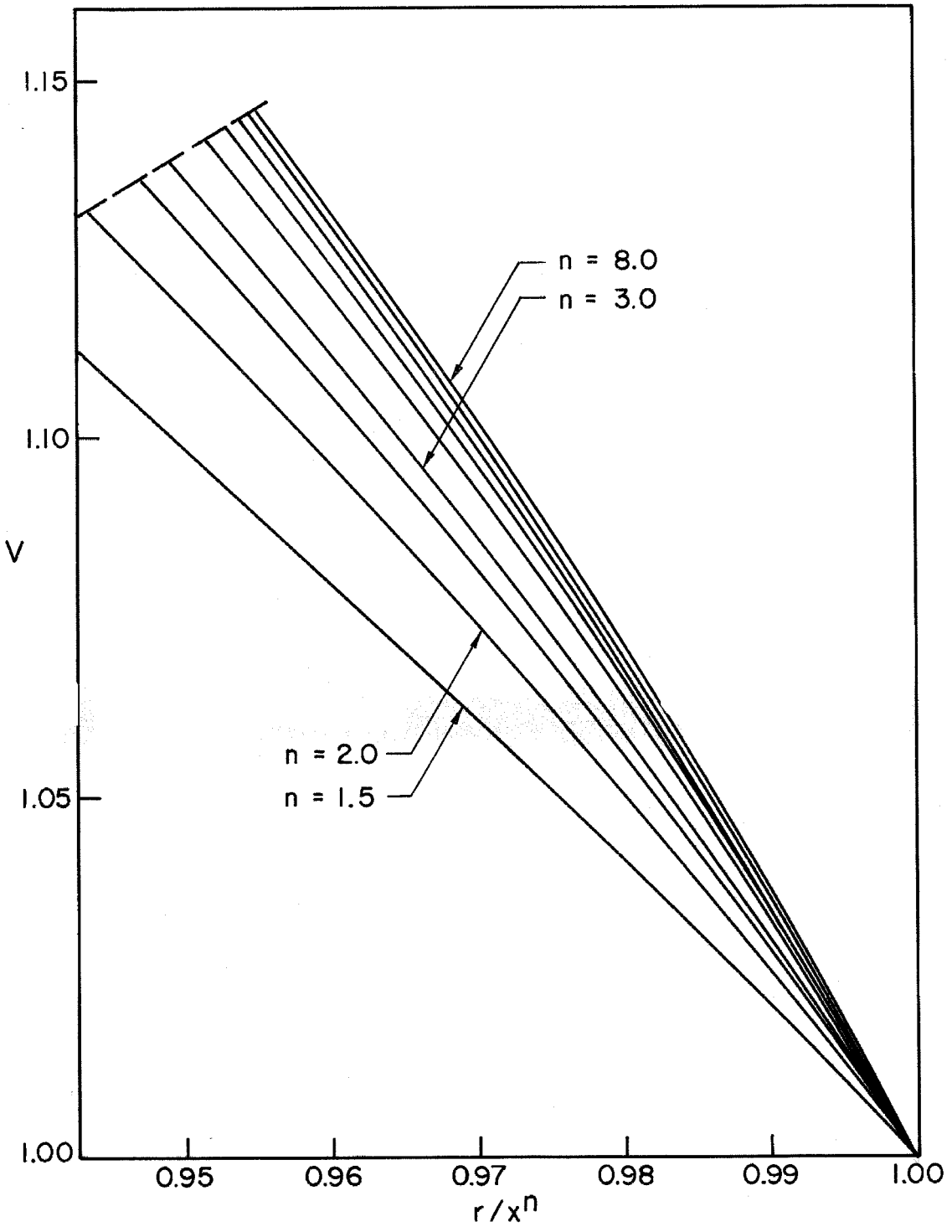

Fig. 3 VELOCITY FIELD ($\gamma = 1.40$)

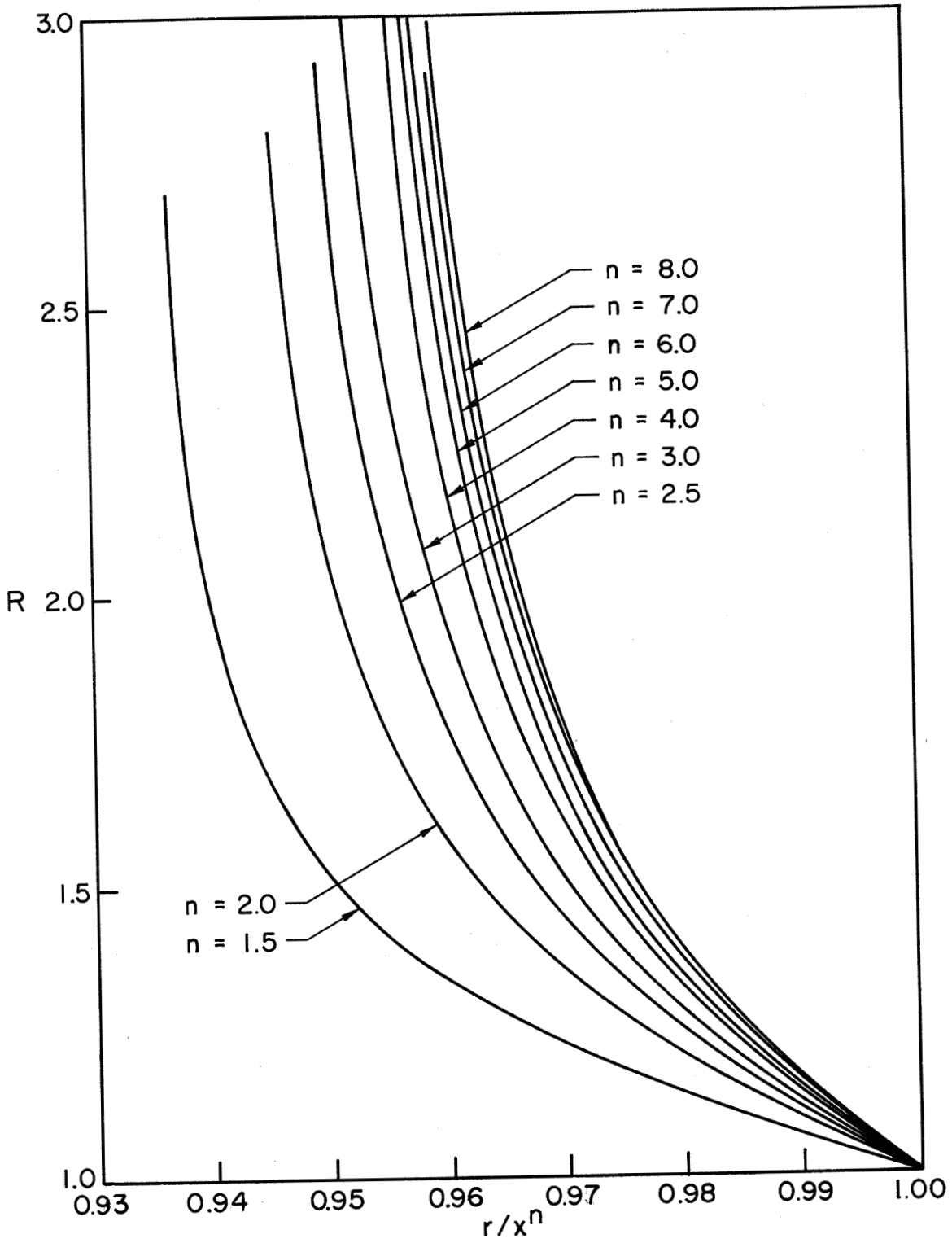

Fig. 4 DENSITY FIELD ($\gamma = 1.40$)

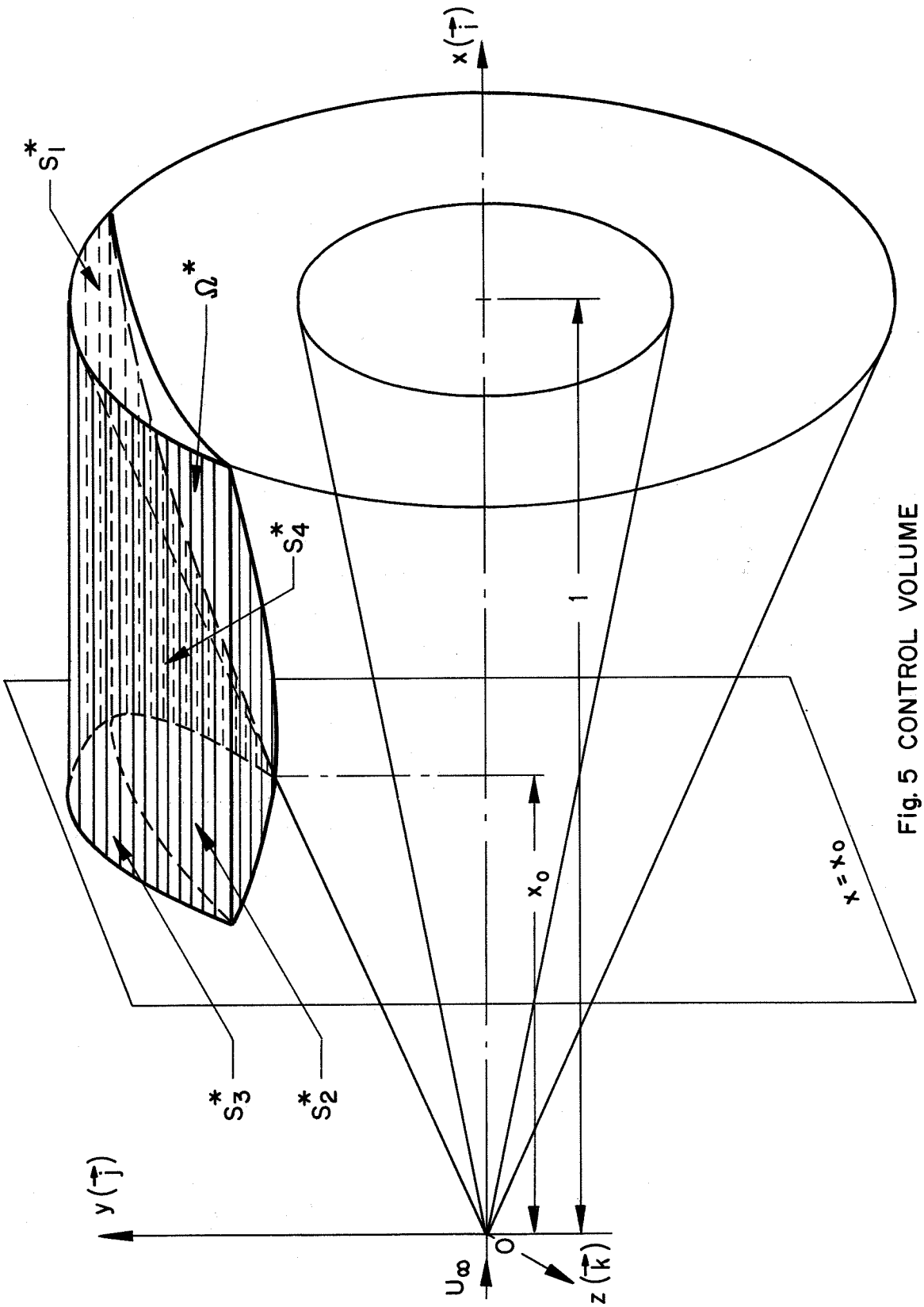

Fig. 5 CONTROL VOLUME

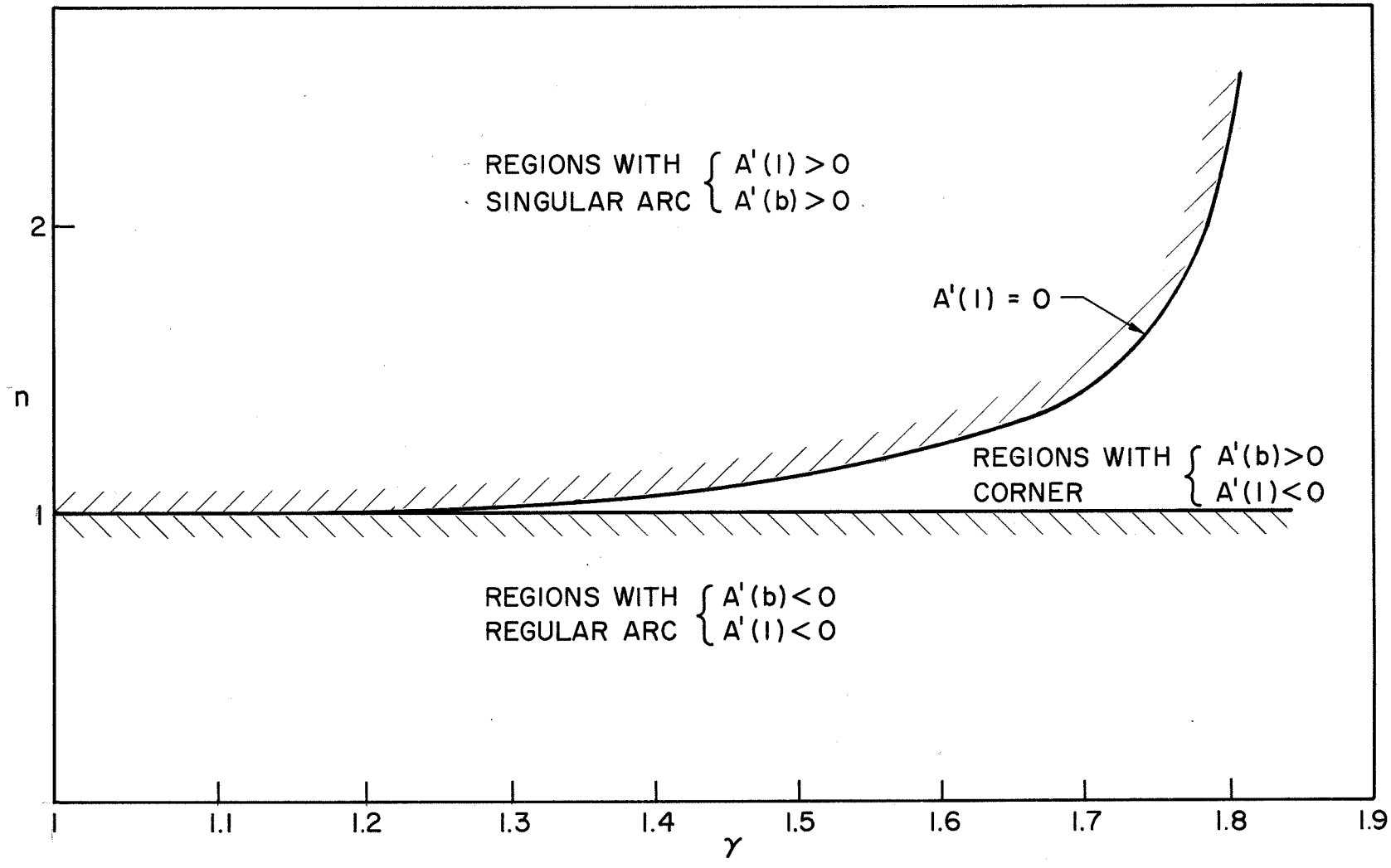

Fig. 6 THE CURVE $A'(1; n, \gamma) = 0$

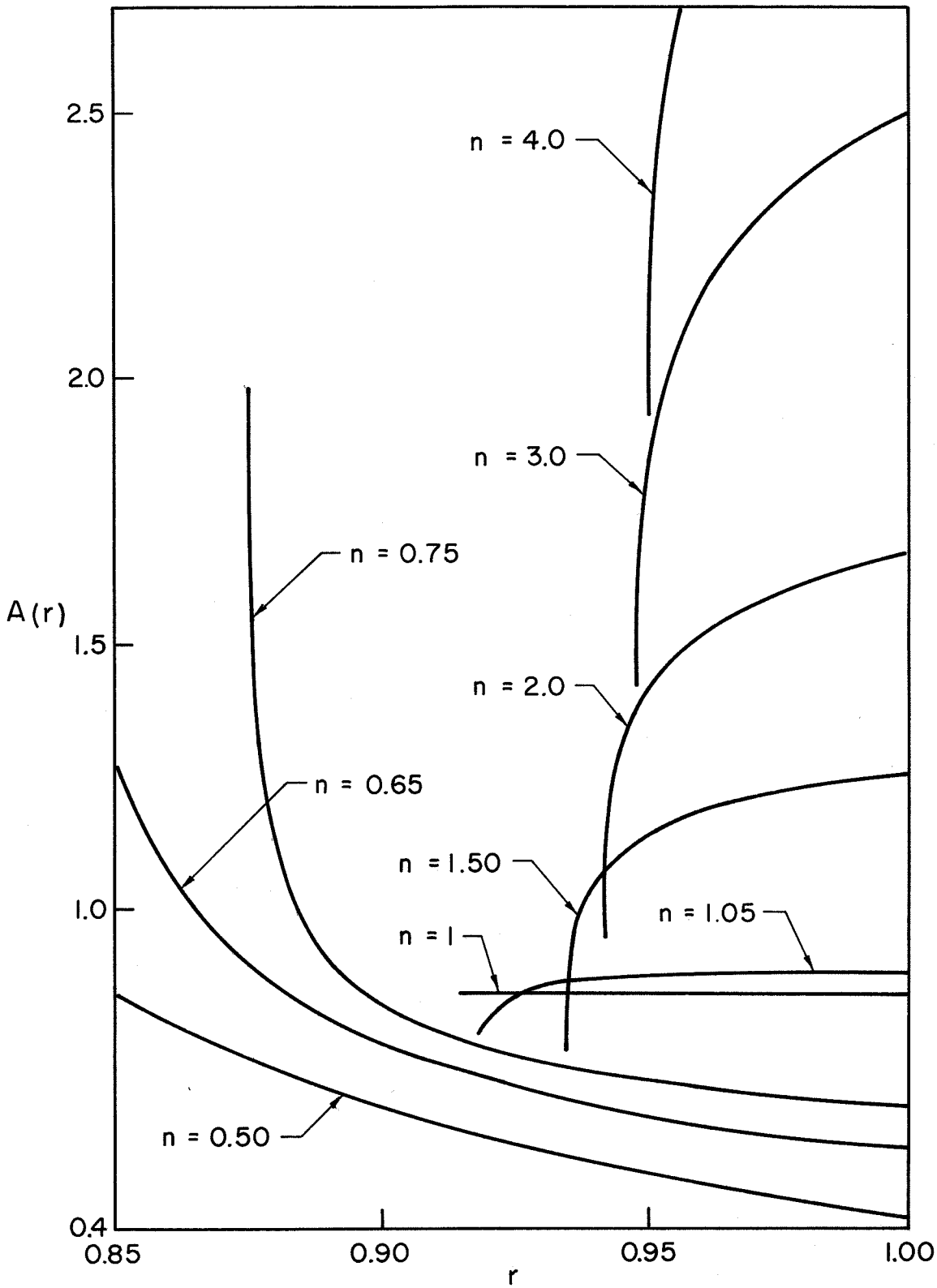

Fig. 7 THE FUNCTION $A(1; n, \gamma)$ FOR $\gamma = 1.40$

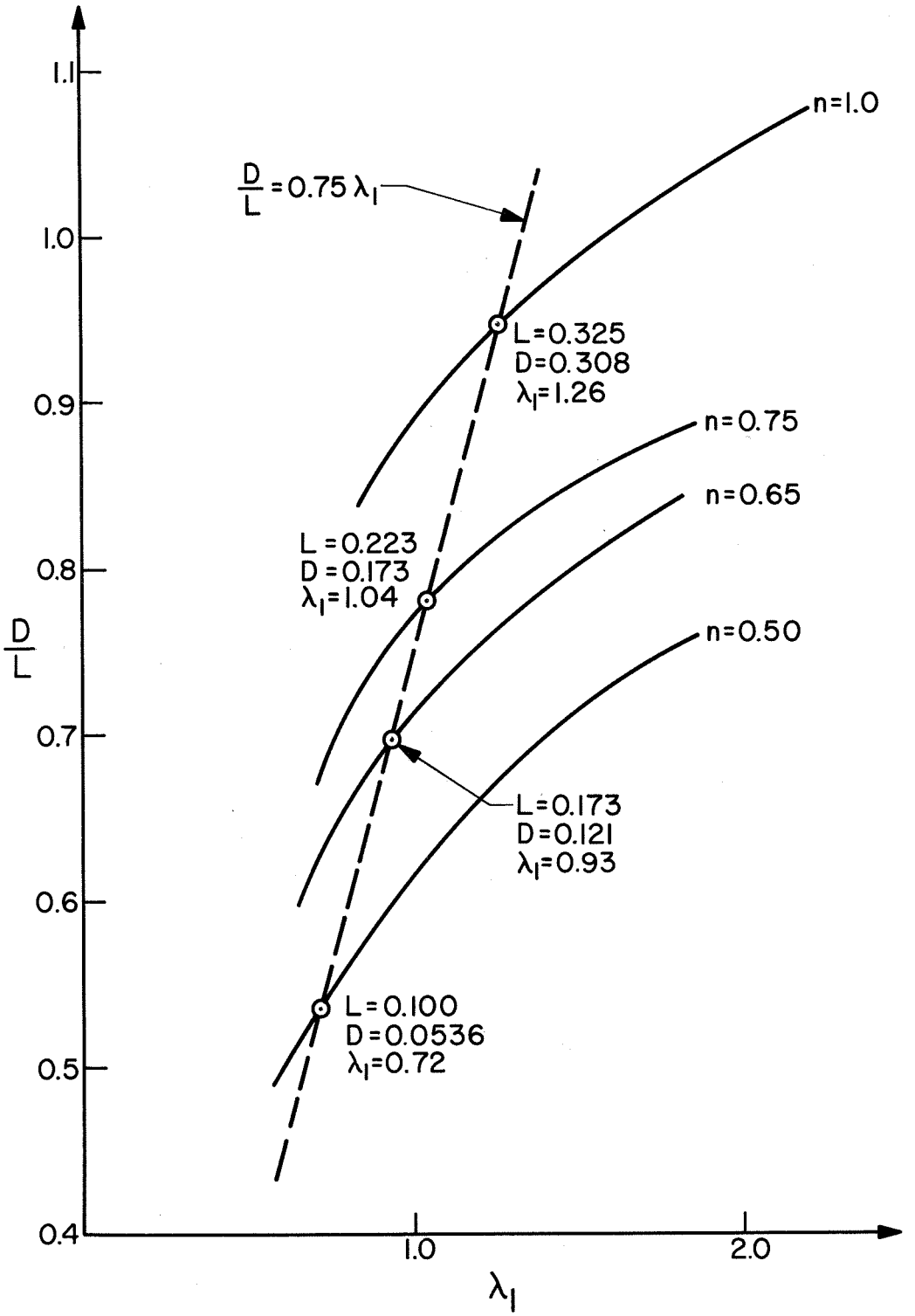

Fig. 8 GRAPHICAL SOLUTION FOR λ_1

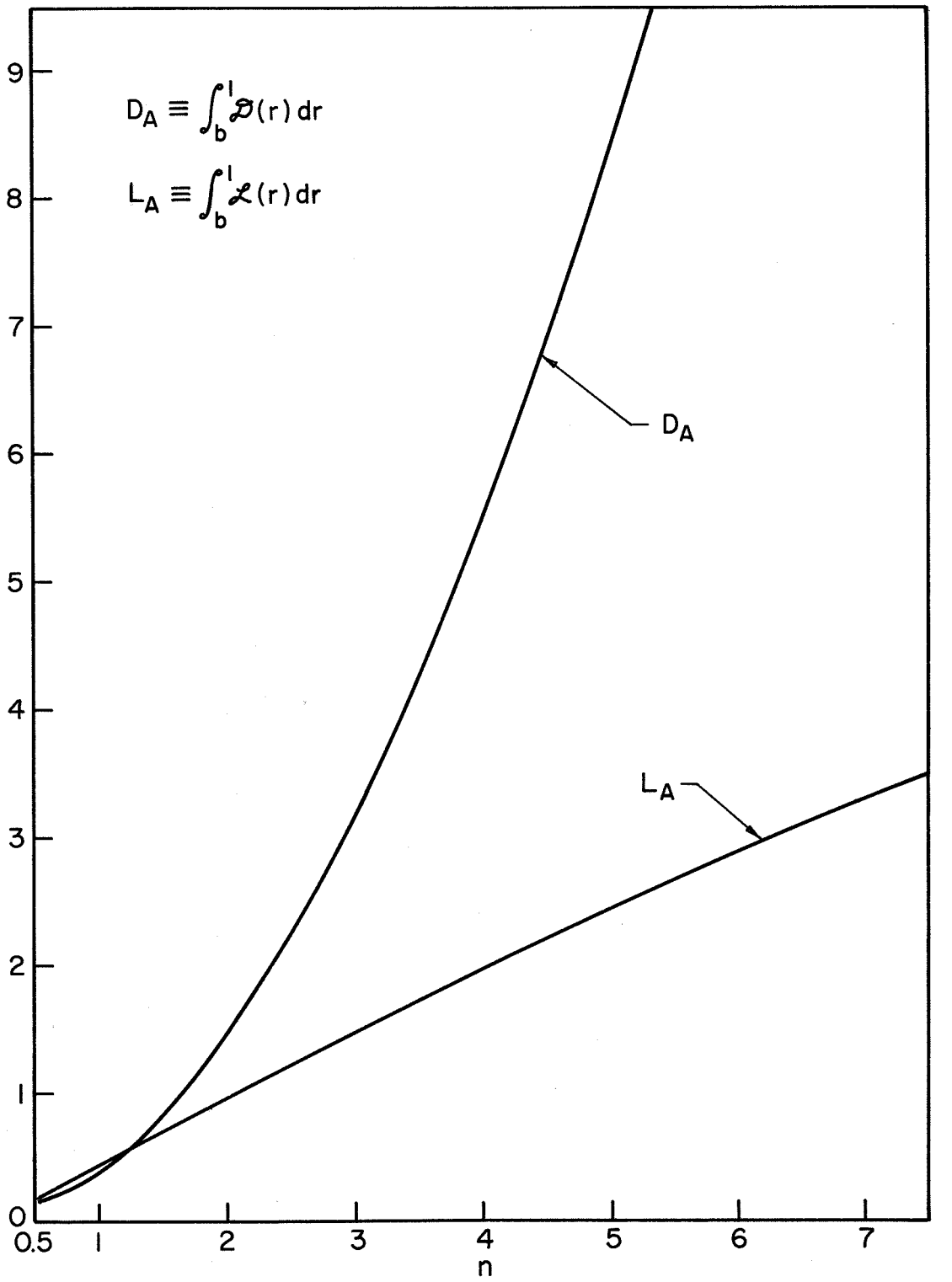

Fig. 9 D_A AND L_A AT $\gamma = 1.40$

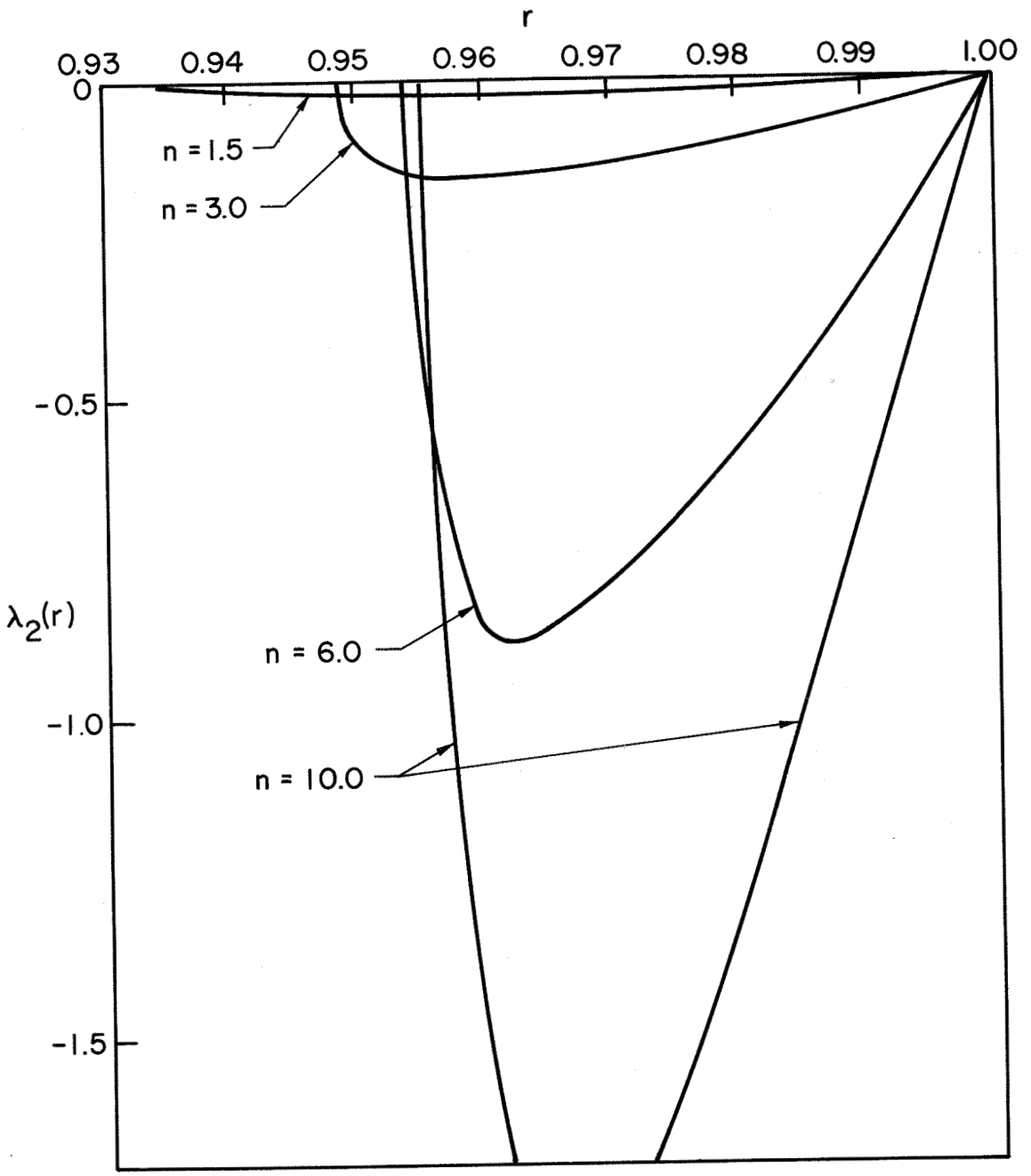

Fig. 10 $\lambda_2(r)$ FOR $\gamma = 1.40$

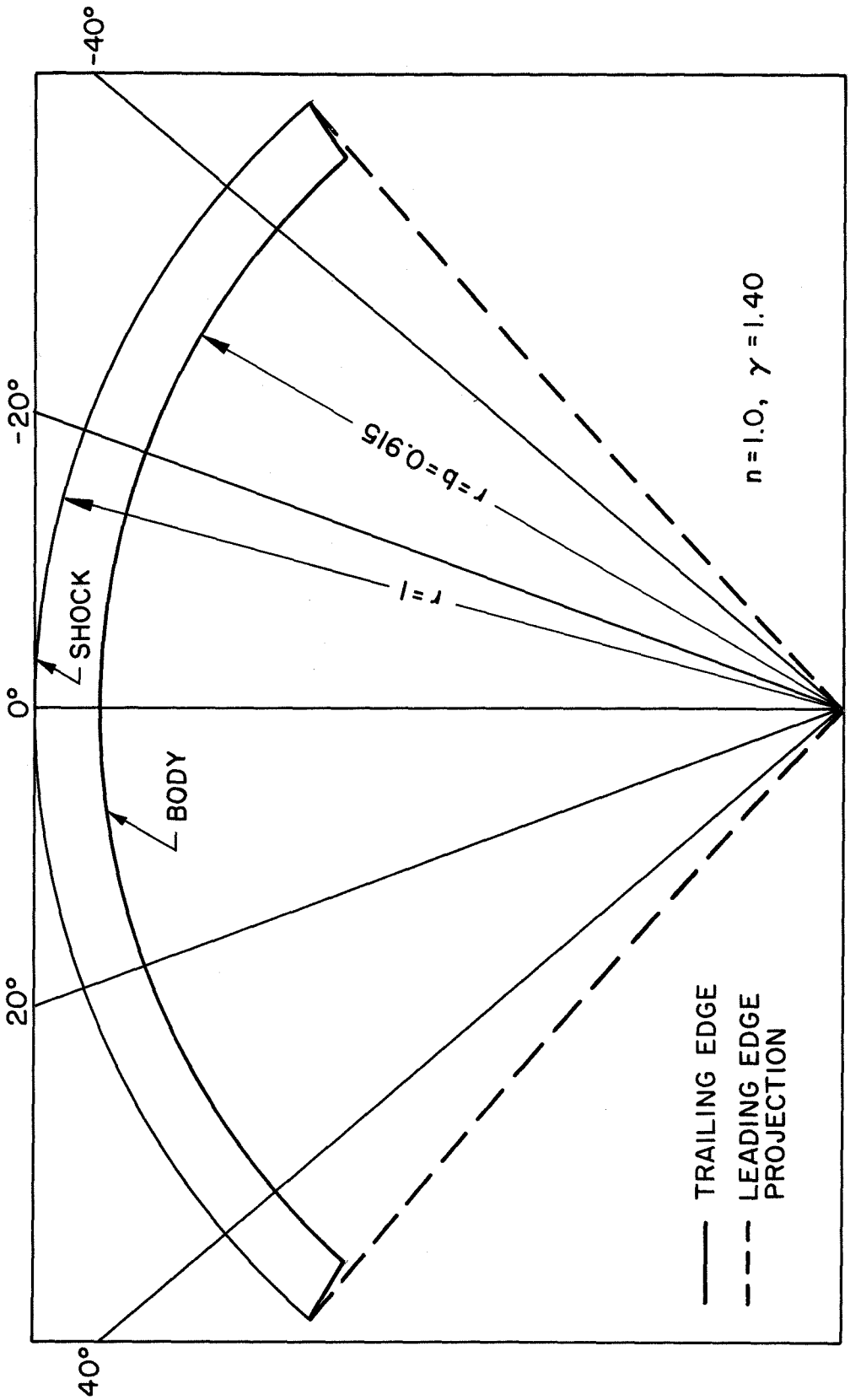

Fig. 11 OPTIMUM SHAPE (TRAILING EDGE PLANE)

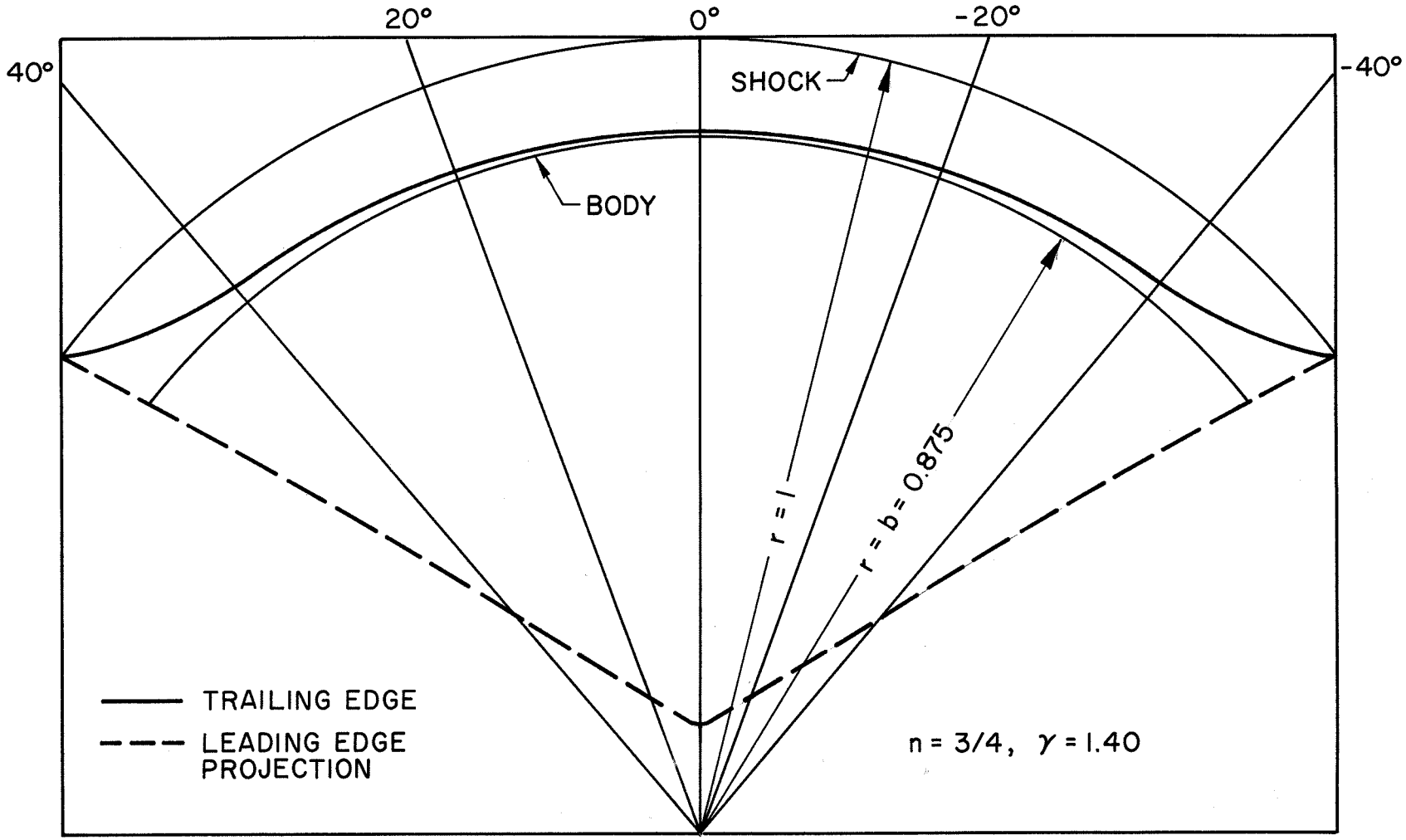

Fig. 12 OPTIMUM SHAPE (TRAILING EDGE PLANE)

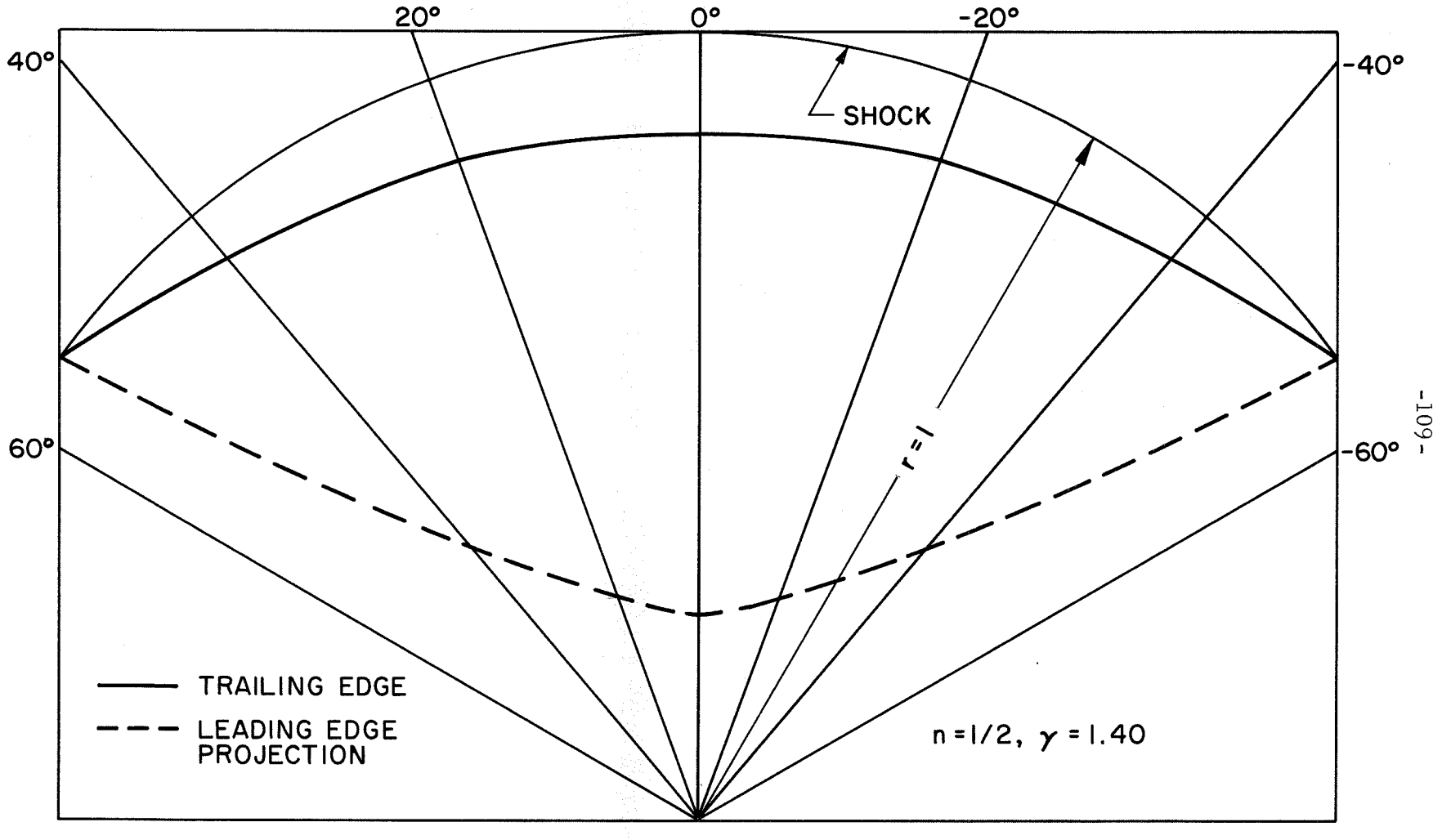

Fig. 13 OPTIMUM SHAPE (TRAILING EDGE PLANE)

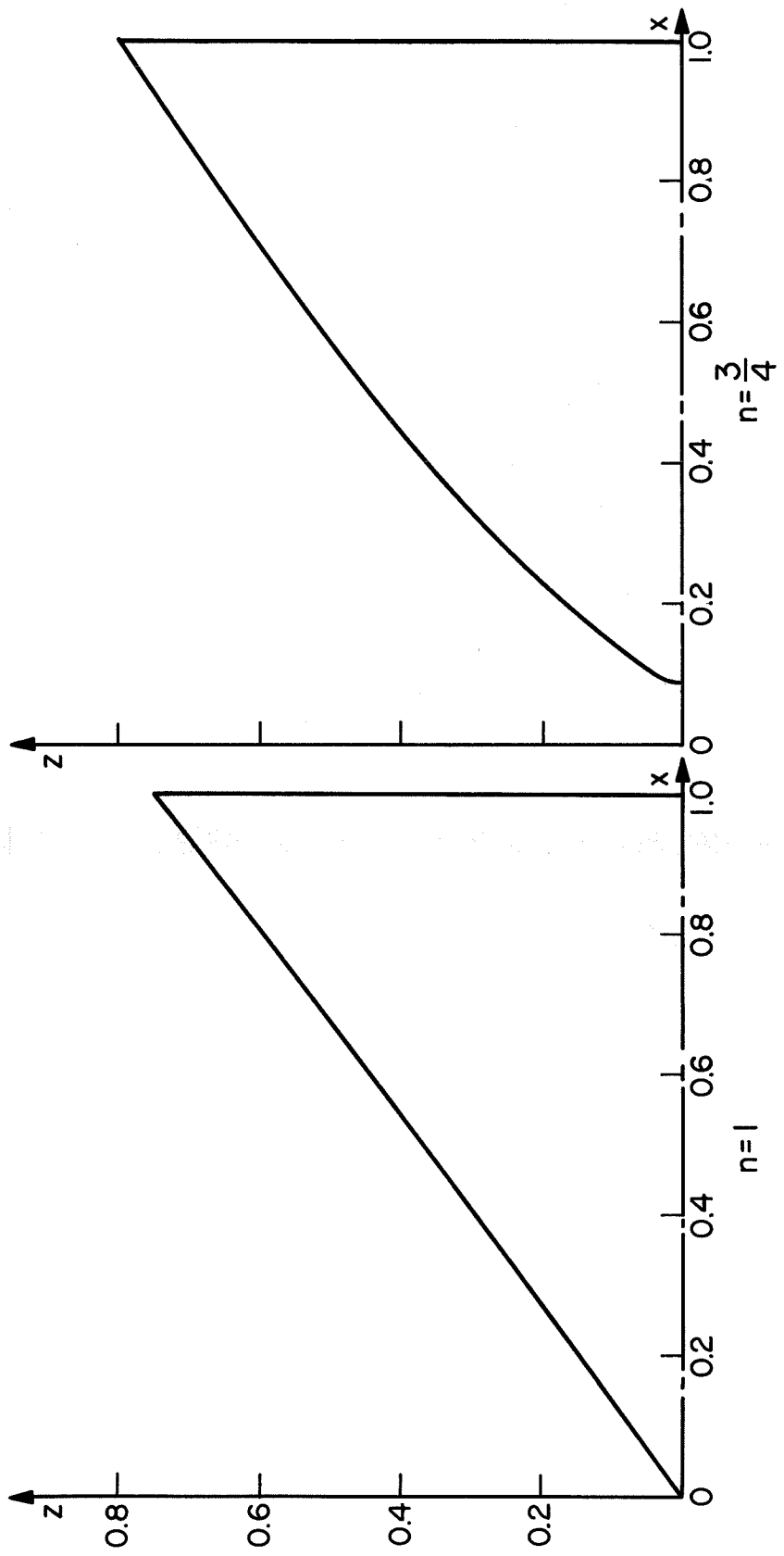

Fig. 14 PLANFORMS OF THE OPTIMUM SHAPES

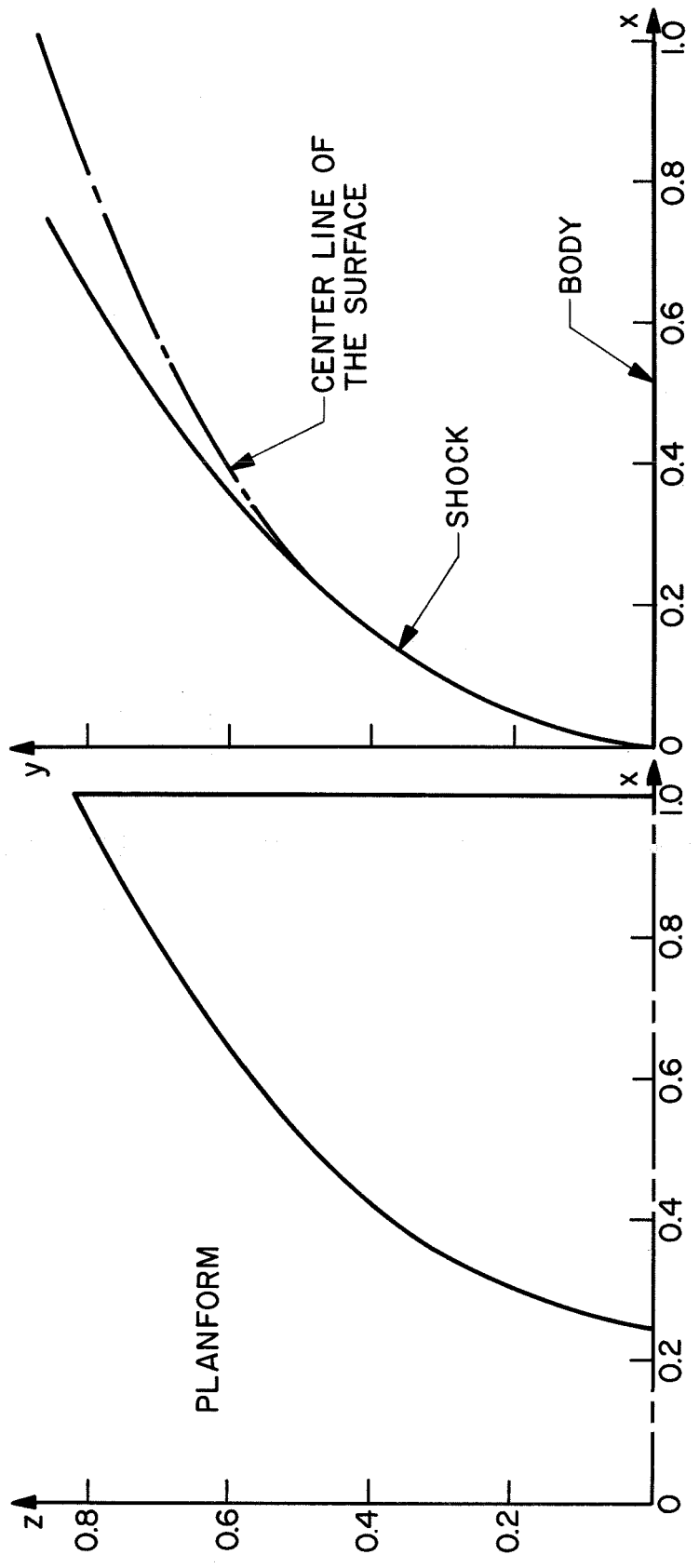

Fig. 15 PLANFORM AND CENTER LINE OF THE OPTIMUM SHAPE ($n=\frac{1}{2}$)

Table 1. Numerical Results of Flow Fields ($\gamma = 1.40$)

n = 1.5				n = 2.0			
r/x^n	P	V	R	r/x^n	P	V	R
1	1	1	1	1	1	1	1
0.998	1.0084	1.0043	1.0117	0.998	1.0114	1.0054	1.0170
6	1.0165	1.0086	1.0239	6	1.0225	1.0105	1.0342
4	1.0246	1.0128	1.0360	4	1.0337	1.0157	1.0524
2	1.0328	1.0170	1.0487	2	1.0450	1.0208	1.0710
0.990	1.0408	1.0211	1.0617	0.990	1.0560	1.0258	1.0904
8	1.0487	1.0252	1.0747	8	1.0672	1.0308	1.1105
6	1.0566	1.0292	1.0885	6	1.0783	1.0357	1.1315
4	1.0645	1.0333	1.1027	4	1.0894	1.0406	1.1535
2	1.0723	1.0373	1.1172	2	1.1006	1.0454	1.1767
0.980	1.0800	1.0414	1.1324	0.980	1.1117	1.0502	1.2010
8	1.0877	1.0452	1.1480	8	1.1229	1.0549	1.2265
6	1.0954	1.0492	1.1645	6	1.1342	1.0598	1.2550
4	1.1031	1.0530	1.1817	4	1.1454	1.0643	1.2830
2	1.1106	1.0568	1.1994	2	1.1568	1.0688	1.3144
0.970	1.1183	1.0608	1.2184	0.970	1.1682	1.0735	1.3479
8	1.1258	1.0645	1.2384	8	1.1797	1.0781	1.3844
6	1.1334	1.0685	1.2602	6	1.1913	1.0825	1.4242
4	1.1409	1.0721	1.2820	4	1.2031	1.0870	1.4682
2	1.1484	1.0759	1.3064	2	1.2150	1.0915	1.5174
0.960	1.1560	1.0796	1.3324	0.960	1.2272	1.0958	1.5730
8	1.1635	1.0834	1.3607	8	1.2396	1.1003	1.6367
6	1.1712	1.0871	1.3924	6	1.2524	1.1046	1.7115
4	1.1788	1.0907	1.4269	4	1.2656	1.1089	1.8019
2	1.1864	1.0944	1.4660	2	1.2792	1.1132	1.7479
0.950	1.1942	1.0981	1.5109	0.950	1.2936	1.1176	2.0632
8	1.2020	1.1017	1.5632	8	1.3090	1.1218	2.2775
6	1.2099	1.1053	1.6264	6	1.3261	1.1260	2.6432
4	1.2182	1.1089	1.7055	4	1.3470	1.1302	3.6936
2	1.2266	1.1125	1.8114	0.9438	1.3496	1.1305	3.9792
0.940	1.2355	1.1161	1.9687	36	1.3525	1.1310	4.4181
0.938	1.2452	1.1197	2.2630	34	1.3557	1.1314	5.2391
0.936	1.2577	1.1231	∞	32	1.3601	1.1317	∞
n = 2.5				n = 3.0			
0.998	1.0132	1.0058	1.0202	0.998	1.0143	1.0063	1.0222
6	1.0262	1.0117	1.0407	6	1.0286	1.0125	1.0452
4	1.0393	1.0174	1.0624	4	1.0430	1.0186	1.0692
2	1.0523	1.0230	1.0849	2	1.0574	1.0246	1.0942
0.990	1.0653	1.0285	1.1082	0.990	1.0717	1.0304	1.1205
8	1.0785	1.0342	1.1329	8	1.0862	1.0363	1.1482
6	1.0917	1.0396	1.1590	6	1.1007	1.0422	1.1777
4	1.1049	1.0450	1.1860	4	1.1154	1.0478	1.2089
2	1.1182	1.0502	1.2150	2	1.1301	1.0535	1.2420

Table 1 (cont'd)

	n = 2.5				n = 3.0		
r/x^n	P	V	R	r/x^n	P	V	R
1	1	1	1	1	1	1	1
0.980	1.1315	1.0555	1.2460	0.980	1.1449	1.0590	1.2775
8	1.1450	1.0607	1.2789	8	1.1601	1.0645	1.3159
6	1.1585	1.0658	1.3144	6	1.1753	1.0700	1.3560
4	1.1723	1.0710	1.3524	4	1.1908	1.0753	1.4029
2	1.1861	1.0760	1.3939	2	1.2065	1.0807	1.4527
0.970	1.2000	1.0811	1.4395	0.970	1.2225	1.0860	1.5080
8	1.2145	1.0860	1.4900	8	1.2389	1.0912	1.5700
6	1.2291	1.0909	1.5464	6	1.2557	1.0964	1.6404
4	1.2440	1.0958	1.6100	4	1.2729	1.1016	1.7222
2	1.2592	1.1005	1.6835	2	1.2910	1.1066	1.8187
0.960	1.2750	1.1054	1.7702	0.960	1.3097	1.1117	1.9355
8	1.2915	1.1102	1.8737	8	1.3294	1.1167	2.0832
6	1.3086	1.1149	2.0039	6	1.3505	1.1216	2.2792
4	1.3268	1.1196	2.1745	4	1.3735	1.1266	2.5622
2	1.3465	1.1243	2.4190	2	1.3994	1.1314	3.0462
0.950	1.3683	1.1288	2.8209	0.950	1.4323	1.1362	4.3421
0.948	1.3951	1.1334	3.8171	0.949	1.4589	1.1386	1.0594
0.947	1.4142	1.1356	6.365	0.9489	1.4630	1.1387	∞
0.9468	1.4220	1.1362	∞				
	n = 4.0				n = 6.0		
0.998	1.0158	1.0068	1.0247	0.998	1.0173	1.0073	1.0272
6	1.0318	1.0134	1.0505	6	1.0348	1.0144	1.0560
4	1.0476	1.0200	1.0775	4	1.0523	1.0214	1.0862
2	1.0636	1.0265	1.1062	2	1.0700	1.0283	1.1182
0.990	1.0799	1.0327	1.1364	0.990	1.0877	1.0351	1.1520
8	1.0959	1.0391	1.1680	8	1.1057	1.0418	1.1885
6	1.1121	1.0452	1.2020	6	1.1239	1.0484	1.2274
4	1.1287	1.0513	1.2384	4	1.1423	1.0549	1.2690
2	1.1454	1.0573	1.2774	2	1.1608	1.0613	1.3144
0.980	1.1623	1.0633	1.3195	0.980	1.1800	1.0676	1.3640
8	1.1794	1.0692	1.3652	8	1.1994	1.0740	1.4185
6	1.1969	1.0751	1.4157	6	1.2192	1.0801	1.4789
4	1.2147	1.0808	1.4712	4	1.2397	1.0862	1.5467
2	1.2329	1.0865	1.5332	2	1.2607	1.0922	1.6234
0.970	1.2517	1.0921	1.6034	0.970	1.2824	1.0982	1.7117
8	1.2710	1.0976	1.6837	8	1.3050	1.1041	1.8157
6	1.2909	1.1032	1.7770	6	1.3286	1.1099	1.9405
4	1.3117	1.1087	1.8884	4	1.3537	1.1158	2.0957
2	1.3336	1.1141	2.0259	2	1.3805	1.1214	2.2957

Table 1 (cont'd)

n = 4.0				n = 6.0			
r/x^n	P	V	R	r/x^n	P	V	R
1	1	1	1	1	1	1	1
0.960	1.3569	1.1195	2.2019	0.960	1.4098	1.1270	2.5747
8	1.3820	1.1248	2.4410	8	1.4427	1.1326	3.0036
6	1.4100	1.1299	2.8017	6	1.4821	1.1381	3.8366
4	1.4425	1.1351	3.4636	4	1.5405	1.1435	7.9740
2	1.4871	1.1402	5.8818	0.9538	1.5511	1.1440	10.967
0.9518	1.4935	1.1407	6.7905	0.9537	1.5585	1.1442	16.464
0.9516	1.5014	1.1412	8.6860	0.9536	1.5656	1.1444	∞
0.9515	1.5063	1.1414	11.075				
0.9514	1.5142	1.1416	∞				
n = 8.0				n = 10.0			
0.998	1.0181	1.0075	1.0287	0.998	1.0186	1.0076	1.0295
6	1.0363	1.0148	1.0587	6	1.0373	1.0152	1.0605
4	1.0547	1.0222	1.0905	4	1.0560	1.0225	1.0932
2	1.0731	1.0292	1.1257	2	1.0750	1.0298	1.1280
0.990	1.0918	1.0363	1.1604	0.990	1.0942	1.0369	1.1652
8	1.1106	1.0432	1.1987	8	1.1136	1.0440	1.2052
6	1.1298	1.0500	1.2402	6	1.1332	1.0510	1.2480
4	1.1491	1.0566	1.2850	4	1.1533	1.0577	1.2947
2	1.1689	1.0633	1.3337	2	1.1737	1.0644	1.3457
0.980	1.1890	1.0698	1.3874	0.980	1.1946	1.0710	1.4017
8	1.2096	1.0763	1.4464	8	1.2159	1.0776	1.4639
6	1.2307	1.0826	1.5124	6	1.2377	1.0841	1.5334
4	1.2525	1.0889	1.5872	4	1.2604	1.0904	1.6125
2	1.2750	1.0950	1.6729	2	1.2839	1.0968	1.7035
0.970	1.2983	1.1012	1.7719	0.970	1.3082	1.1030	1.8104
8	1.3228	1.1072	1.8905	8	1.3339	1.1092	1.9387
6	1.3486	1.1132	2.0352	6	1.3610	1.1153	2.0972
4	1.3762	1.1192	2.2195	4	1.3902	1.1213	2.3017
2	1.4059	1.1250	2.4657	2	1.4219	1.1272	2.5826
0.960	1.4390	1.1308	2.8256	0.960	1.4576	1.1330	3.0086
8	1.4774	1.1365	3.4406	8	1.5003	1.1388	3.8009
6	1.5270	1.1420	5.1334	6	1.5601	1.1444	6.6025
0.9548	1.5782	1.1454	13.624	0.9558	1.5688	1.1450	7.5653
0.9547	1.5910	1.1456	∞	0.9556	1.5792	1.1455	9.3065
				0.9554	1.5931	1.1461	14.605
				0.9553	1.6065	1.1464	∞

References

1. Miele, A. (ed.), Theory of Optimum Aerodynamic Shapes. Vol. 9. Applied Mathematics and Mechanics Monographs. Academic Press Inc. New York (1965).

2a. Nonweiler, T. R. F., Aerodynamic Problems of Manned Space Vehicles. J. Roy. Ae. Soc. 63 (505) September, 1959.

2b. Nonweiler, T. R. F., Delta Wings of Shapes Amenable to Exact Shock Wave Theory. J. Roy. Ae. Soc. 67 (625) January, 1963.

3. Jones, J. G., A Method for Designing Lifting Configurations for High Supersonic Speeds Using the Flow Fields of Non-Lifting Cones. R. A. E. Report No. Aero. 2674, March, 1963.

4. Woods, B. A., The Construction of a Compression Surface Based on an Axisymmetrical Conical Flow Field. R. A. E. Tech. Note No. Aero 2900, June, 1963.

5. Woods, B. A., The Forces on a Compression Surface Based on an Axisymmetrical Conical Flow Field. R. A. E. Tech. Report No. 64035, October, 1964.

6. Mirels, H., Hypersonic Flow Over Slender Bodies Associated with Power-Law Shocks. Advances in Applied Mechanics, Vol. 7, 1962.

7. Chernyi, G. G., Introduction to Hypersonic Flow. Academic Press, New York and London, 1961.

8. Gersten, K. and Nicolai, D., Die Hyperschallstromung um schlanke Koper mit Konturen der Form $\overline{R} \sim x^n$. Deutsche Luft-und Raumfahrt Forschungsbericht 64-19, Juli, 1964

9. Sullivan, P. A., Inviscid Hypersonic Flow on Cusped Concave Surfaces. J. Fluid Mechanics 24, Part 1, (99), 1966.

10. Van Dyke, M. D., A Study of Hypersonic Small-Disturbance Theory, NACA Report 1194, 1954.

11. Liepmann, H. W. and Roshko, A., Elements of Gasdynamics. John Wiley and Sons, Inc. New York, (1957)

12. Sedov, L. I., Similarity and Dimensional Methods in Mechanics. Academic Press Inc. New York and London, 1959.

13. Gelfand, I. M. and Fomin, S. V., Calculus of Variations. Prentice-Hall, Inc. Englewood Cliffs, New Jersey, 1963.